Automotive Body Structure Assembly

Mass & Cost Saving Potential of Laser Welding Compared to Spot Welding

Julius F. Klinger

Master Thesis in Vehicle Engineering

Department of Aeronautical and Vehicle Engineering
KTH Royal Institute of Technology

TRITA-AVE 2012:04
ISSN 1651-7660

Postal address	***Visiting Address***	***Telephone***	***Telefax***	***Internet***
KTH Vehicle Dynamics SE-100 44 Stockholm, Sweden	Teknikringen 8 Stockholm	+46 8 790 6000	+46 8 790 9290	www.kth.se

Abstract

Due to the continuously increasing demands on the efficiency of road passenger vehicles the National Highway Safety Traffic Administration (NHTSA) commissioned a project to determine the achievable mass savings on an average, mass produced passenger car, which are obtainable with today's or within close reach technology. The major part of this project is conducted at EDAG, Inc.

One of the approaches made within this program is to reduce the weight of a vehicle's body structure by replacing the commonly on a mass production vehicle applied joining technology resistance spot welding with laser beam welding. The main advantage is the possibility to bisect the size of the flanges since laser welding requires less flange width compared to spot welding. A sample structure is remodeled twice to create one almost solely spot welded and one almost solely laser welded body structure of the same vehicle. Those body structures are represented by two FEM models. Proper representation of the joining technology is applied to both FEM models in preparation of NVH computation runs, ensuring the comparability of the two body structures regarding their performance. In cooperation with experienced production engineers two assembly layouts for the spot welded and the laser welded structures are developed. For those assembly layouts cost calculations are done to oppose the attained mass savings to the increase in production costs.

The weight difference between the two versions is determined to a remarkable *12.2 kg* for the analyzed sample structure. The laser welded structure thereby displays a slightly improved NVH performance compared to the spot welded structure. Taking the exemplary cost increase for the assembly of certain parts of the lower body structure into account gave a weight saving efficiency of *4.58 $* per saved *kg*. For the field of automotive engineering this is a rather high value, mainly caused by the still very extensive costs for laser welding equipment. With laser welding technology being more and more adopted in mass production applications and most probably due technical improvements those costs are likely to decrease within the next few years. Even more mass savings could be achieved by adapting the design of the body structure more to the usage of laser beam welding.

Acknowledgements

The present study was conducted at the Auburn Hills, Michigan, facility of EDAG, Inc. between July and December 2012. Many thanks go to program manager Harry Singh and the team members of the product development advanced engineering team. They supported this master thesis with a lot of valuable information and advice. Also thanks are due to the supervising professor at KTH, Lars Drugge.

Abbreviations

2T	two thicknesses
3T	three thicknesses
ACM2	area connection model 2
BH	bake hardening
BIW	body in white
BoM	bill of materials
ca.	circa
CAD	computer aided design
CAE	computer aided engineering
CO_2	carbon dioxide
CP	complex phase
DIN	Deutsches Institut für Normung (German Institute of Standardization)
DP	dual phase
etc.	et cetera
e.g.	example given
FEM	finite element method
HAZ	heat affected zone (of the creation of a joint)
HF	hot formed
HSLA	high strength low alloy
i.e.	id est (that is)
LASER	Light amplification by stimulated emission of radiation
LH	left hand
MAG	metal active gas
MIG	metal inert gas
MS	martensitic
NHTSA	National Highway Traffic and Safety Administration
NdYAG	neodymium yttrium-aluminum garnet
NVH	noise, vibration and harshness
N/A	not applicable
OEM	original equipment manufacturer
PID	property identification (number)
RBE	rigid body element
RH	right hand
S	stainless

Table of Contents

1. Introduction

The demands on a road vehicle regarding efficiency are further increasing nowadays. With respect to the ecological impact of road vehicles and the drain of resources the energy consumption of passenger cars needs to be further decreased. This leads to enhanced efforts concerning the reduction of weight of vehicles. All components of a modern passenger car are continuously tested for further weight reduction potential.

In a conventional vehicle propelled by an internal combustion engine the body structure is the second heaviest main module right after the power train. So engineers are constantly seeking for new paths to take weight from the body in white (BIW). Different approaches as well with different materials like aluminum and recently also composite materials have been tackled. But since the processing of such materials is much more expensive and energy consuming than manufacturing of steel, the latter remains a very competitive option. On top of that steel is much more temperature independent and easier to recycle, at least compared to composite materials.

Several global research studies like the UltraLight Steel Auto Body and the Future Steel Vehicle (autosteel.org, 2012) have shown that the conventional steel body still has large mass saving potentials. The research program commissioned on behalf of the National Highway Traffic and Safety Administration (NHTSA), which this thesis work is part of, identifies further possibilities to reduce the weight of a body structure manufactured in a cost efficient way. Not necessarily relying on the use of steel the program's main aspect is to only apply measures feasible with mass production. The starting basis for this project is the North American edition of the Honda Accord, model year 2011, whose body style was first launched in 2008. In line with the program the body structure weight already could be significantly decreased, mainly on the behalf of the application of high strength steels.

Being a subpart of the NHTSA program the present thesis scrutinizes another approach to reduce the weight, i.e. to seek possibilities to be able to downsize the weld flanges, which are attached to each single part with respect to the bonding process. All flanges of the inspected Accord have an approximated total weight of roughly *25 kg*. The average flange width of those flanges is about *16 mm*, since this is the required width for a resistance spot weld bond. The spot weld point itself has a diameter of ca. *4.5 mm*, but further space is needed to allow the weld gun to access the flange to be bonded. Since decades spot welding is the dominating joining process for the body structure of mass production vehicles.

If the resistance spot weld procedure would be replaced by laser beam welding the flange width could be considerably reduced. Since the remote laser weld gun does not need to physically contact the part, small clamps are the only tools getting in touch with the flange. So it can be designed much leaner, typically with a flange width of *8 mm*. In this thesis project all the flanges of the sample body structure are investigated on whether they are suitable for laser welding having the flanges trimmed as described and thereby reducing the weight.

Further mass savings possibly could be achieved by dint of the continuous seam created by laser welding. The linear connections may lead to a larger body structure stiffness compared to the punctual connections of spot welding. In this case some parts not relevant for crash impact load cases could be reduced in thickness to achieve the same stiffness performance as the spot welded body structure which would result in further mass reductions. To survey this approach finite element

computation models of the resistance spot welded and the laser beam welded body structure are established and compared.

If a comprehensive study of the benefits of laser welding is pursued also the costs need to be studied. Therefore in line with this thesis project the assembly layouts of a BIW manufactured by resistance spot welding and one manufactured by laser beam welding were compared. Those assembly layouts were designed with the help of experienced manufacturing engineers who also were able to establish a cost estimation.

As indicated above the trimming of the flanges by switching to laser welding is just one of many measures covered by the NHTSA program study. For all the analyzed measures the expenses were identified to point out the most cost efficient ones in terms of the gained weight reduction compared to the required financial efforts. According to *Figure 1* welding only causes *12 %* of the total costs in the BIW production. This means that even if the welding costs do considerably increase due to the introduction of laser welding, the total costs for the BIW might just rise moderately. On the other hand the application of laser welding does not only affect the welding costs. Since this joining technology requires much lower tolerances than resistance spot welding also the stamping costs will increase. However, all those aspects are going to be studied in the present thesis work.

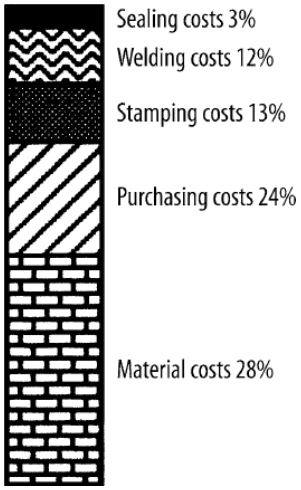

Figure 1 **Cost distribution for a common vehicle's body in white (Steen & Mazumder, 2010, p. 243)**

2. Theory

2.1. Introduction to Joining Technology

Joining is an important part in the process chain of manufacturing, which is divided into six sections according to one of the standardizations, the German DIN 8580: primary shaping, forming, cutting, joining, coating and adjustment of material properties (Koether & Rau, 2007, p. 14).
Since this thesis study deals with the weight saving potential on a body structure by altering the joining technology, this chapter aims to give a brief overview about the general groups joining is subdivided into. In chapter 2.1 all those groups, some subgroups and actual processes are touched on. Of course only the most relevant ones can be mentioned and the elucidations here make no claim to be complete.

2.1.1. Overview of Joining Processes

Joining processes are one of the weightiest parts of the metal processing industry. During the last one hundred years joining technology developed from a rather basic manufacturing procedure to an expanding sector, containing a large variety of processes adapting to the material properties, the design load cases and the design of the structure to be bonded. Those processes are continuously extended and improved and are pointing in the direction of micro-joining for the future development (Grote & Antonsson, 2009, p. 656 f.).

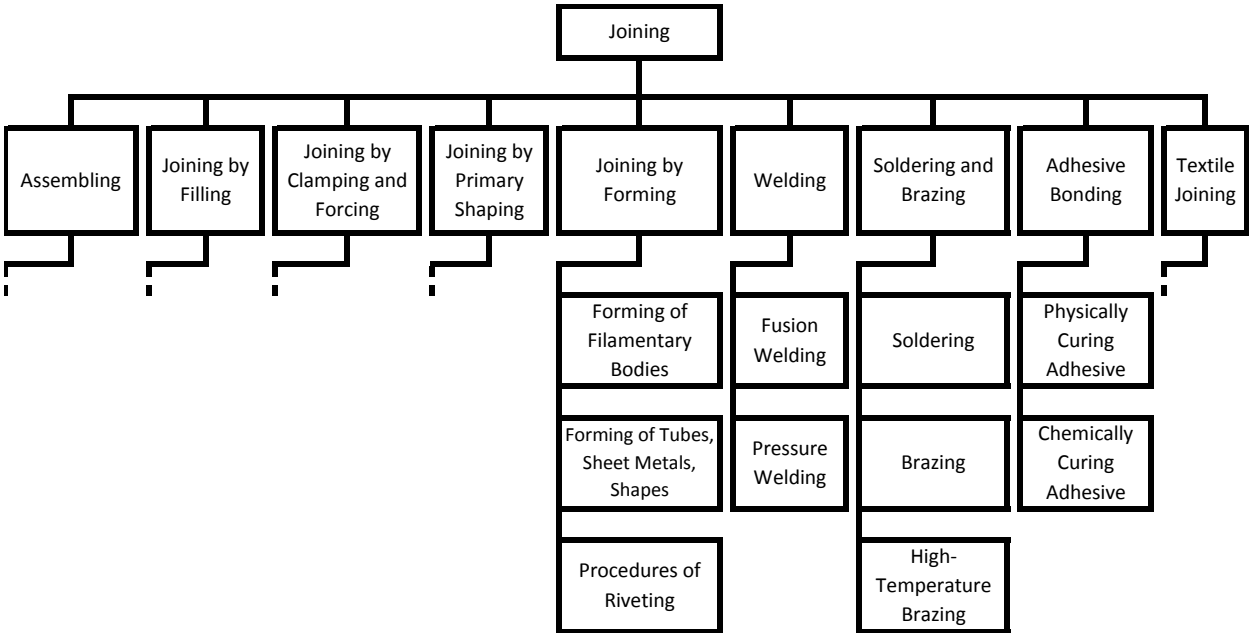

Figure 2 **Classification of joining processes highlighting typical body strucutre applications (Grote & Antonsson, 2009, p. 658)**

There are many different approaches to create a joint. By now there was no international classification for joining created. According to the German DIN 8593 the procedures can be divided into the main groups shown in *Figure 2*. For a usual mass production body in white (BIW) design, filling, joining by primary shaping and textile joining are not applied. Not considering the hang on parts and

closures also assembling and clamping and forcing is rarely used. So while the other procedures are elucidated in the following chapters, these are just briefly outlined in the next few lines.

Joining by assembling includes only positive locking connections. The bonded parts are directly in touch with each other without any aid in between and are not plastically deformed by the joining process. Being sub classified into six sections the group includes laying, donning and piling, engaging, telescoping and inserting, hinging, setting and elastic spreading (Spur & Stöferle, 1986, p. 19 ff.). Filling covers inserting of liquids, gasses, dry chemicals or compounds into interstices, which then if necessary consolidate and thereby fasten the parts, conduct heat, isolate or similar (Matthes & Riedel, 2003, p. 29).

The group of clamping and forcing contains joining by screwing, clamping, cramping, a crimp connection, tacking and impact driving, wedging and guying. So all the procedures that have the joint created by mainly elastically deforming the parts and if applicable the ancillary parts and preserve that joint by traction are gathered here (Spur & Stöferle, 1986, p. 44). Implying all screwing operations and crimp connections, this group is very important in the field of vehicle engineering. But considering only the body in white without hang on parts and closures it is not playing a decisive role.

Primary shaping as a joining technology involves having a liquid, pulpy or pasty material poured onto one or several surfaces of a part to cast a counter piece which automatically is bonded to the part. This is done by effusion, embedding, grouting or electroplating into a part (Matthes & Riedel, 2003, p. 31). Textile joining includes processes where the creation of twines, threads and nonwovens from textile fibers is involved (Hennecke & Czichos, 2008, p. L40 f.).

2.1.2. Processes Important for Automotive Body Structure Manufacturing

2.1.2.1. Joining by Forming

Non-thermal joining technologies are very common in most fields of mechanical engineering. Joining by forming, sometimes also referred to as mechanical joining, is one of them, characterizing a permanent connection whereat at least one part or a fastener, which is an additional part required for the bond, is plastically deformed. The first subgroup contains forming of filamentary bodies which is not applied on BIW (Spur & Stöferle, 1986, p. 78 ff.). Concerning sheet and sectional metals and tubes there are procedures without fasteners, so that only the work piece or pieces are deformed, which among others include hemming, crimping, clinching, notching and center punching, joining by expanding, joining by flanging, coiling, lock forming and spread forming. Creating the bond with fasteners can be achieved by only deforming the parts, the fasteners or the fasteners and the parts. The first case includes punch riveting, riveting by transforming spigots and joining by flow drilling screws. Distorting only the fastener includes blind riveting, riveting with full rivets, riveting with hollow rivets and locking ring bolt. The latter case contains self-pierce riveting, joining by pressing and joining by squeezing (Grote & Antonsson, 2009, p. 687 f.).

2.1.2.1.1. Joining by Forming without Fasteners

With hemming and crimping overlapped edges are bend in conjunction to create a form and force closure. Crimping thereby refers to the bonding by contracting of curved sheet metals such as certain containers, barrels and tube ends, while hemming is applied if the part is flat along the joining seam. For those processes the parts do not need to be prepared, so it can be divided into three

steps: adjusting, whereat the flanges are bend to a hemmable respectively crimpable angle, hemming or crimping itself, what may need more than one run, and redressing, which assures the joint by further plastically deformation. Therefore at least one of the part materials needs to be capable of large plastic deformation (Grote & Antonsson, 2009, p. 688 f.). Since the bonding is achieved on a macro level a lot of different materials can be joined together, which in general holds for joining by forming.

Another method of joining by forming without fasteners is clinching. A punch is pressing the so called punch-side piece into the die-side piece creating a mechanical interlocking by plastically deformation of the two parts. Because there is a die acting as a counterpart to the punch ensuring the correct shape of deformation, clinching requires double-sided accessibility. The materials used need to provide even more deformability than for hemming or crimping, which applies to all parts involved in the bond. The process can also be carried out joining more than two parts (Grote & Antonsson, 2009, p. 689 ff.).

Notching and center punching mainly refers to the bonding of two parts. Thereby one part is inserted into another part, which then is subject to a punctiform or linear plastically deformation to make the joint last. Expanding refers to a similar process, but here the inner part is expanded to achieve a form or a force closure. Joining by flanging shows more similarity to crimping again. The skirt of one part is shaped to create a form closure with the other part. Completely wrapping a strap shaped part around another part to create a bond is referred to as coiling (Matthes & Riedel, 2003, p. 34 f.). Lock forming is achieved by bending or twisting the edges of two parts to create a positive locking while spread forming only plastically deforms one of the parts by fitting it into an excavation of the other part (Lange, 1993, p. 292 p.).

2.1.2.1.2. Joining by Forming with Fasteners

As mentioned above obtaining the bond by the deformation of a fastener includes among others all the riveting processes. Blind riveting only deforms the fastener and has the main advantage of only requiring single-side access. The rivet is inserted into a hole in the two parts lying on top of each other followed by the inside mandrel being dragged out and then broken off. This distorts the not accessible end of the rivet in a way that a form and force closure is created (Matthes & Riedel, 2003, p. 37). The only prerequisite is that both parts have to have a hole at the bonding location; there is no other preparation required and many material combinations as well as a large range of thicknesses can be joined. The materials of the rivet itself are chosen according to corrosion aspects, connection strength and costs from a selection of aluminums, steels, nickels and coppers. Before the blind riveting process was introduced almost 200 years ago full rivets were common, which require double-sided access (Grote & Antonsson, 2009, p. 693 f.). Those deform the rivet with a die from the opposite site where the rivet is inserted.

Using hollow rivets also requires double-sided access. The main difference separating it from full rivets is that it does not seal the prepunched holes (Klemens & Hahn, 1994). Characterized by similar properties as a screw joint the locking ring bolt is a special kind of rivet. But here the preload is preserved permanently which makes the connection vibration resistant. Due to the high strength capability of the bolt itself the connection is also suitable for high strength connections (Grote & Antonsson, 2009, p. 695 f.).

Other rivet connections are also deforming the parts to be joined. This holds for example for procedures, which are creating the hole right with the riveting process. Applying self-pierce riveting the parts do not have to be pierced in advance, since the rivet itself creates the holes in the work pieces. By being stamped into the work pieces it shapes those and is plastically spread itself so a connection is achieved (Matthes & Riedel, 2003, p. 37). This requires double-sided access. The non-riveting procedures in this category include the inspirable methods pressing and squeezing. Those are most commonly used on joining ropes and similar work pieces or attaching ferrules onto those.
As indicated above there are also methods which only distort the work pieces, but not the fastener. Flow drill screwing refers to a bond, which is created by drilling a screw through the raw work pieces and thereby creating the hole as well as cutting the thread into it. Being very similar to self-pierce riveting punch riveting is a rivet application in this group. The rivet is blanking a hole into the work pieces and having the ejection direction facing piece clamped onto it without being deformed itself. A benefit of this procedure is the light impact on the work pieces surfaces, which makes it very suitable for coated parts (Grote & Antonsson, 2009, p. 393 f.). To attach a pin to a work piece riveting by transforming spigots is applied. The rivet with the attached pin is pressed in a prepierced whole of the work piece (Klemens & Hahn, 1994).

2.1.2.2. Soldering and Brazing

Classified as thermal procedures, soldering and brazing are not only applied to join parts, but also to coat them. This is achieved by creating a liquid phase between the parts or on the surface of the one part. Besides mechanical applications soldering is the most important joining technology in electric engineering. The range of operating temperature splits the group of soldering and brazing into three subgroups. If the liquidus temperature, which is the temperature where all phases of the solder are completely molten, is in the scope below *450°C*, the process is called soldering. Temperatures in the interval between *450°C* and *900°C* are characteristic for brazing, while a brazing solder temperature of more than *900°C* refers to high-temperature brazing.
The main difference between soldering respectively brazing and welding is the lower temperature. With soldering and brazing the solidus temperature of the material of the parts is not reached, instead either there is only diffusion taking place at their boundary layers, or an added solder is melting, having much lower solidus and liquidus temperatures than and being not of the same kind as the main materials. The established connection is firmly bonded and of a chemical type, creating a new crystal lattice either from diffused material or solder (Matthes & Riedel, 2003, p. 94 ff.).

2.1.2.2.1. Soldering

Soldering usually uses solder which contains zinc, tin or lead (Spur & Stöferle, 1986, p. 408) and is divided into five subcategories. Applying solder onto a part with the help of a rotating roll is called soldering by solid bodies. Soldering by liquids refers to all procedures, which have the part to be covered with solder or the parts, which are to be joined by soldering, come into direct contact with the soldering bath. Some methods have the solid solder and the parts brought into position and then melt the solder by heating up the parts by fire, having a hot air current pass by the set up or heating the assembly by convection in a gas furnace, classifying those procedures as soldering by gas. Soldering by ray refers to the required soldering heat being created by a non coherent light beam. The last soldering process is carried out by electric current. The electric power is converted to soldering heat

by induction or resistance or by convection, thermal radiation or heat conduction in an electrical furnace.

2.1.2.2.2. Brazing

The higher temperatures involving brazing processes mainly use silver-, copper-, or aluminum-based solders. Brazing by liquids, gases, rays and electric current are similar to the equivalent soldering processes. But the methods not able to create the required high operating temperature are of course excluded, while other methods like using coherent light beams or more advanced electrical furnace technologies are supplementing the category. An additional subgroup is brazing by electrical gas discharge, which contains arc brazing, an application with increasing importance to joining coated thin sheets in the automotive industry (Matthes & Riedel, 2003, p. 44 ff.).

For high temperature brazing, nickel-, copper- as well as noble metal-based solders are typical. Due to the high temperature only brazing by ray and by electrical current are applicable, similar to the previously mentioned normal brazing procedures, but carried out in a vacuum or shielding gas environment. In contrast to most soldering or brazing joints, these connections actually are capable of reaching the strength level of the base materials (Spur & Stöferle, 1986, p. 443).

2.1.2.3. Adhesive Bonding

In the automotive industry adhesive has, besides interior applications, mainly been used on outer parts, where for visual reasons no welding, especially no spot welding, could be employed. Only in the last few years and in particular for alternative materials like aluminum adhesive bonding became an option also for structural joints. It became very popular as a hybrid bonding technology in conjunction with mechanical joining or welding. For high strength steels this can increase the fatigue strength considerably. But even if the bonding is not generally combined with another joining technology, it is recommended to add another connection at the end of a bond seam, since adhesive bonding is very sensitive to peeling loads. In the field of aviation engineering adhesive bonding is crucial, also because the used sandwich technology, where different materials are united to form a high-strength interconnection, is relying on bonding.

According to the curing behavior adhesives are classified into physical, also known as hot melt adhesives, and chemical adhesives, which include the curing adhesives. For steel applications usually thermosets, which provide high shear strength, stiffness and durability, and thermoplastics, which show good energy absorption behavior and performance at low temperatures, are used. One-part thermosets cure due to applied heat, while two-part adhesives of course react with the cure agent (Davies, 2003, p. 183 f.). However, the curing process requires time. This needs to be considered when designing the assembly layout with adhesive bonding involved, if necessary some kind of local heating must be applied to accelerate the curing process (Morello, et al., 2011, p. 138 f.).

2.1.2.4. Welding Processes

Since decades welding has been the dominating joining technology when it comes to automotive body structures. This doubtless is mainly caused by the very good weld ability of steel. Joining by a matching or similar continuity is in general often technically and economically advantageous. Since welding is such a very popular method there are more than one hundred different processes.

Up to date most mass production welding operations are completely automated, which makes them highly reliable and reproducible processes. Compared to soldering, brazing, adhesive bonding and specific mechanical joints, welding benefits from the usually larger strength of the connection (especially at high temperatures), the larger tolerances at the joint, the lower requirements on the purity of the surfaces and the similarity between the seam and the part material. This leads to a decreased tendency to corrosion compared to soldering, brazing and specific mechanical joints. Also welding is not subject to ageing phenomena, as adhesive bonding is.

According to DIN 1910 T1 welding is joining of substances in the weld zone by the application of heat and/or a force and optionally adding filler metal. Welding consumables like shielding gas, welding flux or welding paste may be utilized to enable or alleviate the process. This standard also classifies welding after the energy transfer medium, the work piece parent material, the purpose of the welding, the physical sequence of the process and the kind of manufacturing.

Referring to the energy transfer medium one can distinguish between welding through a solid body, by liquid, by gas, by electrical gas discharge, by beam, by motion or by electrical current. The weldable parent materials are metals, plastics and other materials like graphite, ceramics and material combinations. For the purpose there are two categories, joint welding and built-up welding. Joint welding is of course referring to the joining of one or more work pieces and thereby the kind to be focused in this study. Built-up welding is applied to coat a work piece, increasing the wear resistance or suppressing chemical reactions for example (Spur & Stöferle, 1986, p. 143 f.). Breaking down the procedures with respect to manufacturing one comes by manual welding, partly or fully mechanized welding and automatic welding. The physical sequence allows dividing the methods into fusion welding and pressure welding. This is the basis for the most used classification in practice, regulated in DIN ISO standard 857-1 (Zeissler, 2011, p. 7).

2.1.2.4.1. Pressure Welding

If there is no filler material added and the weld is obtained by applying pressure and if applicable regional heat the process is referred to as pressure welding (Zeissler, 2011, p. 9). The group of pressure welding of course contains many subgroups. The most important ones are briefly described in the following.

Diffusion welding is also referred to as welding in a solid state. The surfaces need to be cleaned and polished to be joined in the vacuum by pressure and temperature, which creates a diffusion connection. This costly procedure is applied, if dissimilar materials need to be joined without activating a microstructural transformation. If the materials are too different, interlayers usually made from nickel, copper or vanadium are added.

By high compacting pressure cold pressure welding initiates deformation of the surfaces to be joined. The bond between similar or dissimilar materials is created by reducing the distance between the surfaces to an atomic level and thereby creating transposition activity as well as cohesion and adhesion attractions.

Destroying the surface layers of the parts by supersonic vibration ultrasonic welding creates a punctual connection by deforming the surface while facing a very short and locally restricted heat input. The vibration energy is applied in the contact surface plane while the overlapping pieces of the part are compressed (Dilthey, 2006, p. 265 ff.).

Similar to this also friction welding creates the required temperature by friction, as the name indicates. Usually this method is applied to axially symmetric work pieces. So the surfaces to be bonded are compressed and one part is set to rotation to heat-up the connection area. This process is used on pipes or shafts, especially hollow shafts can be economically produced like this (Koether & Rau, 2007, p. 206).

A method applied since ancient times is forge welding, whereat the faying surface gets free formed, swaged or driven through after being heated up in the fire (Matthes & Riedel, 2003, p. 38). A similar process but much more modern is gas pressure welding. Heat is introduced to the ends of the work pieces by high performance gas burners so that the joining surfaces are heated up to their melting point. Then the pieces get butt joint compressed, mostly by a hydraulic created force. The shape of the gas burner must match the shape of the bond surfaces. Due to the compact layout of the apparatus this technique is for example popular on construction sites (Dilthey, 2006, p. 113 f.).

Arc pressure welding differs from this by using not a gas burner, but an electric arc to briefly induce heat into the contact surfaces before compressing them. Another way of heating-up the part section to be joined is applied by cast pressure welding which has the part ends encapsulated by a liquid energy transfer medium in a mold (Matthes & Riedel, 2003, p. 38 f.).

For the body structure and thereby for this study the most important subgroup is resistance welding. In general with resistance welding the parts to be joined are compressed between two electrodes. Through those a current is introduced to the work pieces and due to the ohmic resistance at the boundary between the parts heat is generated which locally melts the material. The subgroup contains the crucial process of resistance spot welding, whereat electrode holders create a punctual bond. This is described in depth in a chapter below.

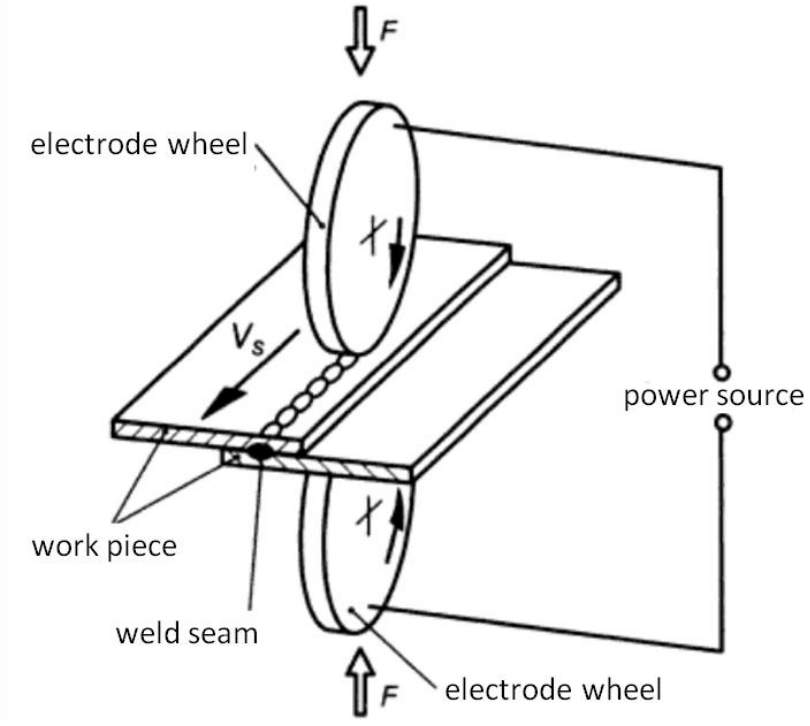

Figure 3 **Process of resistance seam welding (Koether & Rau, 2007, p. 207)**

Another operation of this subgroup is resistance seam welding. Hereby a pair of wheels, which are usually made of a copper alloy and cooled with water, compresses the parts and also functions as the electrodes. The wheels are turning with a specified speed creating a line of weld points with a particular distance (see *Figure 3*). This way sealing seams and with special filler material also butt joints can be created. Other advantages compared to spot welding are the higher weld speed, since no adjustment and no closing travel of the holders is required, and the reduced wear of the wheels compared to the spot welding electrodes. This makes the process capable of mass production applications, e. g. for the manufacturing of fuel tanks, silencers, suspension bars and pipes. However the need of accessibility on a grand scale keeps it from being used to a great extend at the body structure.

Large-area electrodes are used for resistance projection welding. Those plates compress the metal sheets to be welded, of which one has knolls formed into it. Where those knolls are in touch with the other part the welding does take place; in doing so the knolls get at least partly leveled and a not sealing connection is achieved. This actually is one of the most efficient resistance welding processes, but the large plate electrodes of course also require extensive accessibility.

Bonding thicker parts by creating a butt joint is done by flash butt welding. While the edges to be joined are positioned close together a current is induced into both parts creating a short-circuit between the joint surfaces and thereby heating them up. Right after, both work pieces are compressed abruptly and thereby upset and welded. A welding burr is arising which afterwards has to be removed. An automotive application of this method is the power train area (Koether & Rau, 2007, p. 204 ff.).

Similarly resistance butt welding is working, but the joint surfaces are in touch and the heat is initiated by the ohmic resistance of the part transition. Therefore both surfaces have to match exactly and be free of contaminants and oxides. Due to the usually relatively large surface area the resistance is quite low and high current is required. Once the desired temperature is obtained the current is shut off and the upset pressure of the parts is increased which creates the characteristic flaring at the joint patch (Dilthey, 2006, p. 114 f.).

2.1.2.4.2. Fusion Welding

Creating the bond by a localized melt flow, usually adding filler material, without applying any external forces is called fusion welding (Zeissler, 2011, p. 15). With most of these processes an open weld pool at the welding location is generated which is very sensitive to the ambient environment, i.e. the circumjacent atmosphere. A proper insulation of the weld pool from air admission is crucial to prevent absorption of gases from the environment which would lead to oxidization and thereby to a porous weld.

Fusion welding also is sectioned into several subgroups. One of them is gas welding, also known as autogenous welding. Usually applied as a manual method the weld pool is created by the combustion of an acetylene oxygen mixture at the weld seam, into which typically also filler material is fed (Spur & Stöferle, 1986, p. 243).

As the name indicates, manual arc welding also is a manual application, but here the welding is initiated by a current. Nowadays only covered rod electrodes are used, which consist of a metallic core rod and a mineral cladding and also serve as the filler material. While the part is connected to one electric pole, the rod electrode is connected to the other. To ignite the arc the rod is brought to rest

on the part and is then slightly lifted, which causes a strike ignition. The mineral cover of the rod electrode becomes dross which gets to rest on top of the seam weld and thereby shields it (Dilthey, 2006, p. 11 f.).

Another way to protect the seam weld from oxidations is the application of shielding gas. Many kinds of gases can be used, like argon, helium or carbon dioxide; they are conveyed to the welding location by the welding torch. There are two kinds of gas-shielded arc welding depending on the kind of electrode used. If the fed wire functions as the filler material and as the electrode, one alludes to gas-shielded metal-arc welding, see *Figure 4*. Depending on which of the gases mentioned above is used, one refers to metal inert gas (MIG) welding or metal active gas (MAG) welding. Due to the open weld pool the welding torch is exposed to very high temperatures. So except for very small welding currents the torch needs to be water-cooled. The arc is ignited by a short-circuit, which usually causes spillings. This only can be prevented by special control mechanisms of the welding current (Dilthey, 2006, p. 61 ff.).

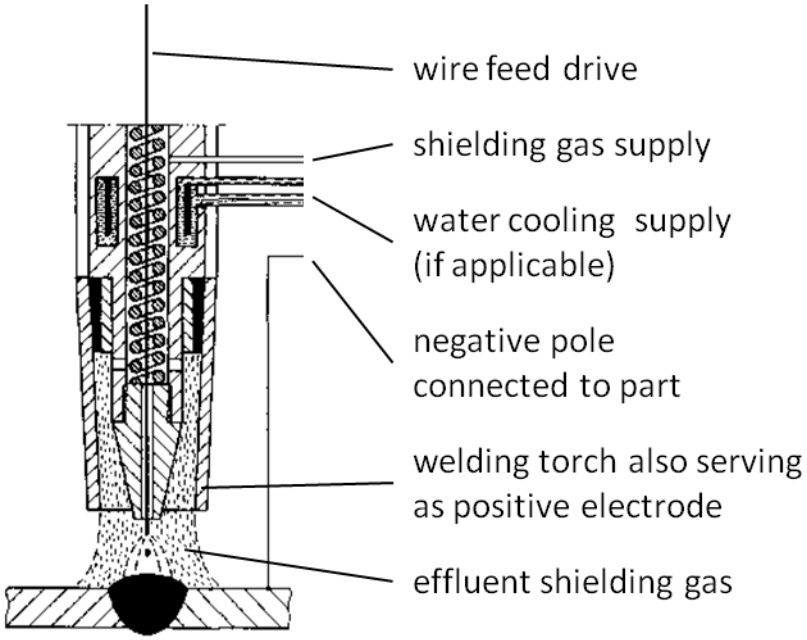

Figure 4 **Gas-shielded metal-arc welding (Dilthey, 2006, p. 63)**

The other kind of gas-shielded arc welding is called tungsten inert gas welding. Since the peaked tungsten electrode is not melting filler material is fed separately from the welding torch, if applicable, as shown in *Figure 5*. Generally the electrode does not get in touch with the part, but the ignition of the arc is produced by a short circuit originating in high-frequency high-voltage pulses. Also here for high welding currents water cooling is installed and the well heat conducting tip is made of copper. Most materials are welded with direct current. Then again interchanging the poles to plus on the electrode can help destroying the bothersome oxide film when welding aluminum or magnesium alloys, but the welding performance itself then fades. So some materials are welded with alternating current (Dilthey, 2006, p. 43 ff.). Usually there are the same inert gases applied as for gas-shielded metal-arc welding.

An outlier is tungsten plasma arc welding, were the regular gas is made conductive by introducing electrical energy with the help of an arc. This helps to create a more stable, definite and energy dense welding arc (Koether & Rau, 2007, p. 200).

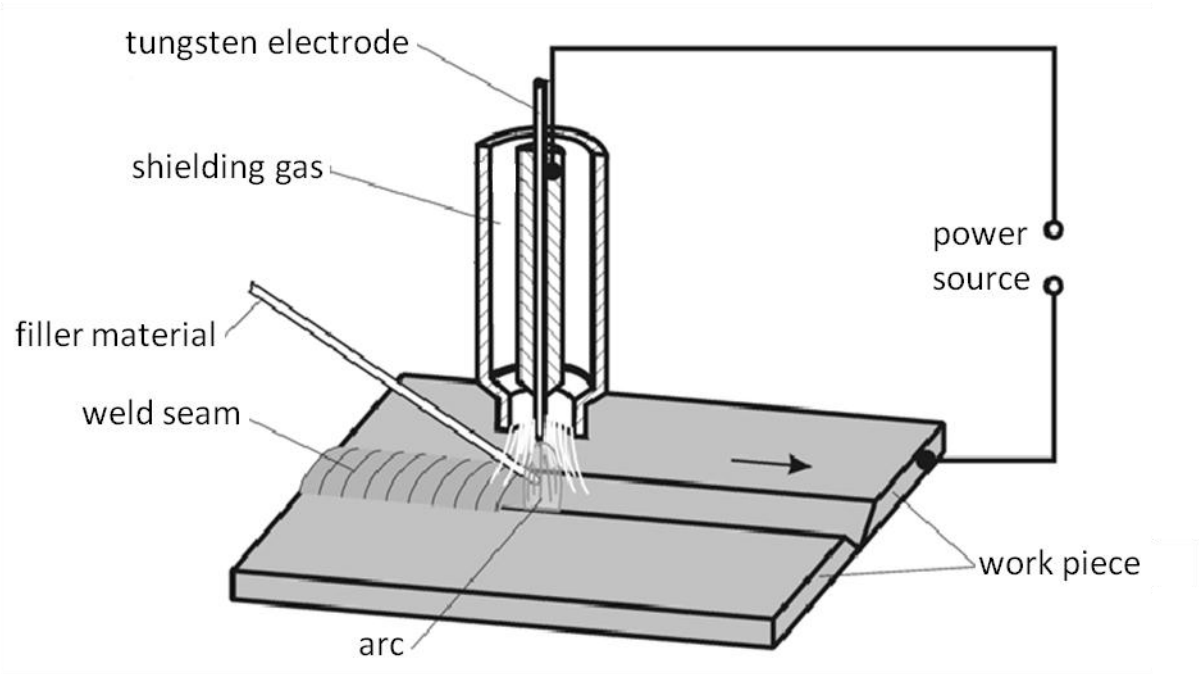

Figure 5 **Tungsten inert gas welding (Dilthey, 2006, p. 44)**

As known from other methods the ignition for submerged arc welding is either caused by a short tangency of the electrode and the part or a high-voltage pulse. Also concerning the kind of current this method is versatile; either direct or alternating current can be used. The specialty of this process is the insulation of the weld pool by a specific welding flux. The flux is applied on the seam weld right before the welding torch passes it. The electrode continuously runs inside the flux so that the arc is not visible but covered by flux. This creates a cavern which is filled with vaporized base material and flux and margined by the weld pool to its bottom and by dross on the top side (Dilthey, 2006, p. 33 f.).

Resistance fusion welding processes are similar; dross similar to the mentioned flux is involved, which usually is one of the resistance causing elements to introduce the weld heat. One procedure of this family is electro slag welding, where the dross is supported and formed by cooled cooper brackets (Grote & Feldhusen, 2011, p. G3).

For this study the most relevant subgroup of fusion welding is laser beam welding, which is described in detail in chapter 2.2.2. This technique uses a bundled light beam to induce heat into the work pieces and thereby creating a weld pool. Another kind of beam welding is electron-beam welding. But since this technique is only applicable in the vacuum it is hardly manageable and rarely applied in mass production (Koether & Rau, 2007, p. 200 ff.).

2.2. Joining Processes Investigated in This Study

In this chapter the joining processes which are compared in this thesis work are described in a higher level of detail. Since the study refers to a mass production vehicle and thereby the body structure's material is steel only the application of the joining technologies on this material will be discussed. The regular sheet metals used on today's body structures are zinc coated to provide a better corrosion resistance. This also is an aspect which needs to be considered describing joining technologies.

2.2.1. Resistance Spot Welding

2.2.1.1. Process

Being the most widely used example of lap joining processes resistance spot welding is a highly developed BIW manufacturing operation perfectly adapted for the use in mass production due to the short weld time achievable and the good eligibility for automation and robotic techniques. Belonging to the group of pressure welding the electrodes of the spot weld gun impact the parts to be joined with a high force, of which the magnitude is one of the crucial spot welding parameters. The electrodes are made of either precipitationed strengthened copper-chromium and / or zirconium alloy or a dispersion strengthened copper alumina system and have to be exchanged after a certain amount of welds. A typical BIW of a mass production car nowadays contains about 5000 spot welds. Their quality is a key criterion for the NVH behavior and the strength of the body structure (Davies, 2003, p. 171 f.).

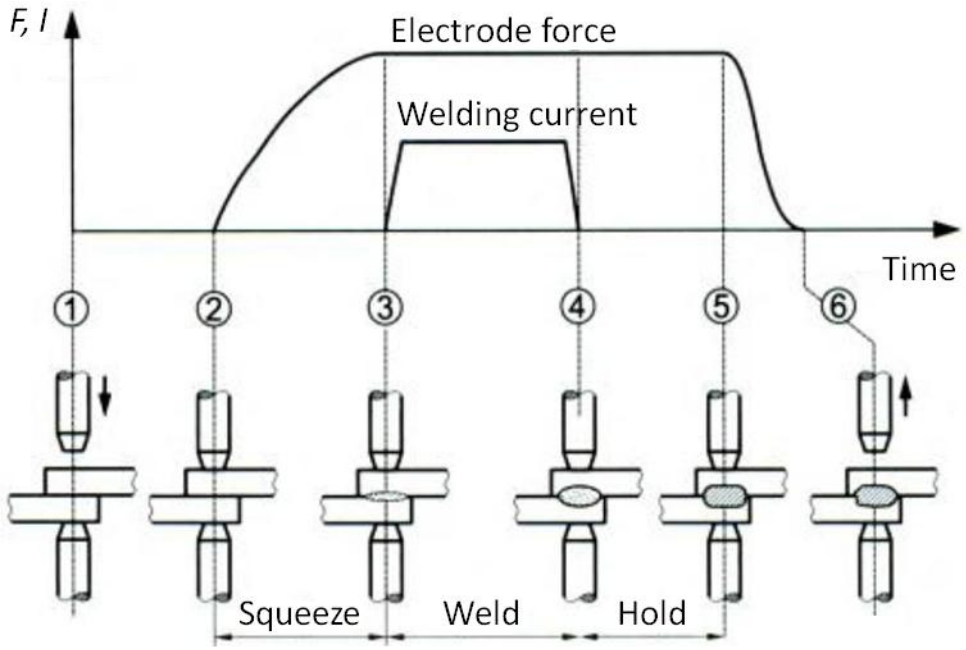

Figure 6 **Cycle of resistance spot welding (Koether & Rau, 2007, p. 205)**

The pure welding time usually is in the range of *0.1* to *0.4* seconds, whilst the water cooled electrodes apply a welding current of *5* to *25 kA* creating a lentoid spot connection (Zeissler, 2011, p. 12). The squeeze time and the hold time are two other important weld parameters. The whole cycle

of creating a spot weld is shown in *Figure 6*. The squeeze phase serves to overcome a poor fitting of the parts due to a rough surface or other reasons and has about the same length for coated and uncoated steels. During the weld phase the actual connection is created, demanding a higher weld current and a longer weld time for zinc-coated steels compared to not coated steels. Afterwards the electrode force is kept up for a specified hold time to ensure the consolidation of the weld. All this adds up to an approximate welding time of about *3* seconds per spot, of course depending on the different welding parameters.

The spacing between two spot welds is usually *30* to *100 mm*. One of the restrictions for the minimum spacing is the quality of the weld nugget. As displayed in *Figure 7* with too close positioned spot welds there is a shunt established through the previously created spot weld. This reduces the current flow right between the electrodes so that the heat input decreases. At which distance the risk of a shunt occurs depends on the weld parameters, the sheet's coating and thicknesses. The mentioned upper limit only guarantees sufficient strength in combination with adhesive bonding. In practice the spacing averages to about *40 mm* for solely spot welding.

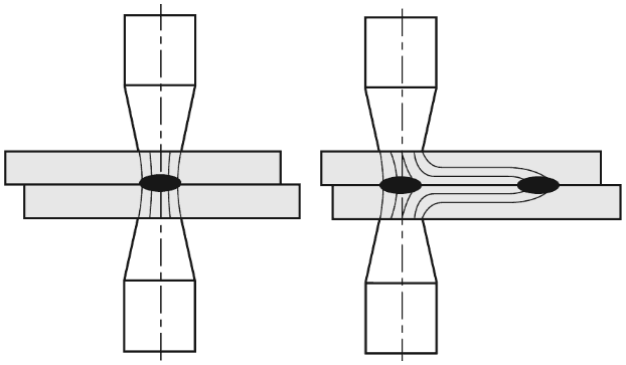

Figure 7 **Desired current flow (left) and current flow with shunt (right) (Fritz & Schulze, 2010, p. 202)**

Nowadays it also is common to apply resistance spot welding of three thicknesses (3T) in mass production. If the weld parameters are adapted carefully a satisfying process stability can be achieved, creating the two weld nuggets at the two interfaces at a time.

2.2.1.2. Limits

An electrode force chosen too large, a too high weld current or a too long weld time can cause splash and expulsion from the weld interface, having the weld pool leaking out between the metal sheets or braking through the outer surface of a sheet. On the other hand, if one of those factors is too small respectively too short, the nugget diameter will be too small and the strength of the connection too low. The minimum diameter for the nugget should be $d_{min} = 3.5 \cdot \sqrt{t}$, where t is the single sheet thickness. If this diameter is not reached, there may is a bond created between the sheets without creating a real weld nugget, which is referred to as stuck weld condition. Another kind of failure is called electrode sticking, at which a bond between an electrode and a sheet is created (Davies, 2003, p. 173 f.).

The acceptable ranges of electrode force, weld time and weld current, which allow the generation of a proper spot weld, form a window referred to as weld lobe. The size of this lobe is an indicator for

the weldability of the material and thickness configuration. A larger lobe allows larger tolerances to the parameters. The tolerance for the weld current depends on the basic resistance of the steel welded, its coating and the thicknesses.

Apart from the differing weld parameters resistance spot welding of zinc-coated sheets mainly is a challenge for the process reliability. While for uncoated sheets over *10 000* spots can be created with one electrode, for zinc-coated steels the limit is usually below *3 000*. If the diameter of the weld nugget decreases below the previously specified value the electrodes need to be replaced. Moreover the mentioned figures show a great spread for welding of zinc-coated steels. The variations between electrode life tests may be up to *100 %*. Besides this the electrode life in general is dependent on a large amount of factors, such as the electrode shape and material, the weld parameters and the sheet's thicknesses and materials (Davies, 2003, p. 174 f.).

Electrode failure primarily is caused by the welding heat softening the electrode, the reaction of the zinc coating with the electrode copper forming brasses at its tip or the deformation of the electrode tip leading to a diminished contact patch and thereby a decreased current density and surface damage to the electrode tip. Depending on the coating type one of those issues will be decisive; in general zinc and iron-zinc alloy coatings are preferable regarding electrode life compared to hot-dip equivalents. To respond to the electrode wear adaptive weld current controls were introduced increasing the weld current at predetermined intervals. Preferential the electrode replacement takes place during the shift change. But due to the hardly predictable electrode life time for spot welding of zinc-coated sheets a backup solution for electrode failure is required (Davies, 2003, p. 175 f.). A solution for this could be an electrode tray right at the weld gun.

For high strength steels the process is not much different than for mild steels. Only some parameters like the weld current may be a bit lower due to the higher resistance caused by the alloying additions. The electrode force will have to be increased, also due to the more pronounced spring back behavior of high strength steels. But all this can be handled quite well by now which is essential for a mass production process. Stainless steel as well needs adjusted parameters to be welded and displays decreased process stability. Welding different thickness combinations actually becomes simplified compared to mild steels due to the higher resistance of the stainless steel.

The fatigue performance of the spot welds is not improved by high strength steels. By fatigue failure being caused by the notch effect of the weld the base material strength is not the key criterion (Davies, 2003, p. 177 f.).

2.2.2. Laser Beam Welding

The laser technology is applied by quite a lot of manufacturing processes in mechanical engineering. Besides the welding discussed here there is cutting by laser beam and the heat treatment of surfaces. Together with the electron beam the laser beam is one of the most power-dense techniques available today and referred to as high-energy-density processing. Due to the high energy input with all those methods evaporation of material takes place (Steen & Mazumder, 2010, p. 199).

Many voices proclaim a bright future for laser beam welding. In 1995 a Japanese study suggested that *25 %* of the industrial weld operations could be carried out by laser welding. At that time the laser actually was applied for only *0.5 %* (Steen & Mazumder, 2010, p. 201 f.). Though this figure certainly has increased by now there still is a lot of potential. Tailored blanks for example are made

almost only by laser welding today. And also other applications on the vehicle's body structure have been established.

Since noncontact joining is possible with laser applications it has a large potential in matters of automation and high processing speed. Extensive research has made laser beam welding capable to weld thicker sheets and improve its weld quality. However, it is still a challenge to make defect-free welds at high speeds and to achieve a high level of process reliability. But since there still is a lot of research dealing with laser welding, continuous progress is made making the process more and more available for mass production (Dahotre & Harimkar, 2008, p. 412).

To apply laser welding, the laser (Light amplification by stimulated emission of radiation) beam is becoming focused and redirected to the weld seam by a lens system containing mirrors, lenses and optical fibers (see *Figure 8*). The radiation being absorbed by the work piece is inducing the heat into the part, which then spreads by conduction (Grote & Antonsson, 2009, p. 668). Since the beam is highly concentrated very narrow seams can be welded which limits the heat impact into the work piece.

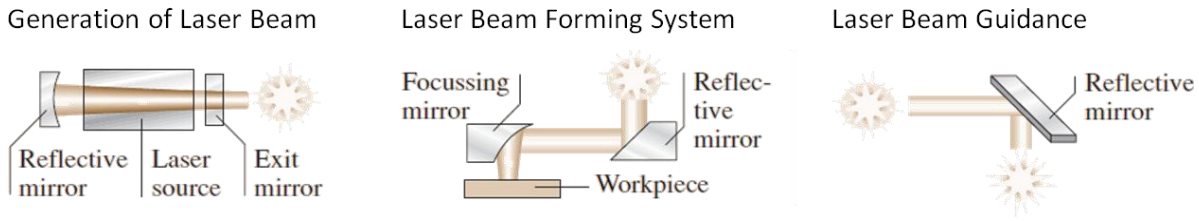

Figure 8 **Laser beam creation and direction (Grote & Antonsson, 2009, p. 654)**

2.2.2.1. Process

There are two modes of operation for laser welding as shown in *Figure 9*. A threshold intensity characteristic for the material, also referred to as critical intensity, divides the process into a lower region also called conduction welding, where the surface of the weld pool remains smooth, and an upper region, which is referred to as deep penetration welding and reached if a so called keyhole is created. This is the characteristic operation mode for laser welding achieving a high joining efficiency by obtaining a proportionally large penetration compared to the laser seam width.

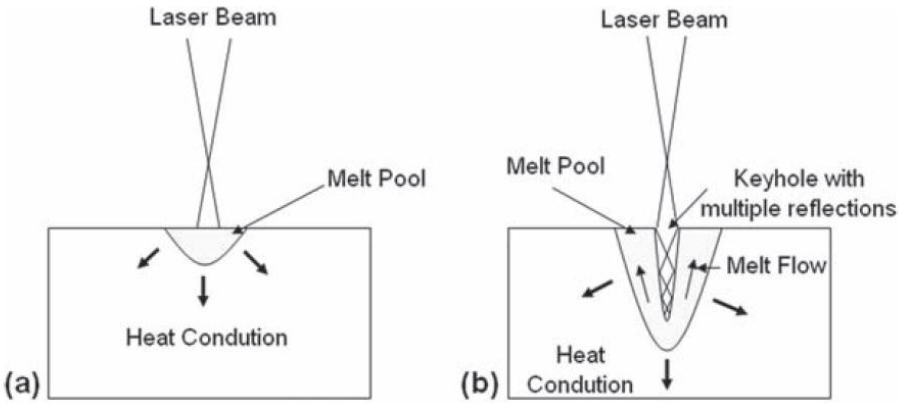

Figure 9 **The two laser welding modes of operation: conduction welding (a) and deep penetration welding (b) (Dahotre & Harimkar, 2008, p. 413)**

By introducing the energy beam perpendicular into the material the heat invades the sheet almost one-dimensional up to the interface of the sheets to be joined, instead of inducing a lot of heat in the surrounding area of the weld, which is a very efficient application of the welding energy. Another advantage is the arising relatively small heat affected zone (HAZ) (Steen & Mazumder, 2010, p. 200). Due to the heat impact the HAZ shows worse properties than the base material and the weld itself, which is why it needs to be avoided if possible.

The highly dense heat input will lead to exceeding the material's capability of dissipation, which causes vaporization of the base material and creates a metal plasma cloud when the vapor becomes ionized by the laser beam (see *Figure 10*), minimizing the laser beam reflection at the part's surface. Further thereby the typical keyhole is created; a lean, tubular opening filled with metal vapor allowing the laser beam to further invade the work piece (Spur & Stöferle, 1986, p. 295 f.). The keyhole is rapidly changing its shape and pulsing in size. It is stabilized by the pressure generated from the vapor. The melt pool surrounding the keyhole contains vortices in front of and behind the keyhole. Humps on the front keyhole surface will be evaporated abruptly, setting the keyhole to an oscillating motion and thereby increasing the risk of porosity. This calls for a smooth surface to obtain a stable keyhole.

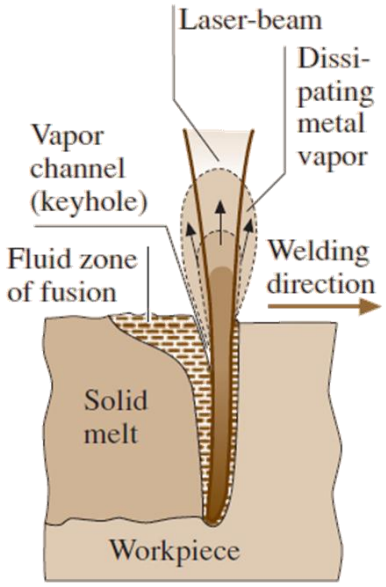

Figure 10 **Deep penetration laser welding creating keyhole and metal plasma cloud (Grote & Antonsson, 2009, p. 668)**

The not directly absorbed parts of the laser radiation become reflected several times inside the emerging plasma plume in the keyhole which leads to a higher total absorption of the laser beam. This makes the absorption behavior of the laser beam and base material combination become less important. Once the keyhole is created the absorption of the laser beam jumps from *3 %* to *98 %*. So there is a lot of energy input required to create the keyhole, but once it is established the required energy decreases dramatically. On the one hand side this is the desirable state of very high efficiency welding, but on the other hand side the transition needs very advanced controlling technology and the risk of damaging the weld structure is high (Steen & Mazumder, 2010, p. 203 f.).

Figure 11 shows the cross section of the weld pool at a laser weld speed of *50 mm/s* with *z = 0* representing the work piece surface and *x = 0* the laser beam center. The left picture displays the position of the approximately *0.4 mm* width laser beam in the weld pool, indicating that due to the welding speed the beam is not only eccentric to the weld pool but also to the keyhole it is creating. The other illustration shows the different levels of the plasma absorption coefficient in the key hole. Most of the radiation is absorbed close to the keyhole wall, but not right next to it. Due to its importance for the welding operation the stability of the key whole has a large impact on the welding speed (Dahotre & Harimkar, 2008, p. 12 ff.).

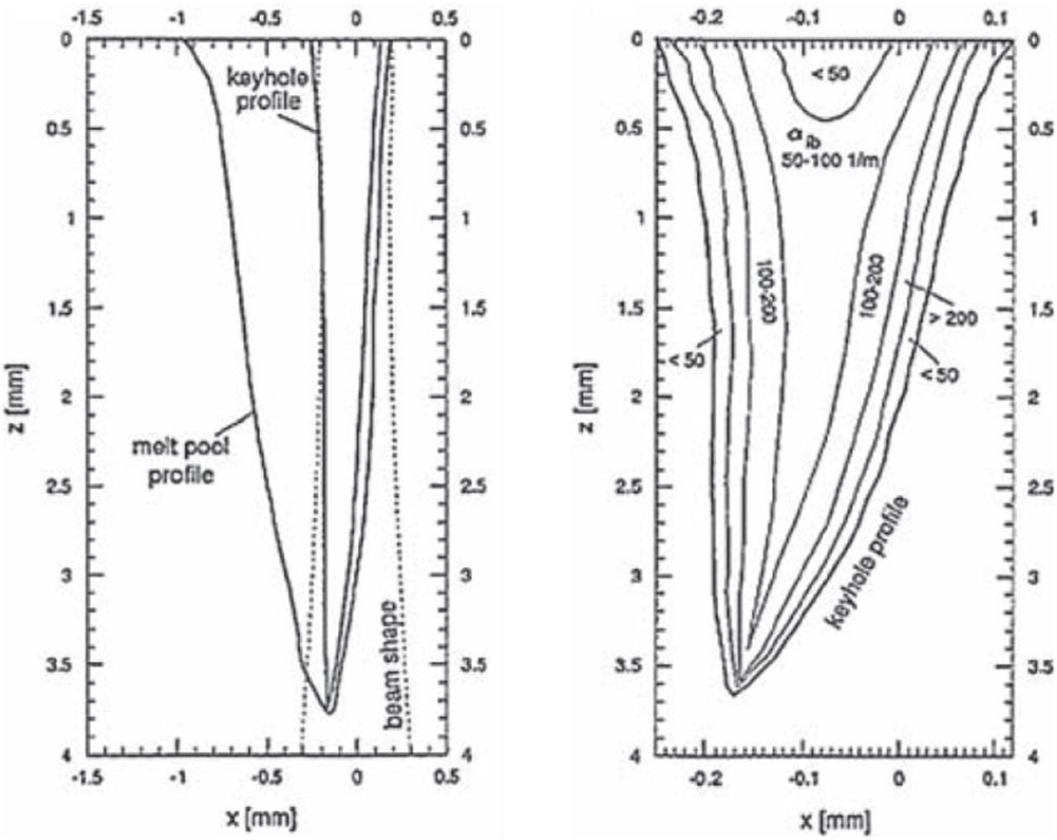

Figure 11 **Calculated melt pool cross section including keyhole (left) and scale-up of keyhole with plasma absorption coefficient contour lines (Dahotre & Harimkar, 2008, p. 422)**

Due to the rapid vaporization in the keyhole vapor is blasting out with very high speeds. Not ionized vapor thereby has a temperature of about *2000 °C* while for the plasma up to *10 000 °C* have been measured. If the plasma is close to the sheet's surface or inside the keyhole it actually is supporting the absorption of the laser beam. But a thick plasma cloud standing above the surface does not only shield the weld pool, but also absorbs and scatters the laser radiation for certain applications (Steen & Mazumder, 2010, p. 225 f.). The electrons of the plasma absorb photons, so the attenuation of the beam is also dependant on the number of electrons and thereby of the plasma temperature. Another source of irritation is the turbulence of the plasma cloud, which causes density variability and thereby has the plasma acting like a lens defocusing the beam. Also the plasma cloud will contain particles and condensate which scatter the beam. So regarding the plasma cloud a laser with a

shorter wavelength is to be preferred, since it creates cooler and less absorbent plasma (Steen & Mazumder, 2010, p. 215 f.).

To obtain an efficient welding procedure there may be shielding gases applied to blow away the plasma cloud (Dahotre & Harimkar, 2008, p. 435 f.). Another function of the supplied gas would be the protection and the cooling of the lense (Spur & Stöferle, 1986, p. 294 f.). This aim obviously is inapplicable for remote laser weld guns. If shielding gas is applied while laser welding zinc-coated sheets the jet can blow the zinc loaded vapor backwards onto the weld bead which will increase the corrosion resistance of the work piece (Steen & Mazumder, 2010, p. 226).

A great advantage of laser welding is the possibility to divide a single laser beam for using only one laser resonator to supply a number of welding stations increasing the efficiency. Moreover remote laser welding was introduced a couple of years ago being able to create a weld seam even if the laser gun is up to *400 mm* away from the work piece (WorldAutoSteel, 2011, p. 478).

2.2.2.2. Laser Beam Source

Laser light is a monochromatic, i.e. containing only a very narrow band of wavelengths, coherent radiation which is able to achieve high power densities in the focal point by using a low beam divergence and focusing. The two most commonly applied laser sources are the neodymium yttrium-aluminum garnet (Nd:YAG) and the carbon dioxide (CO_2) laser with a wave length of *1.06 µm* respectively *10.6 µm*. The latter one has the radiation extracted from gaseous CO_2 and its emission wave length is best absorbed by nonmetallic materials. In contrast the Nd:YAG-laser wavelength supports a high absorption rate by the metallic base material. However, due to its more efficient laser beam creation compared to the Nd:YAG-laser the CO_2-laser also is used for metal welding applications (Spur & Stöferle, 1986, p. 293 f.). It is capable of considerable higher power outputs, up to a two digit kW range. Nd:YAG-lasers currently applied are operating with a maximum power output of about *4 kW* (Steen & Mazumder, 2010).

But then again the Nd:YAG-laser is less impacted by the occurring plasma. Other advantages are the achievable deeper penetration and higher weld speeds as well as the possibility to direct the Nd:YAG-laser beam by fiber optic (Dahotre & Harimkar, 2008, p. 433 f.).

Analyzing the focus position from a laser beam energy point of view, it would be most efficient to have it right on the sheet's surface. On the other hand a focus point at the surface will create a porous weld. That is why the focus point should be shifted *3 mm* away from the surface in either direction (Dahotre & Harimkar, 2008, p. 435).

To improve the performance of the process a pulsed beam can be used. The advantages of a high peak power, like the fast establishment of a keyhole and a greater tolerance regarding focusing, can be combined with the benefits of a moderate average power, e.g. the reduced heat input into the work piece causing less distortion. Increases in penetration of up to *60 %* have been reported with this approach. Also a possibility to control the flow in the weld pool and to reduce porosity is given (Steen & Mazumder, 2010, p. 212 ff.).

2.2.2.3. Laser Welding Three Thicknesses

Since with laser welding one sheet of material is completely molten to reach down to the interface of the two parts there only can be two layers bonded at a time. For punctual connections laser weld-

ing is not able to establish a connection between three thicknesses. For linear connections three layers can be bonded by means of a staggered pattern. As displayed in *Figure 12* the continuous laser weld line is fragmented into sections bonding alternately the lower or the upper sheet to the middle sheet. For a regular pattern the length of a single section t_l could be about *40 mm*, while the spacing between the sections t_s accounts to *5* to *10 mm*.

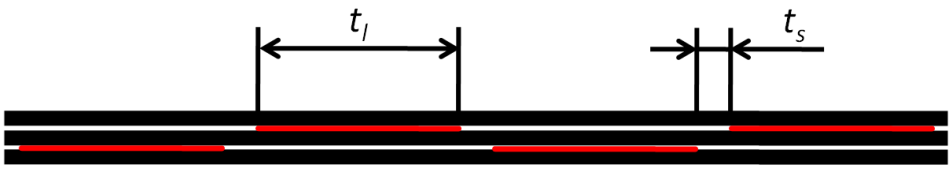

Figure 12 **Staggered pattern for 3T laser weld**

2.2.2.4. Limits for Laser Welding

The two boundary issues occurring with laser welding are the lack of penetration and the so called "dropout", which is the opposite of too little penetration so that the sheets are completely molten thoroughly and material starts to drop out from the bottom side. Similar to the weld lobe for spot welding the weld speed and the laser power create a window within it is possible to achieve an acceptable laser weld for a specific thickness and material. Usually the upper power limit is set by the laser, whose beam exhibits a poor mode structure when operated at peak power, i.e. the energy is not distributed homogeneous anymore throughout the laser beam diameter. In general a larger power level does increase the bandwidth of achievable weld speeds. The penetration is an inverse function of the weld speed for constant laser power. Also the expansion of the HAZ is an inverse root function of the welding speed, being dependant on the laser beam diameter and the thermal diffusivity of the material as well (Steen & Mazumder, 2010, p. 209 ff.).

The upper speed level is not only determined by the achievable penetration. There are also other aspects concerning the shape of the frozen weld bead involved. If the laser is moving too fast the weld pool has not time to redistribute before it is freezing which can lead to a basset in the middle of the weld beam. Also there can be pressure instabilities along the weld pool causing the so called pitch effect which indicates an irregular shape of the weld seam as displayed in *Figure 13*.

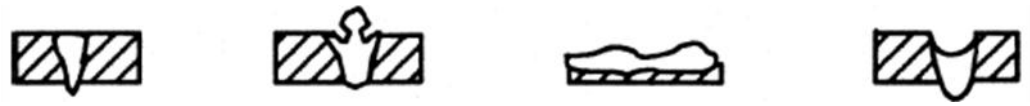

Figure 13 **Different kinds of laser weld failures: cross section of a normal seam, a seam with basset, a longitudinal section of a seam with pitch effect and a cross section of a weld with dropout (Steen & Mazumder, 2010, p. 216)**

One of the quality issues most dependant on the laser welding parameters is porosity. Towards the weld surface there is a risk of formation of small bubbles due to the inclusion of gas during solidification as with most arc welding processes. A specific laser welding issue is the generation of large voids at the bottom of the weld, if the top of the keyhole is closing and solidifying while there still is vapor below. The key to minimize those failures is the stabilization of the keyhole, which can be achieved by increasing the laser welding speed, improving the laser beam quality, increasing the

power density of the beam or optimizing the beam focusing. More elaborate measures like the application of two laser beams or filler wire were also found to reduce porosity (Dahotre & Harimkar, 2008, p. 327 ff.).

The main obstacle keeping laser beam welding from a large scale mass production application in the automotive industry are the restrictions when it comes to welding zinc-coated steel. For a lap joint the two inner zinc layers have to be demolished to create the bond as displayed in *Figure 14*. The vaporizing temperature of zinc is with *1180 K* below the melting temperature of iron, which accounts for *1811 K*. This causes the zinc layers between the overlapping sheets to vaporize before the sheet metal itself is even molten. When the top sheet eventually is liquidized blowouts relief the excited pressure creating failures in the weld seam. Expulsions of metal will ruin the surface finish and remaining vapor causes porosity of the weld seam (Davies, 2003, p. 182).

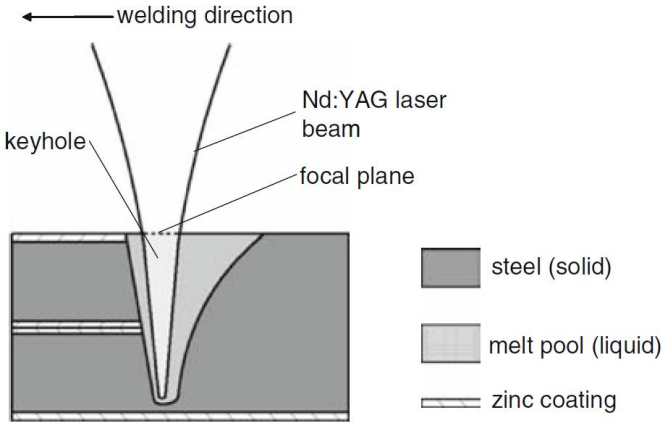

Figure 14 **Lap joint laser beam welding of zinc-coated sheets (Milberg & Trautmann, 2009, p. 10)**

To avoid this there usually is a gap introduced between the two sheets for depressurizing. This gap can be created by surface-fusing certain spots next to the weld bead on one sheet to create small elevations, which is referred to as dimpling. For better efficiency the same laser gun as for the welding itself can be used. Another possibility is to introduce the embossments by a mechanical operation. According to (Steen & Mazumder, 2010, p. 223) the required gap can be calculated as follows:

$$g_{min} \geq \frac{2t_{zn}v\rho_s}{\pi\sqrt{2\rho_v\rho_L g t_p}}$$

This indicates that the gap size is dependent on the thickness of the zinc layer t_{zn}, the welding speed v, the densities of the solid ρ_s, the liquid ρ_L and the vapor ρ_v, the gravitational acceleration g and the sheet thickness t_p. The upper limit for the gap width obviously is set by the dropout risk. There also is a theoretical power limit when it comes to welding of zinc-coated steel. Above roughly *5 kW* there is no gap value which would prevent blowouts without having to deal with dropouts (Steen & Mazumder, 2010, p. 223 f.).

2.2.2.5. Laser Welding Without Gap

Due to manufacturing efficiency the automotive industry of course is seeking a method to weld zinc-coated steels without having to provide a precisely defined gap. One of the approaches is the use of a laser beam with carefully controlled pulsed power and laser speed, whose aim it is to remove the

pores generated in one pulse by the next pulse in form a of zone refining. Another possibility is to put alloy element layers between the sheets to tie the zinc (Steen & Mazumder, 2010, p. 224), which is quite cumbersome. The American Welding Society demands to completely remove the zinc-coating of the metal sheets in the interface area if no gap is introduced. Some manufacturers even went back to abandon the zinc-coating on one side of the whole part. Also multi foci and other variations of multiple laser sources have been tried out. The approach of (Trautmann, 2009) seems to be quite promising, using bifocal hybrid laser welding with one Nd:YAG and one high power diode laser. But further research concerning the application on mass production conditions is required. In general porosity remains an issue for hybrid laser welding processes (Yang, et al., 2011, pp. 9-s).

One of the most recent studies regarding laser welding without a gap was conducted by Yang, Carlson and Kovacevic (Yang, et al., 2011). Being a very up to date paper initially some recent approaches of other researchers are discussed. One of those is the replacement of the zinc-coating by nickel-coating at the respective areas. Since nickel has a vaporization temperature of *3180 K* there is no risk of expulsions, but still some corrosion resistance provided. Of course this measure again is quite elaborate, so that the authors are looking for other opportunities.

Yang et al.'s first approach was the use of a combined welding head, which contained a fiber laser and a gas tungsten arc welding torch. The torch burns the zinc-coating at the top surface which helps to create a thin film of metal oxides and transforms the zinc-coating at the interface into zinc oxides having a higher melting point than steel. However, the authors themselves doubt the mass production capability of this technique, since the offset between the torch and the laser beam must be precisely controlled within very lean tolerances, the additional torch causes extra costs and the welding head would be very bulky.

The most recent approach, which is the main topic of the paper, puts a lot of emphasis on shielding gases. Also according to other sources those are crucial to obtain a proper weld, though their application for laser welding is mostly refused by the manufacturers. Yang et al. introduce three different approaches of shielding gas supplies. The conventional coaxial supply enwraps the laser beam. Applying shielding gas from the side is a method which was mentioned above already. It blows away the plasma from the top of the keyhole achieving an enhanced laser beam absorption by the material and provides a better ventilation of the keyhole leading to an improved removal of the zinc vapor. The side shielding gas outlet was located *10* to *20 mm* away from the laser beam focal point. The third kind of supply is the application of shielding gas on the back side of the seam, which lowers the temperature and thereby the vapor pressure in the gap. But also without this supply sound welds can be obtained, which sustains single sided accessibility, one of the key benefits of laser welding.

Also different kinds of shielding gas mixtures were researched. Pure argon and helium was used, but also blends enriched with miscellaneous shares of oxygen or carbon dioxide were used. The effect of switching from pure argon to pure helium is displayed in *Figure 15*. According to the illustrations of Yang et al. it can be observed that this is one of the measures with the largest impact due to the different ionization potentials of argon and helium leading to a much smaller plasma cloud with helium. Spatters, porosity and insufficient penetration, all clearly visible in *Figure 15 A* and *B*, could be avoided, see *Figure 15 C* and *D*. This improvement could be amplified by the application of side shielding gases and by the deliberate addition of active gases to the shielding gas mixture. Oxygen and carbon dioxide could reverse the melt flow in the pool, making the material urging inwards resulting in a deepened and enlarged key hole. On the other hand the active gases may reduce the

mechanical properties and corrosion resistance of the weld by reducing the amount of deoxidating alloys and if applicable dissociation. But due to the high laser welding speeds the time for those reactions is kept very short and they probably can be neglected. Actually the X-ray spectroscopy of Yang et al. shows no loss of alloying elements for the welds created for the study.

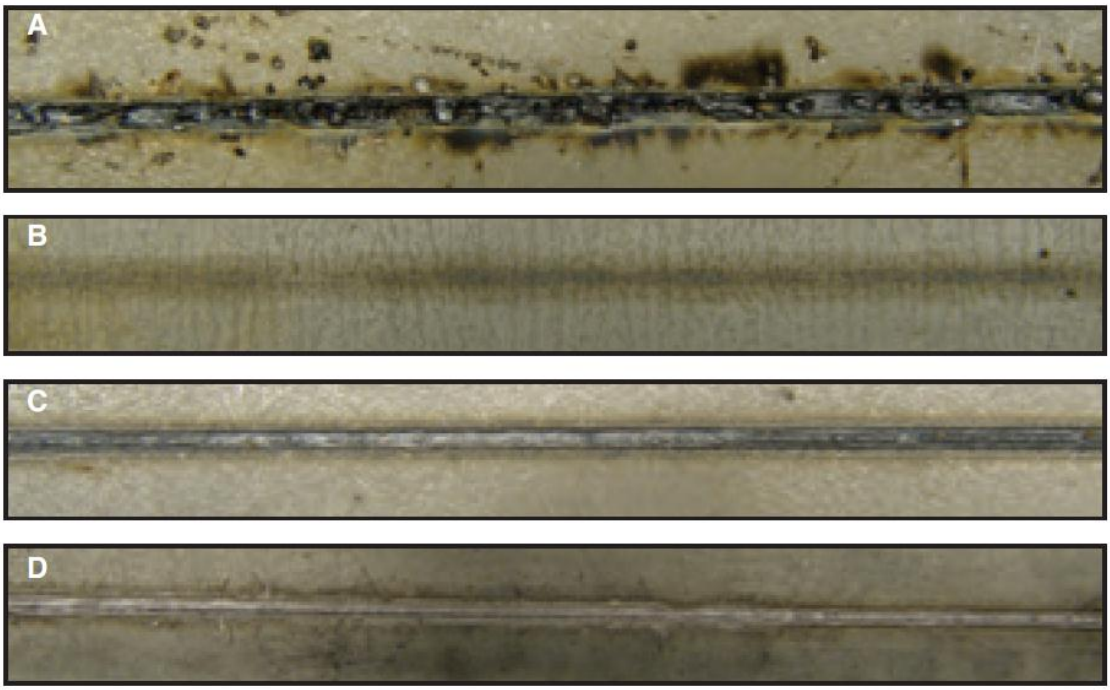

Figure 15 **Top (A/C) and bottom (B/D) view of weld without and with side shielding gas (Yang, et al., 2011, pp. 9-s)**

The sheets tightly clamped together were welded with the laser beam being focused on the top surface. On the basis of the explained shielding gas supply approaches, various combinations of those and different shielding gas mixtures Yang et al. studied the mechanisms of stabilizing the laser welding process, evaluating them with the help of different kinds of photographical tools as well as micro hardness and tensile strength tests.

The paper of Yang et al. gives a very good introduction into the topic. Giving quite detailed information about the general field and recently conducted research related to the discussed approach introduces the reader to the topic and makes it easy to come up to speed. This way it is also made possible for readers less familiar with the subject to get accessibility to it without the paper becoming too superficial. The experimental set-up and procedure are explained very well and in detail. In general also the observed effects are described well and if an approach comes with certain drawbacks, those are clearly outlined, for example the decreased mechanical properties and corrosion resistance of the weld when applying a too large share of active gases, which limits their relative portion in the mixture.

At certain stages the paper lacks of theoretical background though. Some phenomena occurring or procured in purpose could have been explained in greater detail. E.g. even if one is familiar with the details of the Marangoni effect it is not traceable how the application of active shielding gases can flip the flow pattern in the molten pool around by suddenly having raising temperatures increasing

the surface tension. The explanation for the poor weld quality when supplying the side shielding gas with too high through flows is redolent of an ad hoc hypothesis. It is arguable that the ionization due to the higher flow rate grows faster than the effect of the shielding gas blowing the plasma away. Maybe it would make more sense to right away apply helium instead of argon, since its high ionization potential is known from the previous trials. However, it is questionable if the measure introduced to dispossess the plasma cloud actually enlarges it. Concerning the modes of failure in the tensile shear tests further illustration would be valuable. Though the achieved strengths are absolutely satisfactorily, for example for spot welds a failure right at the weld interface means that the realization of the bond has failed. How a behavior like this is to be evaluated for a laser weld would need to be further explained.

Another weak point of the paper is its structure. Because a lot of procedure description, especially concerning the observation and testing procedures, which most properly would be placed within the method section, is put into the results and discussion part this chapter takes up more than half of the whole article and the results are not easy to seize. Also the sample size certainly could be enlarged, since it is quite small compared to the large number of parameters analyzed, leading to a large denominator but only a few values tested per parameter. But this is mentioned by the authors as a future scope, to look at certain parameters with a redefined step width.

The large number of testing methods like photographs, camera shooting, X-ray spectroscopy and mechanical tests allows a widespread analysis of the created welds. This way a comprehensive and differentiated overview of the properties of the weld can be obtained, though the information gained from the X-ray spectroscopy could be processed more intensely. Overall the paper of Yang et al. does not only explain a method to achieve a sound weld without the need of a gap by supplying a precisely adapted configuration and mixture of shielding gas, but also gives an invaluable overview about other research done in this field. To eventually achieve a perfect weld of zinc-coated sheets without a gap of course no exact parameters are given; those have to be determined depending on the weld configuration. Nevertheless the authors have shown that creating such a weld is feasible. Though in the abstract of the paper it actually states that the developed laser welding procedure can be *"directly applied in the industrial conditions"*, no testing of mass production capability seemed to be done. This burden still needs to be taken to establish the new method.

2.2.3. Summary

Comparing the well established joining technology of resistance spot welding to the uprising laser beam welding the former certainly is the process better known. For decades production engineers gained experience with and improved the process of spot welding. This makes it a highly reliable and efficient process. Moreover welding zinc-coated steels already has been introduced years ago and also the welding of three thicknesses is achievable without problems. The distortion of the material properties due to the firm heat input is minor. Spot welding under atmospheric conditions as well as welding of magnetic or reflective materials causes no issues. Compared to laser welding the initial costs of the equipment and the requirements regarding tolerances of the work pieces are lower (Steen & Mazumder, 2010, p. 201).

The benefits of laser welding are the high static and dynamic stiffness of the created joint, the subsistence with only single-sided accessibility, the visual quality of the seam, the weight reduction by being able to trim the flange size and the possibility to improve the structural stiffness by creating

continuous joints (Davies, 2003, p. 181 f.). The thermal impact of laser welding is even lower than for spot welding, mainly due to the narrower heat affected zone owed to the very high energy density. In addition the weld bead exhibits a much nicer finish; the application of after treatment operations makes even a usage on exterior shell parts possible. The single-sided accessibility of the laser gun itself gives more flexibility to the fixture set up and less restrictions to the structure's design. The high costs of the laser equipment can be reduced by using one laser source for up to four laser welding guns (Steen & Mazumder, 2010, p. 201). The laser beam from an Nd:YAG-source can easily be transported by fibers and thereby be time-shared as well as divided.

One of the essential advantages for laser welding is, especially for remote laser welding, the much higher welding speed. For spot welding roughly a time of *3* seconds per spot can be assumed, of course dependent on the weld parameters and configurations. If the gap between two spot welds in now assumed to be *30 mm*, the spot weld gun achieves a speed of *10 mm/s* along the flange. For laser welding the speed for average applications is around say *50 mm/s*, which is highly depending on the kind of materials, the thicknesses and other parameters. For certain configurations a speed of a couple of hundred millimeters per seconds can be achieved.

Mainly due to the much higher speed, the greater flexibility and the lower requirements regarding accessibility laser welding has become a competitive option to spot welding. If the process stability in general was increased and an approach to easily weld zinc-coated sheets proved to be mass production capable, laser welding could be applied in a large scale. Those required progresses are certainly within reach for the next few years.

3. Researched Sample Structure

The effects of the conversion from a resistance spot welded to a laser beam welded body structure were analyzed on the basis of the NHTSA light weight vehicle body structure. NHTSA is the acronym for the National Highway Traffic and Safety Administration, an American governmental organization, which commissioned EDAG, Inc. to accomplish the light weight vehicle study in cooperation with the George Washington University and Electricore, a non-profit organization developing and managing research programs (electricore.org, 2011). EDAG, Inc. is the American affiliate of the German development service provider EDAG, which employs about *130* staff members at its facility in Auburn Hills, Michigan, USA. The goal of the study was to design a concept vehicle which demonstrates that with reasonable efforts there still can be further large-scale weight savings achieved for a common mass production vehicle.

This concept vehicle is based on the American edition of the 2011 Honda Accord (see *Figure 16*), which has a curb weight of *1480 kg,* already making it one of the more lightweight vehicles in its class. The target for the overall vehicle was to reduce this weight significantly under the aspect of mass production. The NHTSA lightweight vehicle had to draw upon production technology which would allow a production volume of *200 000* vehicles per year, which also was the figure all cost calculations would be based on. The production time was assumed to be five years, which led to a complete volume of production of *1 000 000* vehicles. Other demands were that the current base line retail price of *22 730 $* should not be exceeded by more than *10 %* and the performance regarding driving and handling, safety and utility would not abate.

The production-model body structure, referring to the BIW excluding hang on parts and closures, had a weight of *327 kg*. Within the research program this weight up-to-date already could be significantly reduced, mainly by the application of high strength steels, but also by structural modifications. So the measure to reduce weight by the conversion to laser welding is one of many approaches being reviewed in line with the NHTSA light weight vehicle program.

Figure 16 **2011 Honda Accord (cars.com, 2011)**

Since the program is still been worked on, only preliminary statuses of the design could be accessed. For the rough approximation done in the next chapter an earlier status of the NHTSA light weight

vehicle project structure was used than for the main study. The main analysis was only started after the consequent milestone was reached, which resulted in different models than the one used for the rough approximation. So the computer aided design (CAD) and the finite element method (FEM) models, which eventually were used, were representing a design meeting the stiffness and side impact demands while the front and rear end impact performance still needed further attention. The weight of that structure was about *243 kg* and it mainly was bonded by resistance spot welding, but also some flanges designed for laser beam welding were present.

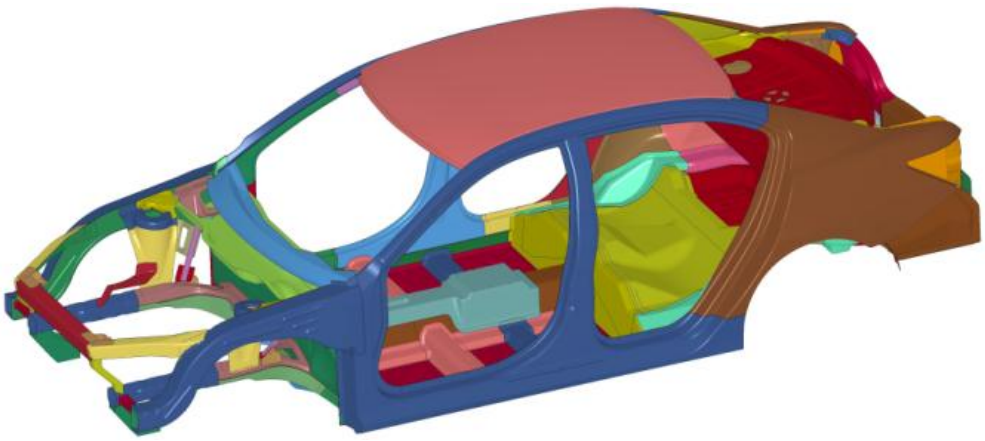

Figure 17 **FEM model of NHTSA light weight vehicle**

Containing *143* parts in total the CAD model (see illustration of similar FEM model in *Figure 17*) was divided into three subassemblies. The largest by far was the lower structure including *96* parts. It contained the whole front end, the dash area, the floor section and most of the rear end (see *Figure 18*). All side panels from the A-pillar to the rear end including the large outer panels, all the pillars, the rockers and the rear wheelhouses, adding up to *32* parts, were gathered in the side structure. Being the smallest subassembly, the upper structure comprised only *15* parts, of which a large share was joined by adhesive bonding.

The panel thicknesses spread between *0.5 mm* and *2.5 mm*, while the average thickness with respect to the size of the parts was *0.858 mm*. The exact value for each part and also its grade of steel can be taken from *Table 1*. Unfortunately the presented bill of materials (BoM) is not complete regarding the material information, since this is not the final status of the NHTSA project structure, as explained. It would go beyond the scope of this thesis to discuss every single part of the BoM in detail, so the table should be regarded as a help to get an idea of the breadth of the body structure and of the steel grades used. As mentioned most applied steels are of high strength grade. The used abbreviations for the different steels are as follows:

BH – Bake Hardening
CP – Phase
DP – Dual Phase
HF – Hot Formed
HSLA – High Strength Low Alloy
MS – Martensitic
S – Stainless

Table 1 **Bill of materials for base structure**

	Body Structure	**N/A**	**N/A**	**N/A**	**N/A**	**N/A**	**223.323**
Number [-]	**Description** [-]	**Side** [-]	**Mate-rial Type** [-]	**Yield** [MPa]	**Tensile** [MPa]	**Thick-ness** [mm]	**Mass** [kg]
	Body Lower Structure	**N/A**	**N/A**	**N/A**	**N/A**	**N/A**	**129.808**
0301	Rear Rail	LH	DP CP DP HSLA	700 1000 700 350	1000 1200 1000 450	1.4 0.6 1.4 0.8	1.596 0.679 1.453 0.645
0314	Rear Rail	RH	See LH	See LH	See LH	See LH	4.373
0201	Floor Panel	LH	DP	500	800	0.6	4.308
0199	Floor Panel	RH	DP	500	800	0.6	4.308
4139	Cradle Mount Bracket	LH	Steel	TBD	TBD	2.5	1.535
4140	Cradle Mount Bracket	RH	Steel	TBD	TBD	2.5	1.535
4141	Support Bracket	LH	HSLA	490	600	1.2	0.196
4142	Support Bracket	RH	HSLA	490	600	1.2	0.196
0302	Rear Rail Reinforcement	LH	DP	700	1000	1.0	2.905
0311	Rear Rail Reinforcement	RH	DP	700	1000	1.0	2.905
1102	Front Rail Tip	LH	Steel	TBD	TBD	1.2	1.808
1101	Front Rail Tip	RH	Steel	TBD	TBD	1.2	1.808
1104	Front Rail Lower	LH	DP	500	800	1.0	1.653
1103	Front Rail Lower	RH	DP	500	800	1.0	1.653
1106	Front Rail Lower to Rocker	LH	DP	500	800	1.2	1.695
1105	Front Rail Lower to Rocker	RH	DP	500	800	1.2	1.695
1108	Front Rail Upper	LH	DP	500	800	1.0	1.084
1107	Front Rail Upper	RH	DP	500	800	1.0	1.084
1005	Close-Out Front Rail	LH	Steel	TBD	TBD	1.0	0.233
1006	Close-Out Front Rail	RH	Steel	TBD	TBD	1.0	0.233
1110	Front Rail to Tunnel	LH	DP	500	800	1.2	0.557
1109	Front Rail to Tunnel	RH	DP	500	800	1.2	0.557
0220	Reinf - Engine Cradle Mount	LH	HSLA	490	600	2.0	1.202
0222	Reinf - Engine Cradle Mount	RH	HSLA	490	600	2.0	1.202
0224	Bulkhead Rear Engine Cradle Mount	LH	HSLA	490	600	2.0	0.226
0226	Bulkhead Rear Engine Cradle Mount	RH	HSLA	490	600	2.0	0.226

Number [-]	Description [-]	Side [-]	Material Type [-]	Yield [MPa]	Tensile [MPa]	Thickness [mm]	Mass [kg]
	Body Lower Structure (continued)						
4145	Shotgun Outer	LH	DP	500	800	0.8	1.802
4152	Shotgun Outer	RH	DP	500	800	0.8	1.802
4146	Shotgun Inner	LH	DP	500	800	0.8	2.139
4153	Shotgun Inner	RH	DP	500	800	0.8	2.139
4148	Upper Rad Support	LH	DP	500	800	0.8	0.691
4155	Upper Rad Support	RH	DP	500	800	0.8	0.691
4149	Lower Rad Support	LH	DP	500	800	0.8	0.458
4154	Lower Rad Support	RH	DP	500	800	0.8	0.458
4147	Support Bracket	LH	Steel	TBD	TBD	0.8	0.345
4156	Support Bracket	RH	Steel	TBD	TBD	0.8	0.345
4150	Radiator Support Upper Main	N/A	HSLA	490	600	0.8	0.820
4151	Radiator Support Lower Main	N/A	HSLA	490	600	0.8	0.608
0258	Cowl Lower	N/A	BH	280	400	1.0	5.932
0275	Cowl Inner	N/A	BH	280	400	0.7	1.941
1100	Front Rail Brkt Center	N/A	Steel	TBD	TBD	1.2	0.307
0300	Cargo Floor	N/A	DP	350	600	0.6	5.632
0350	Back Panel Outer	N/A	DP	350	600	1.0	5.052
0306	Package Tray	N/A	BH	280	400	0.7	4.508
0200	Tunnel Main	N/A	DP	700	1000	0.6	4.378
0016	Seat Pan Rear	N/A	DP	350	600	0.6	4.177
0299	Rear Crossmember	N/A	CP	800	1000	1.4	3.186
0001	Dash Panel	N/A	BH	280	400	0.6	3.139
0252	Tunnel - Dash Interface Panel	N/A	DP	700	1000	0.6	3.080
0253	Crossmember Rear Seat	N/A	DP	500	800	1.2	3.057
0203	Seat Crossmember Front	LH	MS	950	1200	0.8	1.348
0202	Seat Crossmember Front	RH	MS	950	1200	0.8	1.348
0100	Waterfall Panel	N/A	DP	300	500	0.6	2.112
0303	Side Panel Rear Seat	LH	DP	700	1000	0.8	1.035
0304	Side Panel Rear Seat	RH	DP	700	1000	0.8	1.035
0259	Cowl Upper	N/A	BH	280	400	0.8	2.015
0205	Front Seat Crossmember	LH	MS	950	1200	0.8	0.825
0204	Front Seat Crossmember	RH	MS	950	1200	0.8	0.825
0309	Package Tray Crossmember	N/A	DP	350	600	0.7	1.569
0326	Back Panel Inr	LH	DP	300	500	0.7	0.616
0327	Back Panel Inr	RH	DP	300	500	0.7	0.616
0325	Back Panel Inr	N/A	DP	500	800	0.7	1.181

Number [-]	Description [-]	Side [-]	Material Type [-]	Yield [MPa]	Tensile [MPa]	Thickness [mm]	Mass [kg]
	Body Lower Structure (continued)						
0307	Rear Reinf Package Tray	N/A	DP	500	800	0.6	1.163
1016	Shock Tower	LH	S	TBD	TBD	1.0	1.025
1017	Shock Tower	RH	S	TBD	TBD	1.0	1.025
0254	Tunnel Bulkhead Lower	N/A	Steel	TBD	TBD	1.0	1.067
0255	Tunnel Bulkhead Upper	N/A	Steel	TBD	TBD	1.0	0.887
0210	Tunnel Crossmember	N/A	DP	350	600	0.8	0.675
0210	Tunnel Crossmember	N/A	DP	350	600	0.8	0.675
2022	Engine Mount Upper	RH	HSLA	490	600	2.0	0.670
0298	Mount Frame - Suspension Cradle	LH	Steel	TBD	TBD	1.0	0.277
0297	Mount Frame - Suspension Cradle	RH	Steel	TBD	TBD	1.0	0.277
2024	Engine Mount Upper	LH	HSLA	490	600	2.0	0.490
0308	Bracket WH-PT Reinf	LH	BH	280	400	0.7	0.215
0312	Bracket WH-PT Reinf	RH	BH	280	400	0.7	0.215
0256	Close-Off Tunnel Front	LH	DP	500	800	1.0	0.168
0260	Close-Off Tunnel Front	RH	DP	500	800	1.0	0.168
0330	Gutter Reinf	LH	Steel	TBD	TBD	1.0	0.125
0331	Gutter Reinf	RH	Steel	TBD	TBD	1.0	0.125
0317	Rear Rail Inr Brkt LH	LH	HSLA	490	600	1.0	0.221
0318	Rear Rail Inr Brkt RH	RH	HSLA	490	600	1.0	0.221
2372	Gas Tank Mount LH	LH	BH	210	340	1.5	0.453
2373	Gas Tank Mount RH	RH	BH	210	340	1.5	0.453
0265	Shotgun Inr LH	LH	Steel	TBD	TBD	0.7	0.173
0266	Shotgun Inr RH	RH	Steel	TBD	TBD	0.7	0.173
0267	Hood Hinge Reinf LH	LH	HSLA	350	450	1.0	0.967
0268	Hood Hinge Reinf RH	RH	HSLA	350	450	1.0	0.967
0269	Shotgun Inr Brkt LH	LH	Mild	140	270	1.0	0.033
0270	Shotgun Inr Brkt RH	RH	Mild	140	270	1.0	0.033
0271	Brkt Shotgun Inr Rear LH	LH	Mild	140	270	1.0	0.026
0272	Brkt Shotgun Inr Rear RH	RH	Mild	140	270	1.0	0.026
0273	Bracket Hood Damper LH	LH	Steel	TBD	TBD	1.0	0.015
0274	Bracket Hood Damper RH	RH	Steel	TBD	TBD	1.0	0.015
0003	Dash Reinf	N/A	DP	700	1000	1.0	2.023

Number [-]	Description [-]	Side [-]	Material Type [-]	Yield [MPa]	Tensile [MPa]	Thickness [mm]	Mass [kg]
	Body Upper Structure	**N/A**	**N/A**	**N/A**	**N/A**	**N/A**	**15.981**
4084	Bond Beam	N/A	BH	280	400	0.6	0.237
4081	Roof Bow	N/A	MS	950	1200	1.0	1.635
4083	Bracket - Bow	LH	DP	300	500	1.9	0.344
4082	Bracket - Bow	RH	DP	300	500	1.9	0.344
4065	Bracket - Roof Header to Rail	LH	BH	280	400	1.2	0.333
4063	Bracket - Roof Header to Rail	RH	BH	280	400	1.2	0.333
4071	Rear Header	N/A	BH	280	400	1.0	0.797
4061	Roof Header	N/A	BH	280	400	0.72	0.722
4051	Panel - Roof	N/A	DP	300	500	0.6	8.871
4064	Bracket - Center Overhead	N/A	BH	280	400	0.76	0.232
4073	Bracket - Rear Header to Roof Rail	LH	BH	280	400	1.0	0.198
4072	Bracket - Rear Header to Roof Rail	RH	BH	280	400	1.0	0.198
4062	Roof Header Reinf	N/A	BH	280	400	0.5	0.289
4076	Support Roof	LH	BH	280	400	1.0	0.724
4075	Support Roof	RH	BH	280	400	1.0	0.724
	Body Side Structure	**N/A**	**N/A**	**N/A**	**N/A**	**N/A**	**77.534**
0135	**Body Side Asm**	**LH**	**N/A**	**N/A**	**N/A**	**N/A**	**38.767**
1325	Panel - Body Side Outer	LH	DP BH	350 210	600 340	0.8 0.6	8.917 3.752
0066	Rocker	LH	CP	1050	1470	1.0	6.707
1040	FBHP	LH	DP	500	800	1.2	1.437
5140	Reinf - Roof Rail	LH	HF	1050	1500	0.7	2.057
4964	Panel - Wheel House Outer	LH	DP	500	800	0.6	2.517
4960	Panel - Wheel House Inner	LH	BH	210	340	0.6	4.421
4983	Reinf - B-Pillar	LH	HF	1050	1500	0.6 1.0 0.6	0.157 0.260 1.018
5120	Roof Rail Inner Front	LH	HF	1050	1500	0.7 1.0	0.451 0.447
5150	B-Pillar Inner	LH	HF	1050	1500	0.8 0.6 0.8 0.6	0.159 0.132 0.210 1.187
3502	Rocker Cover - Rear Door	LH	HF	1050	1500	0.6	0.190
3500	Rocker Cover - Front Door	LH	HF	1050	1500	0.6	0.177

Number [-]	Description [-]	Side [-]	Material Type [-]	Yield [MPa]	Tensile [MPa]	Thickness [mm]	Mass [kg]
	Body Side Structure (continued)						
5130	Roof Rail Inner Rear	LH	HF	1050	1500	1.1	1.950
5158	Lamp Can	LH	DP	300	500	0.8	1.125
0305	Reinf - Package Tray	LH	BH	280	400	0.7	0.702
0310	Rear Quarter Lower	LH	BH	210	340	0.7	0.794
0140	**Body Side Asm**	**RH**	**N/A**	**N/A**	**N/A**	**N/A**	**38.767**
1327	Panel - Body Side Outer	RH	Steel	See LH	See LH	See LH	12.669
0048	Rocker	RH	CP	1050	1470	1.0	6.707
1042	FBHP	RH	DP	500	800	1.2	1.437
5142	Reinf - Roof Rail	RH	HF	1050	1500	0.7	2.057
4966	Panel - Wheel House Outer	RH	DP	500	800	0.6	2.517
4962	Panel - Wheel House Inner	RH	BH	210	340	0.6	4.421
4985	Reinf - B-Pillar	RH	HF	1050	1500	See LH	1.435
5122	Roof Rail Inner Front	RH	HF	1050	1500	See LH	0.898
5152	B-Pillar Inner	RH	HF	1050	1500	See LH	1.688
3512	Rocker Cover - Rear Door	RH	HF	1050	1500	0.6	0.190
3510	Rocker Cover - Front Door	RH	HF	1050	1500	0.6	0.177
5132	Roof Rail Inner Rear	RH	HF	1050	1500	1.1	1.950
5159	Lamp Can	RH	DP	300	500	0.8	1.125
0313	Reinf - Package Tray	RH	BH	280	400	0.7	0.702
0315	Rear Quarter Lower	RH	BH	210	340	0.7	0.794

Since adaptations improving the crash performance were done directly in the FEM model, before a detailed elaborated design change was made to the CAD, the FEM model differed from the CAD model regarding a few details. That also resulted in the FEM model embedding *102* parts in the lower structure, since the additional support structure, apparent between the right hand shock tower and the dash area in *Figure 17*, was not included in the CAD model. All research was based on the status of the FEM model, which was the one to be edited and worked with. In the main study the CAD model was only used to follow up on the part names and numbers, which were not included in the FEM model, and to better conceive the layout of the body structure.

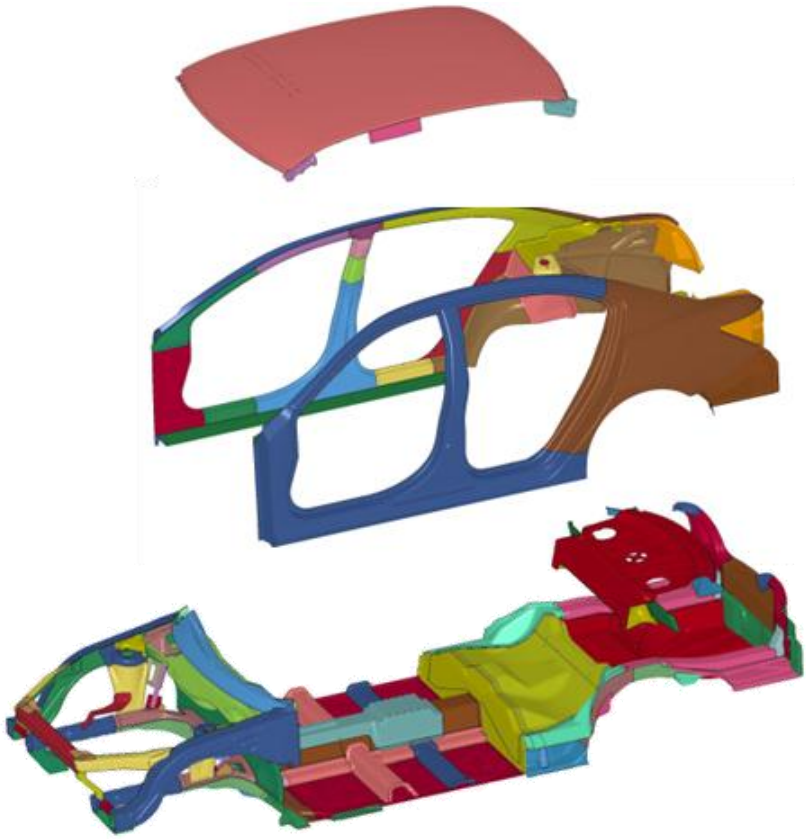

Figure 18 **FEM model separated according to subassemblies upper, side and lower structure (from top)**

4. Weight Saving Potential by Laser Welding on BIW Sample Structure

4.1. Weight Saving Approach

The main idea behind switching from resistance spot welding, which is the standard for usual BIWs made of steel at present time, to laser beam welding is a considerable weight reduction. This can be achieved by the modification of the flanges. While a spot weld connection usually requires a flange width of about *16 mm* for all bonded parts to guarantee accessibility for the spot welding gun, a laser beam weld necessitates only circa *8 mm* of flange width (see *Figure 19*), since the laser gun itself does not need to physically access the flange. Those values are average figures confirmed by experts in this field at EDAG. The actual required flange width of course depends on a lot of parameters, such as the thicknesses of the parts to be joined, if applicable the number of thicknesses, the materials and the welding parameters, but the mentioned values constitute representative average. Information like this also is found in internal papers of the original equipment manufacturers (OEM). Each company has its own design guidelines for resistance spot welding flanges.

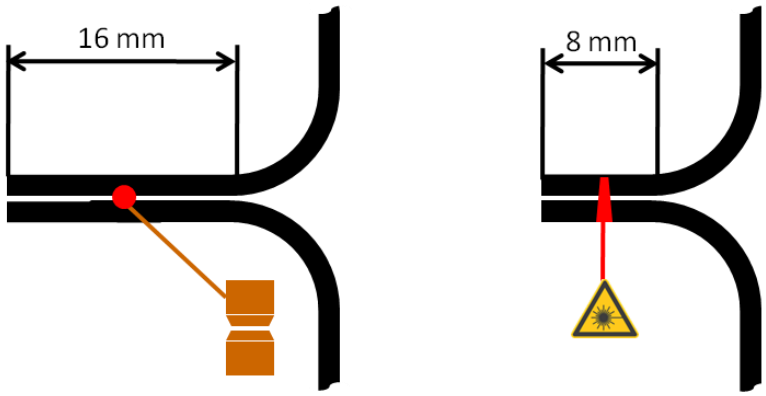

Figure 19 **Flange width comparison between resistance spot weld (left) and laser beam weld flange**

So in general all flanges could be trimmed by *8 mm*. But there are some exceptions, like 3T joints, which have to be treated separately. If all three parts connect to the flange from the same side at least the middle thickness needs a flange of a width considerable larger than *8 mm*. A configuration

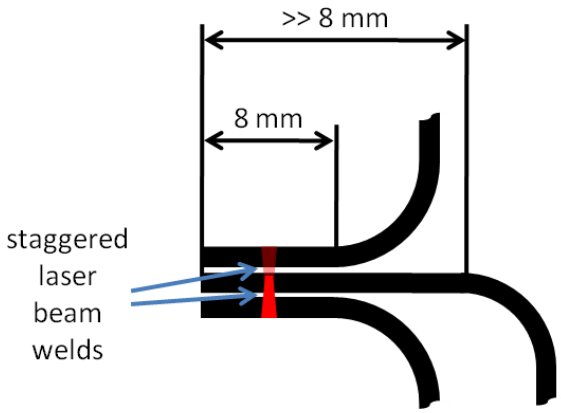

Figure 20 **Flange set-up for a 3T laser beam weld**

like this is displayed in *Figure 20*. Here all components involved in the bond have to be regarded to make sure not to trim one of the concerned flanges excessively.
Another aspect which one needs to be aware of is the distinction between flange joints and lap joints, see *Figure 21*. Converting the flange weld from spot to laser welding the flanges of all parts can be trimmed. Doing the same with a lap joint, only one part can be trimmed to maintain a remaining flange overlap of *8 mm* due to the geometrical configuration. This results in larger mass savings when remodeling a flange joint to a laser beam weld compared to a lap joint.

Figure 21 **Schematic representation of a flange weld (left) and a lap joint weld (right)**

Considering the large amount of functionalities a body structure has to handle, it also is necessary to check whether the flanges to be trimmed serve other purposes, too. It was agreed on, that also trimmed flanges of *8 mm* width could be used to carry e.g. a door seal or the wind screen. But if the flange fulfilled other structural demands than just carrying the bond, it was not trimmed. An example for this occasion is the front rail, where the tip is plugged into the rear part of the rail and the end lap thereby needs to be larger than *8 mm* for the structure not to collapse during the front impact (see *Figure 22*).

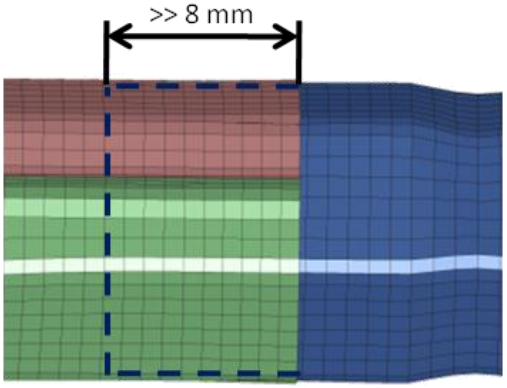

Figure 22 **Front rail tip (right end) inserted into rail counterpart with an overlap much larger than 8 mm**

Another effect of the conversion is the replacement of the punctiform joining approach of the spot welded body structure by continuous connections per laser welding. This probably will lead to an increased stiffness of the structure, which has to be determined with the help of an FEM calculation. If a considerable increase in stiffness can be detected, the thickness of not crash relevant parts can be decreased to bring the laser welded structure down to the same performance level as the spot welded structure. This way it could be possible to save additional weight.

The restricted need in accessibility as well is an advantage of the laser welding technology. If proper clamping of the parts to be bonded can be achieved, only single sided access is required, since the laser gun does not need to access the parts directly. To take full advantage of this property the body structure would need to be completely redesigned from scratch with respect to laser beam welding. This is out of the scope for this study and cannot be carried out.

4.2. Weight Saving Potential Estimation

To get a first ballpark figure of the magnitude of the achievable savings all flanges of the sample structure were investigated regarding trimming possibilities described above. A similar study was done before on the surveyed BIW, which revealed a potential of ca. *15 kg* corresponding to ca. *7 %* of the modified Honda's body structure mass of *223 kg*. But since this study was only roughly estimated, within this thesis project the structure was scrutinized again, analyzing the function of each flange in detail. It was ensured that only the width of flanges was reduced to *8 mm*, where there was no other functionality restricted by doing so.

Considering all the aspects mentioned in chapter 4.1, every part in the Bill of Materials (BoM) was analyzed consulting the body structure's CAD-model. Once a flange to be trimmed was identified, its length was measured as shown in *Figure 23*. If a flange had a relevant in-plane curvature, the length of the outer and the inner flange edge was measured according to *Figure 24*. To gain a representative flange length the average of those two measurements was calculated. Then the width was determined at different locations of the flange to estimate the average jut that could be trimmed to obtain the *8 mm* flange width required for a laser weld. Taking the part's thickness into account this gave the volume of the dispensable flange part. With the steel's density of *7850 kg/m^3* the mass saving potential could be determined.

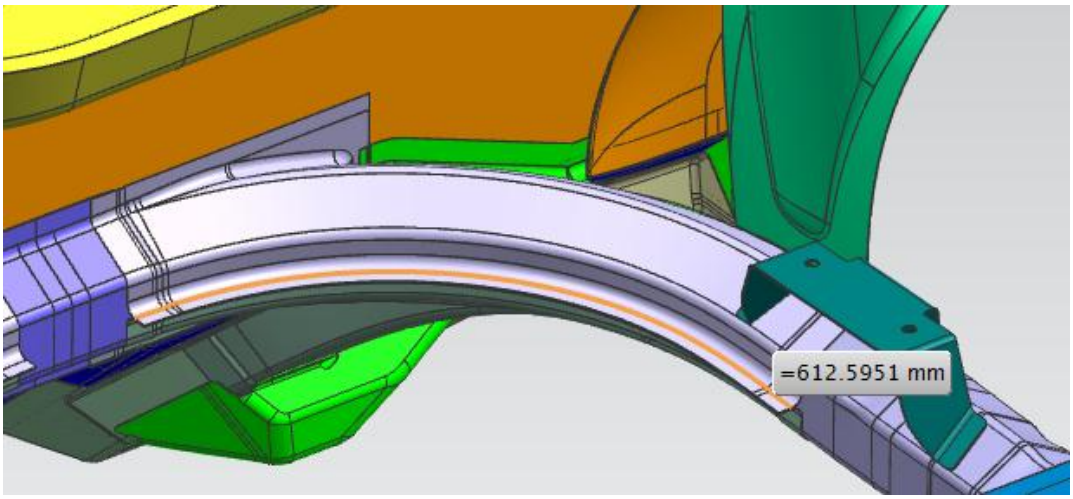

Figure 23 **Example of measuring the length of a flange**

For the total body structure *179 m* of flanges could be somewhat trimmed. This led to more accurately determined mass savings of about *10 kg* respectively *4.5 %*, which still can be considered as a significant saving. This shows that it is actually worth it to research the weight saving potential made possible by laser welding and putting effort in this study.

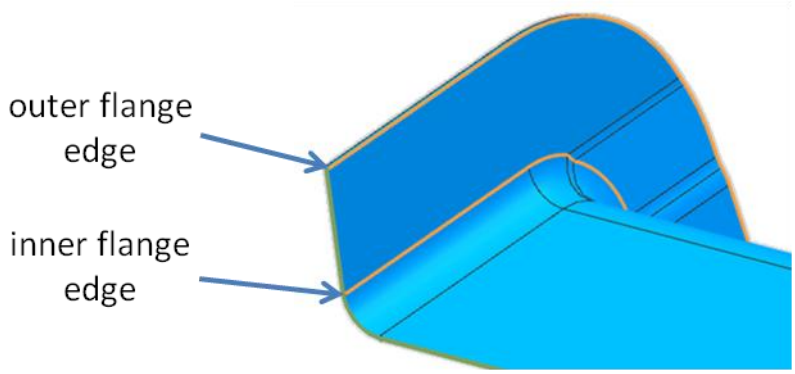

Figure 24 **Inner and outer edge of a flange**

Being by far the largest substructure and representing way more than half of the complete body structure's weight the major share of *7.6 kg* of mass savings originated from the lower substructure. From the upper substructure only about *0.6 kg* could be deducted since adhesive bonding was by the majority applied here; so only few flanges could be trimmed. For the side substructures the situation was similar. Already the basis sample structure was equipped with a lot of laser welds there, especially in the door entry area, so that there were not many flanges to be trimmed. Only *1.8 kg* could be saved here.

5. Creation and Evaluation of Solely Resistance Spot Welded Structure

For the weight saving potential *estimation* the initial state of the model was compared to the trimmed flanges model. But actually the initial model could not be considered as completely spot welded since there were a lot of flanges featuring a width much smaller than *16 mm*, especially in the side structure. To have an appropriate comparison between spot and laser welding, it was not only required to create a representative model of the laser welded body structure, but also one of the solely spot welded structure. So the first step for the main weight reduction analysis was to modify the original model to a completely spot welded structure, i.e. making sure that every flange had a minimum width of *16 mm*.

5.1. Converting Sample Body Structure to a Solely Resistance Spot Welded Structure

Again the bill of materials was used as a guide to make sure every part of the body structure was considered. Starting with the lower structure all flanges of all parts were inspected and if necessary modified following the list. As indicated above, only the FEM model was used for this. The CAD model again was only used as a gateway between the BoM and the FEM model, which was not reflecting any assembly structure.

The main reason, why the flange geometry changes were not accomplished in the CAD system, were the comprehensive topology modification possibilities which ANSA 13.1.1, the FEM tool used by ED-AG, Inc., offered. Those made it possible to do all necessary flange changes right to the FEM model. And since all the material data was also deposited a weight analysis also could be easily carried out with ANSA, the preprocessor program of BETA, Inc. And of course, the other purpose to do these modifications, i.e. carrying out a stiffness analysis, was also done directly with this model. On balance it seemed to be more efficient to directly modify the mesh of the FEM model than to edit the CAD data and then having to create a whole new FEM data set from that.

Each single part of the provided FEM model was analyzed the following way. First off all, all the flanges of the investigeated part were identified, checking whether any of them already was adapted while probably editing a neighboring part. If there were any flanges left which had a width smaller or considerably larger than the discussed *16 mm*, their width were measured all along their full length and the measurements were stored to have a guide for the morphing procedure later on. *Figure 25* displays those preparations on the part of the front structure connecting the left and right front rails at the dash as an example. For this small part there were not too many measurements to be stored, for instance only two on the top flange. If the flanges were more elongate, there also were many more stored measurements. Since the lower flange sits right at the edge of the dash panel it is connected to, its width of only *12.6 mm* could not be increased. So this flange remained unmodified. The top flange shows a width just above the required value, so there was no reason to modify it. On the other hand the side flanges were almost *10 mm* too wide. So the options were to either trim them to *16 mm* at this stage and then further to *8 mm* in the laser welded model, or only considering the comparison aspect, they would not be trimmed at all yet, but just trimmed for the laser welded model later on with a delta of *8 mm*. In this case the first option was chosen, trimming the flanges for both models, but other flanges might needed a larger width for structural reasons, so

only the laser model was trimmed by the delta. Since the flanges in *Figure 25* are lap joints, note that for the side flanges only either the center bracket or the front rails should be trimmed.

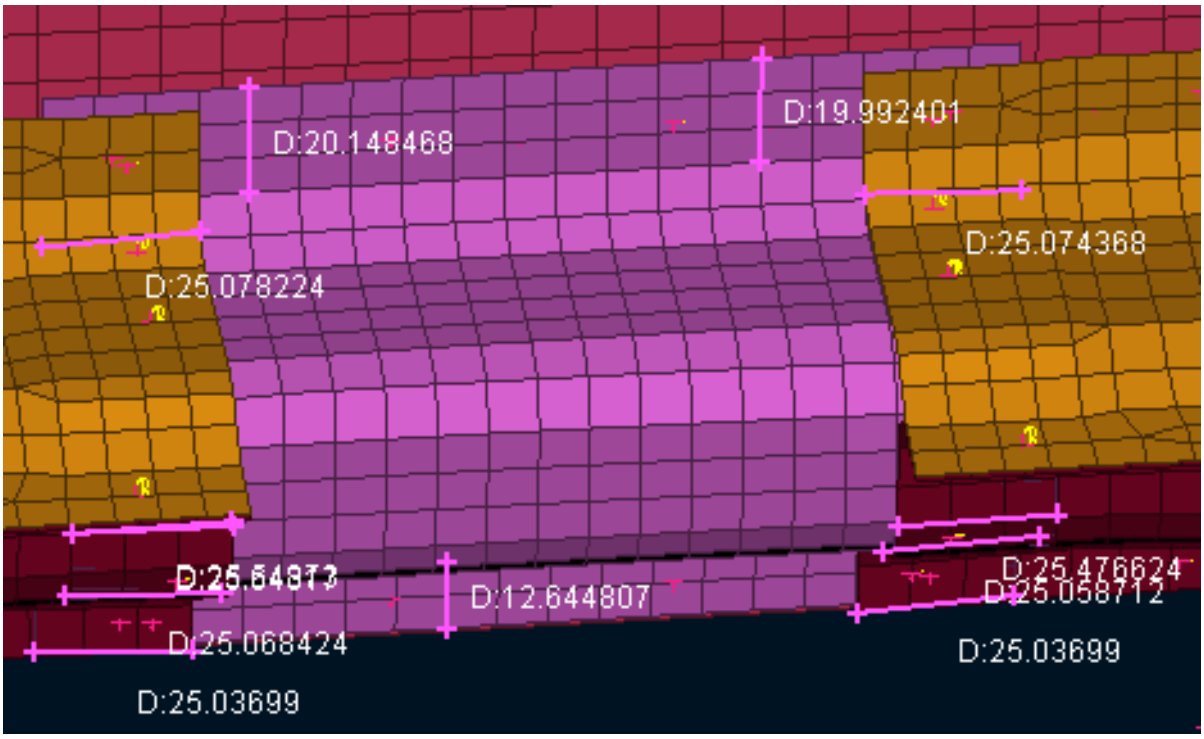

Figure 25 **Flange width analysis of front rail bracket center**

The FEM model used was originally designed for crash impact simulations. All the spot welds shown as violet plus signs and yellow dots on the flanges in *Figure 25* represent 'Dyna Spot Welds', a connection type created for crash impact research. For the stiffness simulations all those spot welds had to be converted into a kind of connection built from rigid body elements (RBE) and a hexagonal element, called the RBE3-HEXA-RBE3 type. As an interstage all the Dyna Spot Welds were converted to connection points (see *Figure 26*), from where they would be realized to RBE3-HEXA-RBE3 later on. But as another indicator to quickly notice which flanges in the model had been modified already regarding width, only those FEM welds were converted to connection points, whose flanges were modified or agreed on not to need any modification. Connection points can be described as a dummy for spot weld connections. They define its position and contain information about the parts

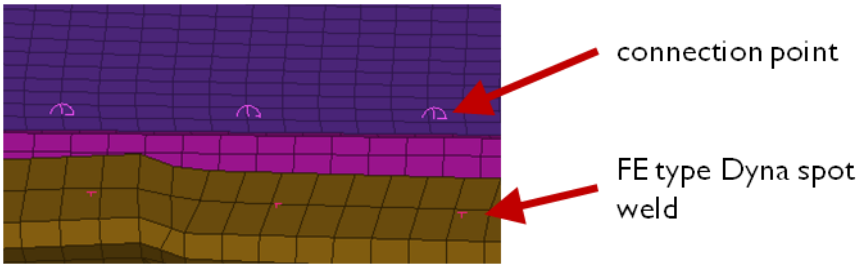

Figure 26 **Connection points and FE representation by "Dyna Spot Weld"**

involved. Since from the connection points new FEM connection could be created subsequent, the Dyna Spot Weld FE which was replaced by the connection point was deleted.
But even if there was already the desired connection FE in the model, it still would have to be redone on the modified flanges. Since the mesh of at least one flange of a modified weld seam was changed, the spot weld FE most probably would have been losing its contact; see an example where it loses both contacts due to trimming in *Figure 27*. Also after the modification the edited mesh was reconstructed, so the connection FE needed to connect to new nodes.

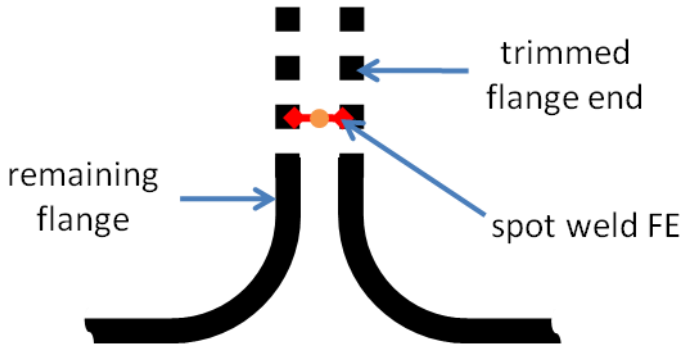

Figure 27 **Spot weld FE sitting on the flange end to be trimmed**

The topology tool of ANSA most used to modify the flanges is called *morphing*. With the most common box morphing, boxes were created containing a certain part of the mesh and then changing their shape, tagging along the mesh. So what was actually always referred to as trimming the flanges usually was a compression or stretching of the flange mesh. *Figure 28* shows one of the morph boxes that have been created. By shifting the upper surface of the box downwards the included mesh became compressed. From the stored measurements one could tell when the desired flange width is reached. In the example the *16 mm* obviously could not be reached for the whole flange at a time. So for only small deviations and small flanges like the one shown, the flange was morphed to meet the desired value approximately as an average. If the flange was longer or the discrepancy of the width along the flange was large, the morph box was split into several subparts all connected and linked at their cross-sectional area, which will then appear as a yellow cross hatch as shown in *Figure 29*. First all subparts were modified to the same level of flange width and then all together where morphed to obtain the desired overall width. For further details on box morphing please see Appendix A.

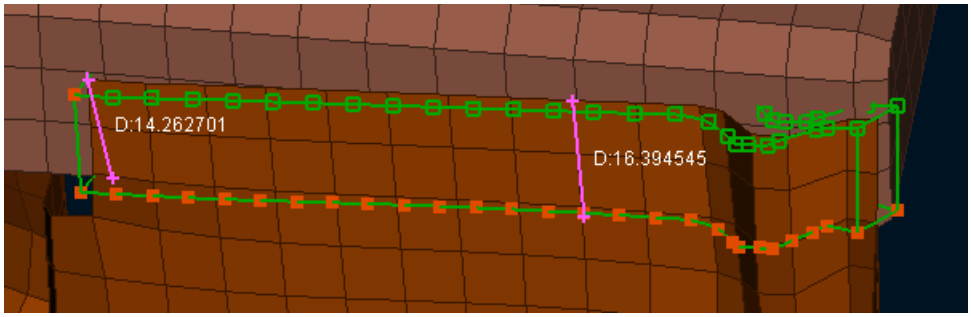

Figure 28 **Box morphing**

Of course one morph box was sufficient for both parts of a flange weld joint. The morphing box simply was created based on only one of the flanges. Since the morph boxes always were generated with a width of ca. *10 mm* (see Appendix A) it would automatically also contain the other flange.

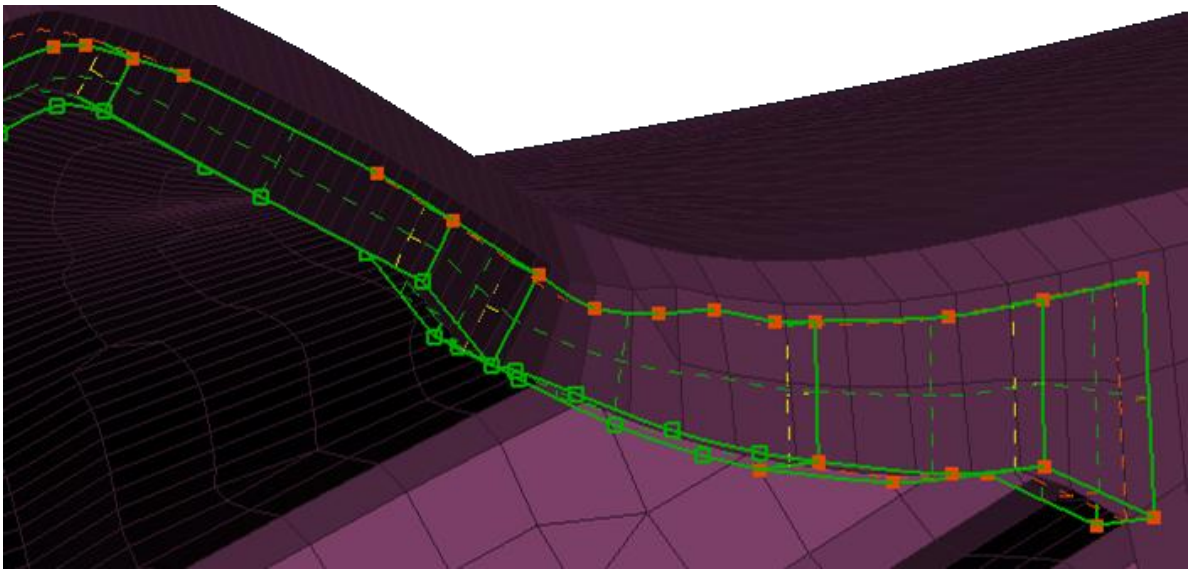

Figure 29 **Subdivided morph box**

For flat flanges another morphing method was more suitable. Direct morphing simply moved all selected nodes in the same direction. The highlighted elements in *Figure 30* were all selected to be involved in the morphing process, i.e. from that area the nodes to be moved or to be frozen could be selected and this area could be automatically reconstructed at the end of the operation if desired. The blue dots are flagging the elements within the morphing area which are chosen to stay in place. Red indicates that the node is going to be moved the way the user specifies it. The non-highlighted nodes are following no particular appointed pattern, but are translating according to keep the mesh as smooth as possible during the morph operation. So similar to the box morphing process flange width measurements were stored and the red dots were translated until the measurements indicated that the desired flange width value was obtained.

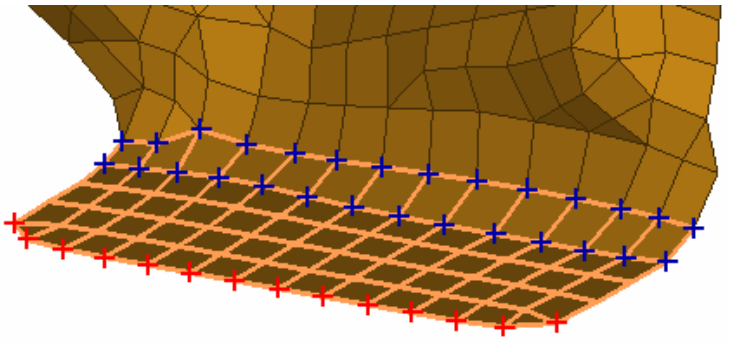

Figure 30 **Direct morphing**

After the flange was modified by applying the suitable morphing method the edited mesh area was reconstructed. All the mesh included and loaded into the morphing box or respectively initially se-

lected for the direct morphing as explained, could be automatically reconstructed after the morphing operation was performed. Right when the spot welded FEM model – or later on the laser welded model – was opened in Ansa, a file separately was loaded containing the mesh evaluation criteria;

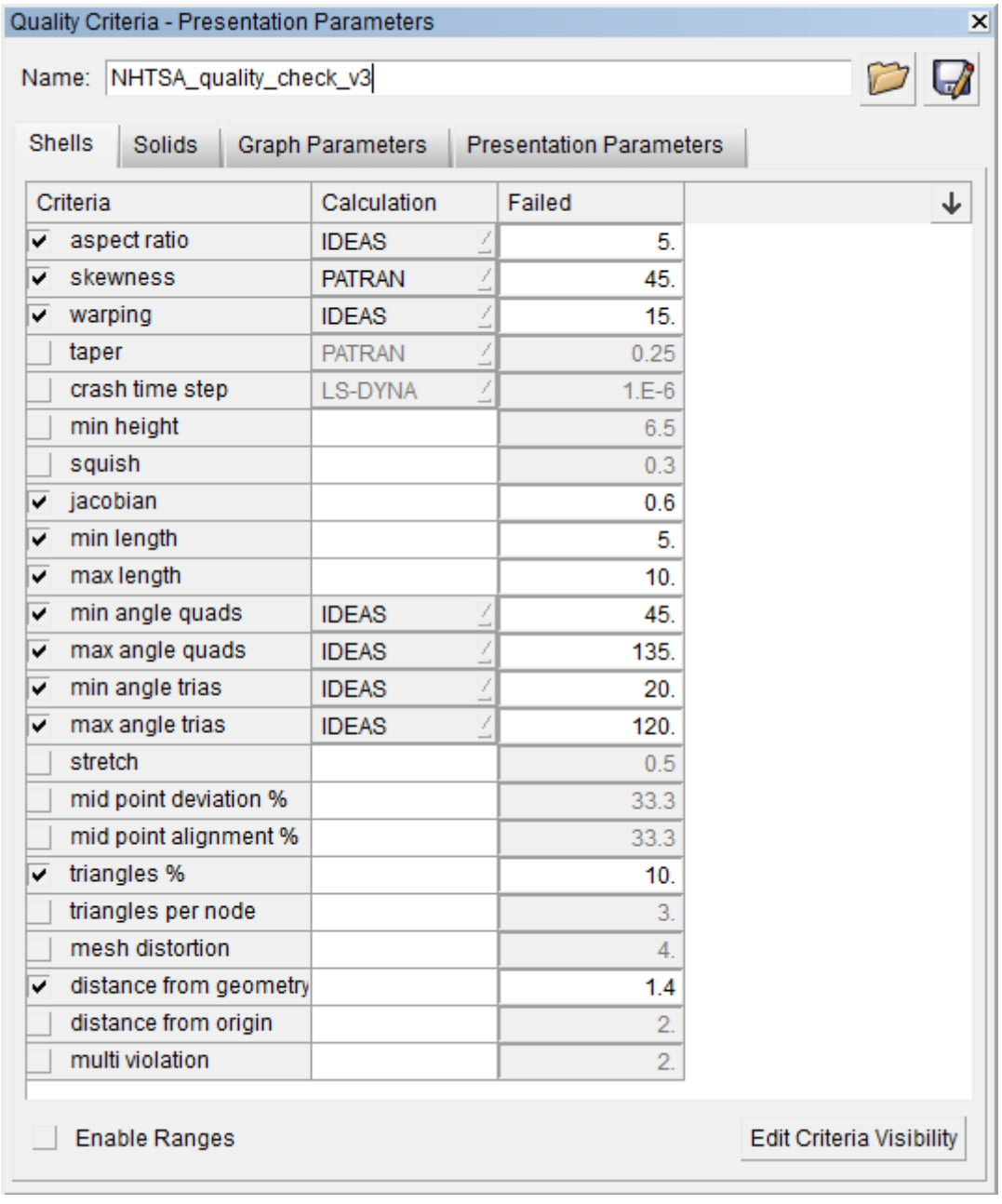

Figure 31 **Quality criteria for FEM models of the NHTSA project**

see limits displayed in "failed"-column of *Figure 31*. Those were defined in cooperation with the George Washington University so that the mentioned file was used for all generated FEM models within the NHTSA project. The automatic reconstruction now referred to this applied reference mesh file and recreated the mesh in line with those target values. If the original adjacent mesh to the flange for some reason did not meet those criteria resulting in a poor transition to the recon-

structed flange mesh, the mesh parameters were by way of exception changed. This phenomenon sometimes occurred regarding the maximum element length. Often the original mesh exhibited an element length of *12 mm* or so. Then the maximum permitted element length for the reconstruction would have to be set to from the default *10 mm* to *12.5 mm* to avoid unwanted additional node lines, which would warp the whole mesh area, as illustrated in *Figure 32*. It was decided to rather achieve a smooth mesh then to stick to the mesh generation standards whatever the cost.

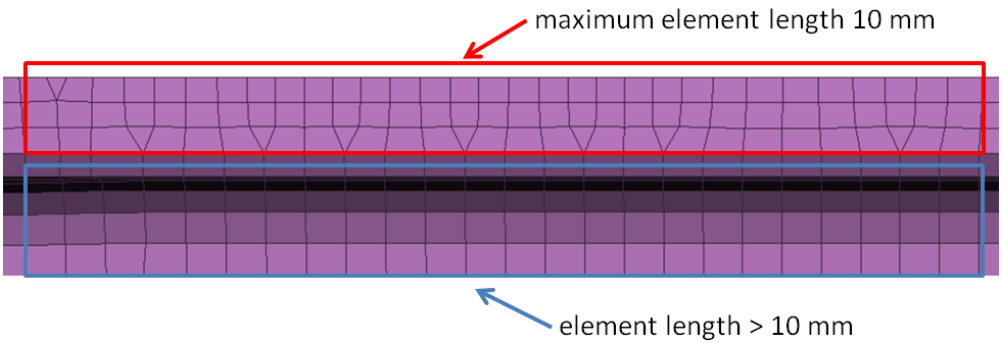

Figure 32 **Reconstructing part of the mesh with different maximum element length**

Another issue requiring attention when reconstructing the mesh was the conservation of certain feature lines. To properly represent shapes, like e.g. edges, feature lines within the area to be remeshed could be defined (see *Figure 33*). The reconstruction tool then would make sure that on exactly this line a node line would be established while remeshing to describe the correct topology.

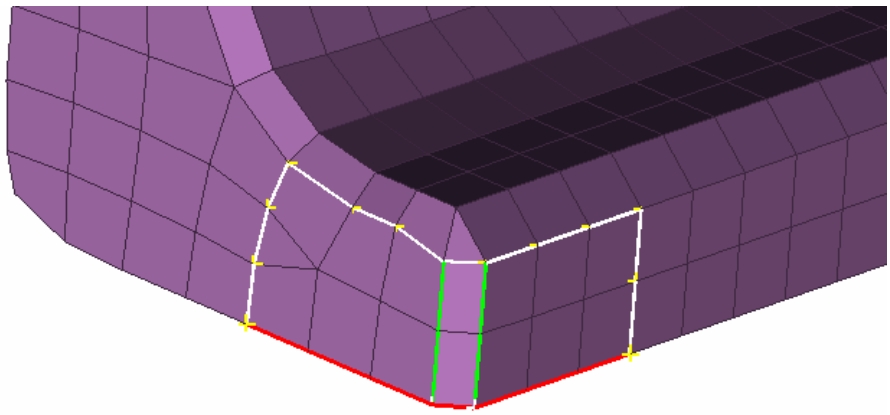

Figure 33 **Feature lines (green) to be kept when reconstructing a mesh area**

All the flanges whose width did not fit were modified applying the methods discussed above after being analyzed and having the spot weld points converted as described at the beginning of this chapter. For the spot welded FEM model this meant that *145* flanges were modified, the majority of those by *38* morph parameters. *Figure 34* shows all the morph boxes created for this model. Note that the lower structure mainly had already sufficiently wide flanges, while the side structure included a lot of laser welding in the base model and thereby needed some attention to its flanges.

For example all entry flanges, including primarily 3T configurations, were stretched together for each door cutout (see *Figure 35*). This was quite a complicated operation, since each front and rear door

involved eight parts to be modified forming the door entry flanges. Moreover morph boxes cannot be designed as a closed loop. So the end surfaces were at least put close together, so there would be no gap with omitted elements and the control points at the ends would move parallel.

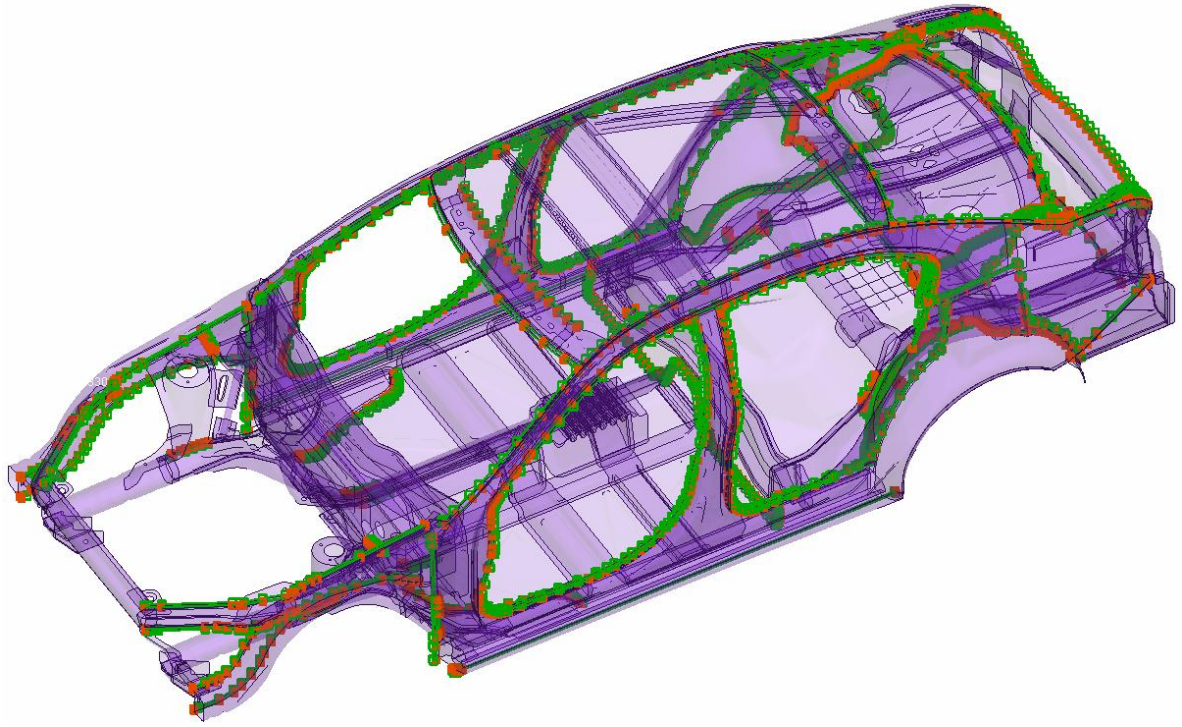

Figure 34 **Morphing boxes created to edit the spot welded model**

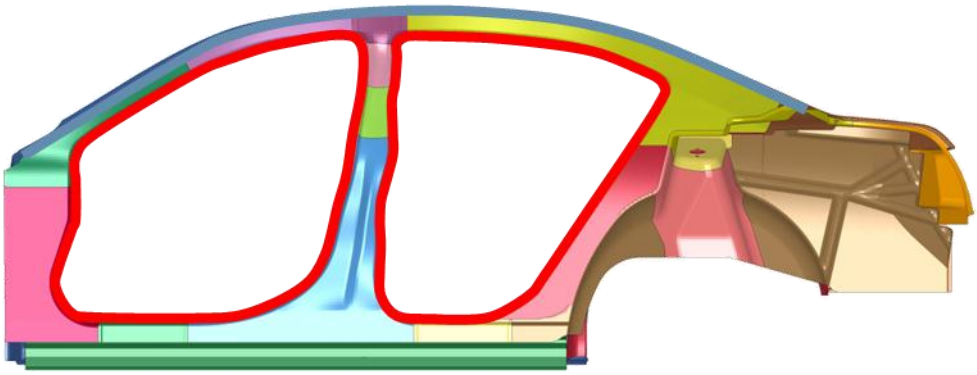

Figure 35 **The door entries (red) needed to be modified for both models**

From the structure modified all the way now, the weight of the solely spot welded body structure could be determined. Since the FEM model contained all relevant information such as thicknesses and material data the mass could be read out right away for each single part or as a total.

5.2. Performance of Solely Spot Welded Structure

It already has been explained that the FEM model adapted to analyze the weight was created with the preprocessor ANSA. So this model could be used more or less straight away to perform a noise,

vibration and harshness (NVH) analysis. Only the joining technology had to be updated. As described the entire originally existing spot weld FEM was converted to connection points. Now those were checked for completeness and whether still the right parts were selected to be connected. Eventually all the connection points were realized to the described RBE3-HEXA-RBE3 spot weld connections (see *Figure 36*). The "*3*" indicates the type of the RBE. As opposed to RBE2s, RBE3-spiders have the center node being dependant on the outer nodes. Moreover RBE3-spiders do not exhibit an equal force distribution among the independent outer nodes as RBE2 elements do, but the distribution is conditioned by the distance from the respective outer node to the center node. On each side of the hexahedra there are four of those RBE3-spiders connecting to the four corners with their center node. The outer nodes of the spiders are in each case attached to the mesh of the parts to be joined. The whole RBE3-HEXA-RBE3 connection also is referred to as area connection model 2 (ACM2).

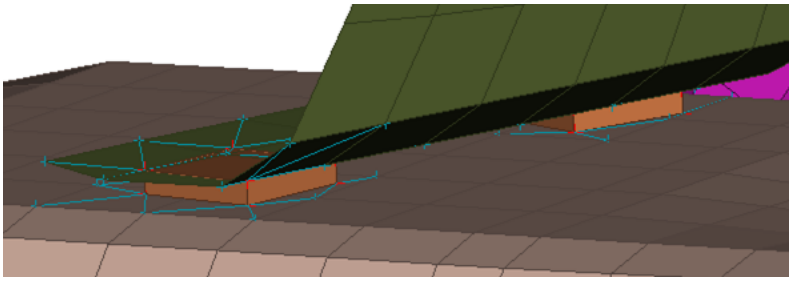

Figure 36 **RBE3-HEXA-RBE3 connection element**

Some connections did fail to realize. This partly was caused by the connection points being located at an inappropriate position after the respective flange was modified. In this case the problem could be solved by slightly translating the connection point in the suitable direction. Another cause of a failed realization was an intersection of the meshes. Since intersections in general have no effect on the NVH calculations or the weight analysis, there was no special attention drawn to them up to this point. But creating any FEM connection right at an intersection of course is not feasible. So by moving certain nodes of affected mesh areas manually or by applying a morph operation to concerned regions all disturbing intersections were erased.

One of those was for example the connection of the bond beam supporting the roof to the roof rails of the side structure. The ends of the beam were intersecting with two layers of the side structure as displayed in *Figure 37*. So the side tips of the beam were both morphed upwards until there was a small gap to the parts of the side structure where the welding FEM would fit in.

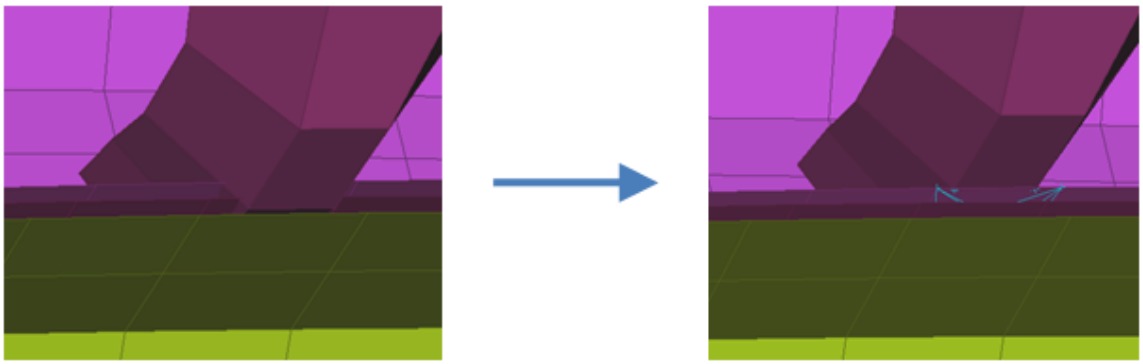

Figure 37 **Intersection of bond beam in roof rail area before (left) and after (right) morphing and properly realizing the spot weld connection**

Finally some parts actually not belonging to the body structure, but usually being taken into account to evaluate the BIW stiffness since they influence the performance significantly, were added to the assembly. The front and rear wind screens were attached with adhesive as can be seen in *Figure 38*. Moreover front and rear bumpers from the regular NHTSA FEM model were bolted onto the structure. Other bolted on parts, which cannot be seen in the illustration, are the rear end tunnel cross member and the instrument panel beam. This turns the structure into a body in prime; alone the subframes are missing, which are included in some definitions of body in prime. Clearly visible in *Figure 38* are also the properly realized spot welds.

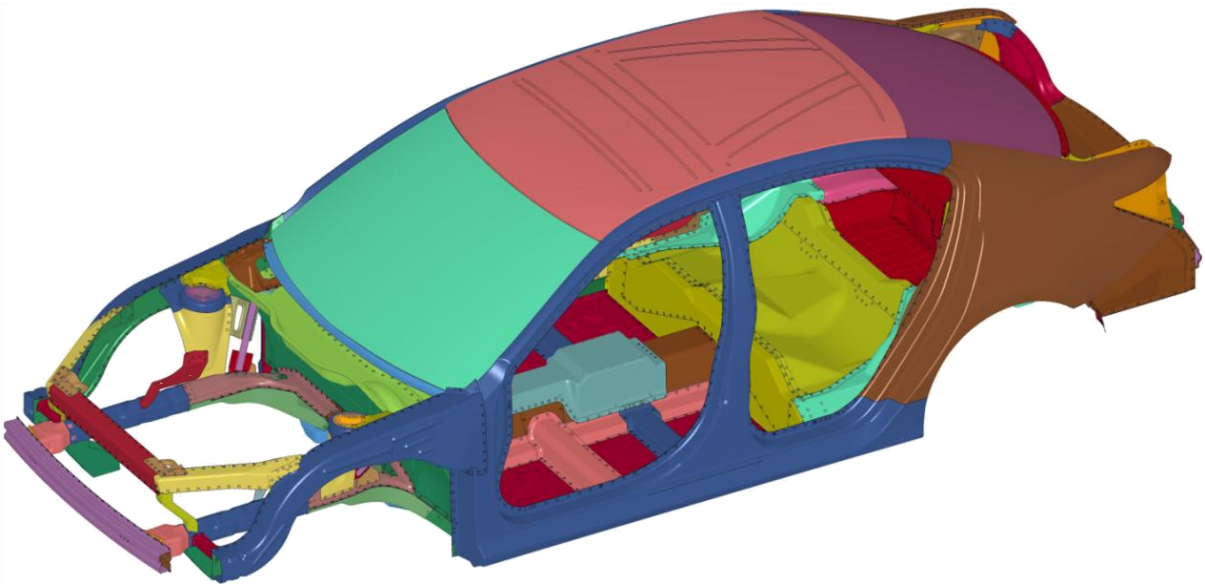

Figure 38 **Trimmed BIW ready for NVH calculations**

The parts brought in from the regular NHTSA FEM model partially were missing connections, which were made up for by RBE2 elements being installed. Also the laser brazing connection between the roof panel and the side roof rails was established by manually installed RBE2s.

After all those preparation efforts the model eventually was ready for calculation. The stiffness behavior was assessed on the basis of the natural frequencies as well as the static torsion and bending stiffness of the body structure. The analysis calculation parameters were not set using ANSA, but one

of the other established FEM pre- and postprocessor tools, HYPERMESH by ALTAIR ENGINEERING Inc. The computation itself was carried out by the solver NASTRAN.

For the free frequency analysis only the frequency range to be investigated for eigen modes needed to be defined, which was set to up to *80 Hz*. Looking at the deformation patterns of the different calculated eigen frequencies the front end lateral mode, the first bending mode and the first torsion mode could be identified and later compared to the ones of the laser welded model.

The static runs needed a little more effort to be set up. For the torsion stiffness RBE2-spiders were connected to the top panels of all four shock towers (see *Figure 39*). The center nodes of the spiders of the rear shock towers were simply respectively freely supported, i.e. all or some translational, but not the rotational degrees of freedom were locked, as shown in *Figure 40*. For the front there were two contra directional vertical forces applied on the center nodes. To stabilize the body structure a node right in the middle of the front bumper at *y = 0* was locked for vertical movement. Creating a statically defined fastening, the y-displacement of one rear shock tower was not locked. The computed displacement at the front shock tower center nodes and the distance between the two center nodes was used to calculate the torsion angle. Relating that angle to the applied forces the stiffness could be determined in *kNm/degree*.

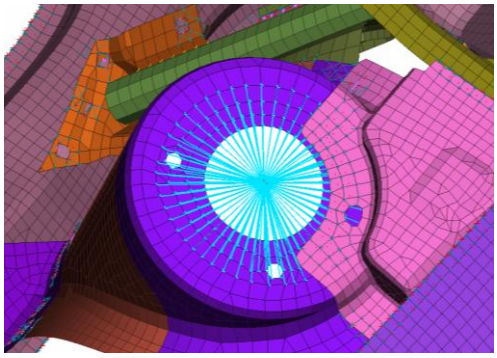

Figure 39 **RBE2-spider connected to front left shock tower**

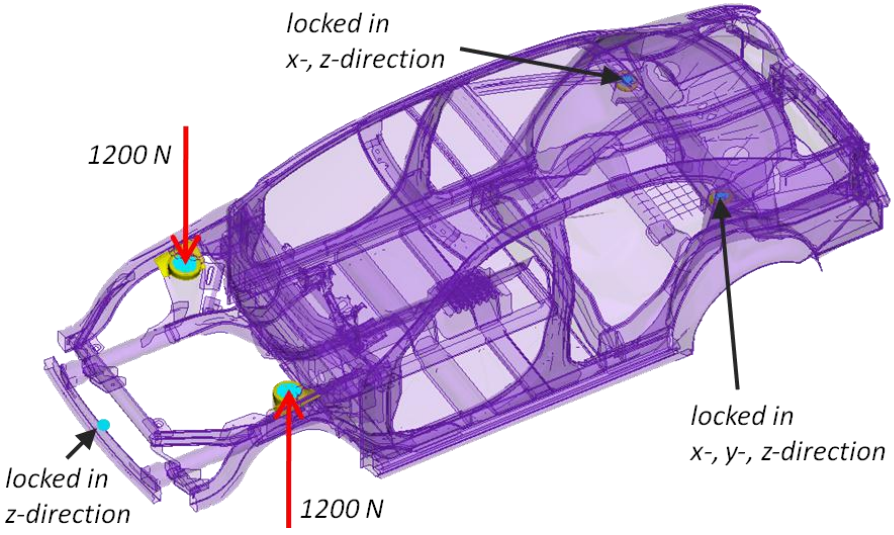

Figure 40 **Set up for determination of static torsion stiffness**

For the bending stiffness measurement all shock tower spider center nodes were simply or freely supported. At the center points of the four seats vertical forces were applied. Via rigid bars those were passed to the front seat supports and the rear seats' points of load transmission, distributing the weights of four worst case passengers on four points each, see *Figure 41*. For the application of the forces to the structure again RBE2-spiders were created (not displayed). Relating the maximum deflection found in the rocker to the forces gave the bending stiffness in *kN/mm*. Hence, besides the eigen frequencies there were two characteristics from static available for comparison.

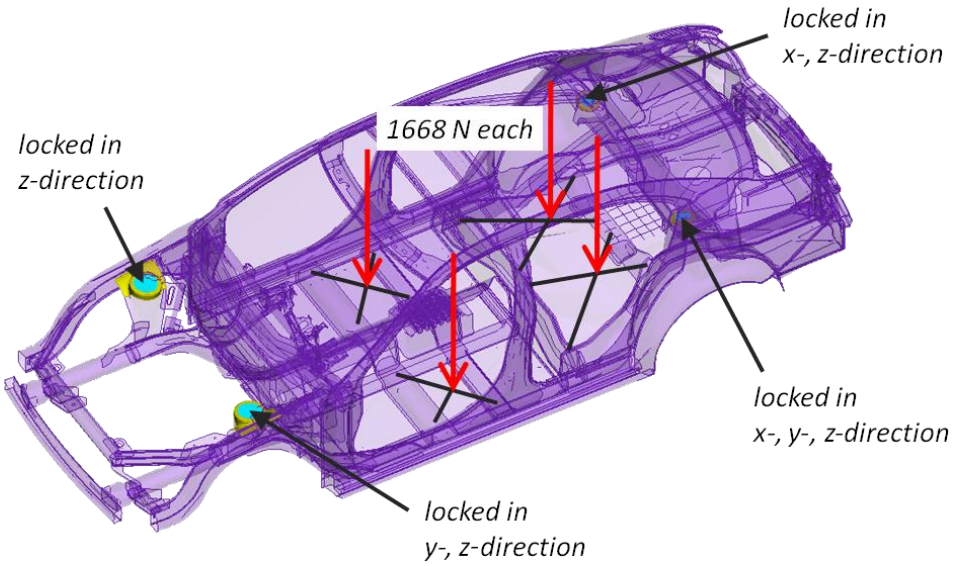

Figure 41 **Set up for determination of bending stiffness**

5.3. Assembly Layout for Solely Resistance Spot Welded Structure

The assembly layout was designed in cooperation with EDAG Germany. Two experienced production engineers were introduced to the project at the EDAG, Inc. USA facility during one week. The cooperation included the compilation of an assembly tree, the designing of an assembly layout according to that and a cost calculation including depreciations on equipment, operating costs, maintenance etc.

As the basic NHTSA project body structure contained not only spot, but also laser welds, small changes to the geometry had to be considered to permit joining by spot welding on almost the whole body structure. This mainly concerned the side structure, where a lot of laser welding was applied for the base model. Those changes were not actually carried out in a CAD or FEM model, but were only analyzed regarding feasibility. It was born in mind that the modifications were small and would be adoptable without a considerable cost impact. Also it was considered to find an assembly sequence which would necessitate the least amount of changes compared to the base model. Prerequisite was that no geometry changes would be required which had to be taken into account for the cost calculation.

One of the joint configurations which required some design changes for spot welding was the rocker area. Since the rocker panel was designed as a rolled, closed profile it was predestined for laser

welding. Converting the structure to spot welding, two more flanges would have to be rolled into the profile (green) to accommodate the main floor panel (blue) and the pillars' inner panel respectively the rocker cover (grey), as displayed in *Figure 42*. Since the profile still would be closed, 3T welds of two parts would be established. The outer side panel (yellow) could be joined by adhesive bonding and single sided spot welding. Both those joining technologies do not show as high tensile strength as regular spot welding. But the connections to the outer panel also were carrying fewer loads, since the outer panel traditional is of lesser structural importance than the other parts surveyed here.

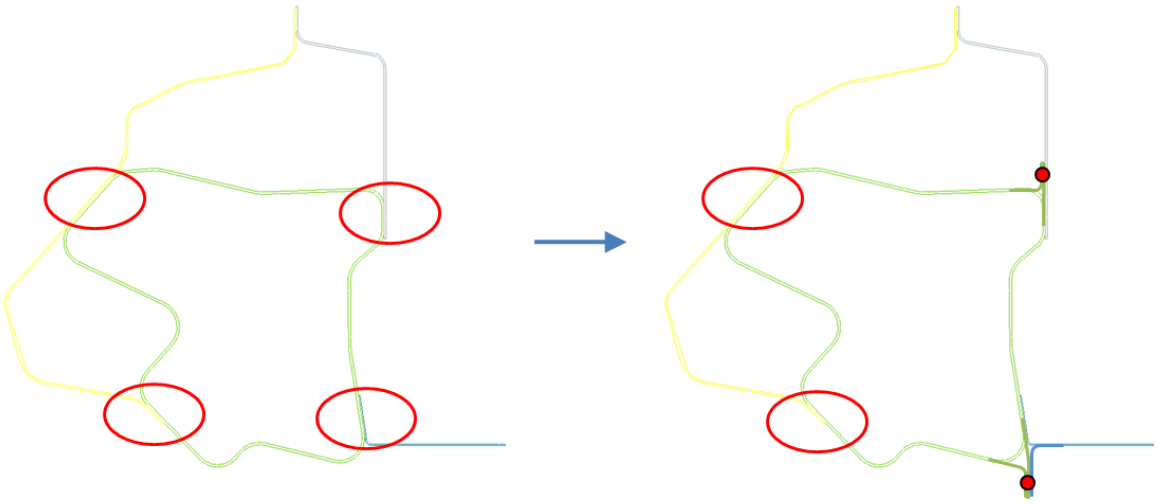

Figure 42 **Cross section of rocker area turning the laser weld joints (red circles in left picture) into spot weld joints**

The modifications to the main floor flange were self-financing and the ones done on the rocker section were negligible regarding costs. So it was assumed that it was feasible to convert this area to spot welding without considerable effort and the attention was drawn to the next laser welded joint. As said no changes were depicted in any CAE model. So also no weight changes conditioned by production requirements were analyzed. For the discussed example there would have been further weight benefits for the laser welded structure caused by the added flanges. But to take aspects like this into account would be out of the scope for this study. Following up on this approach would have led to redesigning the whole structure.

Considering all joints of that kind an assembly tree was developed, showing which parts would affiliate or compose which assembly at which station. Due to the poor manageability the assembly tree cannot be shown in this report, but is explained in detail on the following pages, starting with the front end of the lower structure. The first subassembly to be discussed is the dash panel reinforcement subassembly shown in *Figure 43*. After the parts are loaded into the geometry station they are clamped within very close tolerances to make sure the assembly fulfills the required quality criteria. Then a few spot welds are created to maintain that precisely defined position of the parts relative to each other. This step is called geo welding and contained *22* spot welds for the shown subassembly. Hence the parts are removed from the geometry station for better accessibility and the rest of the designated spot welds are placed. This operation is called respot. The respot sometimes is carried out in separate stations, because the robot may has to change its position holding the part. For the dash reinforcement, there were *30* respots applied within three steps.

The number of weld spots necessary to join an assembly is defined by design requirements. But the distribution of those spot welds to geo welds and respots is fully owed to manufacturability. Also the number of stations is a manufacturing criterion. The cycle time for each single station for this assembly was defined to *55* seconds. Needless to say the number of stations should be kept as low as possible, still ensuring that a welding gun can assess each single spot weld location at some stage and is able to weld the required number of points within the cycle time. So defining the geo welding and respot stations already sets the basic requirements for the assembly layout. That is why this information is provided for each part of the assembly tree discussed in this chapter.

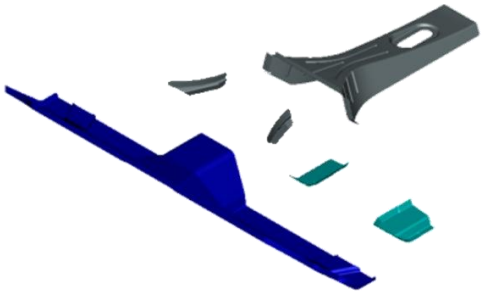

Figure 43 **Dash panel reinforcement subassembly of the spot welded structure**

Discussing spot welds in this section usually refers to 2T welds. If 3T welds were applied, this is clearly indicated. The number of points mentioned refers to the parts displayed, i.e. if of symmetrical parts only one side is displayed, the spot weld figures also just give the number of this one side assembly.

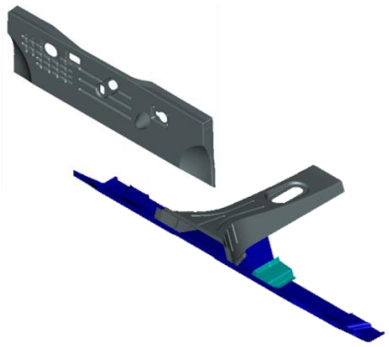

Figure 44 **Dash panel subassembly of the spot welded structure**

Figure 44 shows the dash subassembly. There are *24* geo welds and *18* respots applied to this subassembly. In total eight of those welds are done on three thicknesses. The cowl subassembly shown in *Figure 45* is built in two phases. First the upper cowl and the two hood hinges are welded with 22 spots in the geometry station. The respot contains *6* weld spots. Then the lower and inner cowl are welded with *22* geo welding spots and six respots. Eventually the two created built-ups are joined by *21* geo and *8* respot weld points.

Figure 45 **Cowl panel subassembly of the spot welded structure**

Hence the cowl panel and the dash panel subassemblies are joined to the dash subassembly applying *22* geo welds. After that *9* two thicknesses (2T) and *2* 3T respot welds in the first run and *9* in the second run are established.

The front rail outer subassembly was put together in five stages. First the front rail upper and the upper engine mount (two lower green parts in right half of *Figure 46*) were welded with *8* geo spots and respots each. Then the shock tower (grey) and the shock tower reinforcement (green) were joined by *8* geo spots and two steps of *13* respots and *8* respots. Those two subgroups were connected by again *8* geo spots and *10* respots to establish the upper front rail subassembly. The lower section of the front rail outer was created by joining the lower front rail (blue) and the "lower front rail to rocker" (bronze) with only *10* geo welds. Eventually the two groups were assembled using *24* geo welds and *12* respot welds and again *6* respots. In contrast the front rail inner could be joined in one assembly. This was done by *20* geo and *2* respot welds. The outer and inner rail were put together with *22* geo spot welds.

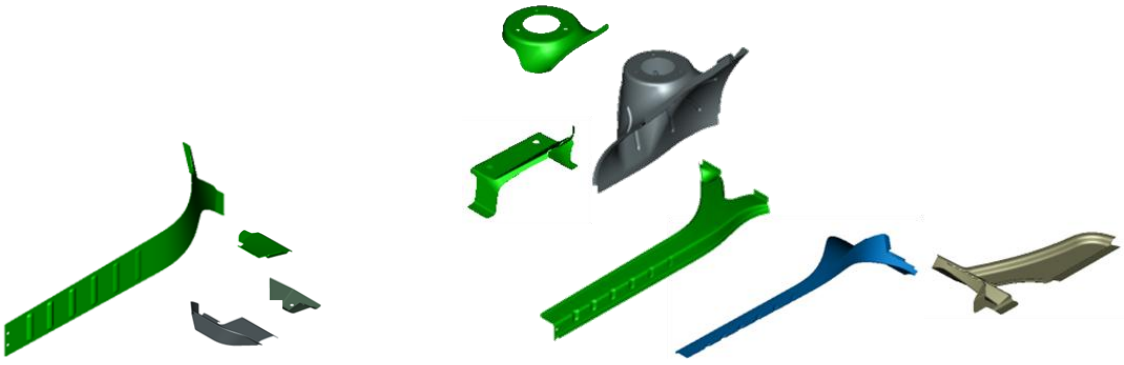

Figure 46 **Front rail inner (left) and outer (right) subassembly of the spot welded structure**

For the shotgun inner two stages were needed. The group shown in *Figure 47* on the left was joined by *12* geo welds and *10* respots. The two parts on the right were connected by *12* geo spot welds and *6* respots. The final subassembly was established by *14* geo welds and *6* respots. To join the front rail and the inner shotgun *24* geo welds and *8* respots were needed.

Figure 47 **Shot gun inner subassembly of the spot welded structure**

The radiator support was joined by *92* 2T and *8* 3T spot welds in total. The lower part, seen right in *Figure 48*, was made with *14* geo welds, while the upper part required only *6*. Putting them together was done with *32* geo welds, *48* respots in the first phase and the mentioned 3T welds as respots in the second phase.

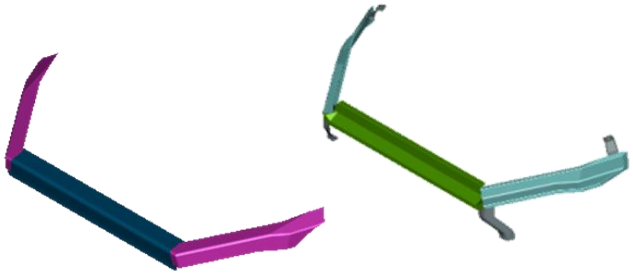

Figure 48 **Upper (left) and lower (right) radiator support subassemblies of the spot welded structure**

At this point the front end of the lower structure could be completely assembled. Therefore *36* geo welds, two times *48* respots and eventually *37* 2T and *4* 3T respots were required, adding up to *169* two layer and *4* three layer spot welds in total.

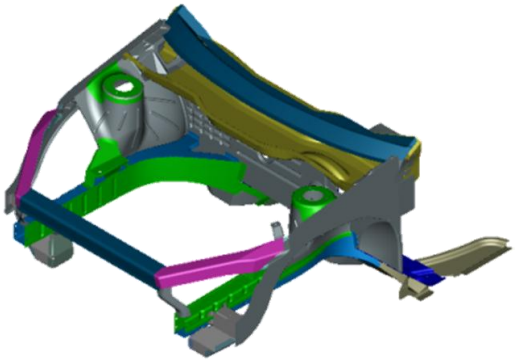

Figure 49 **Lower structure front end assembly of the spot welded structure**

The front floor assembly was created from two subgroups. First the tunnel (dark blue in *Figure 50*), the seat cross members front (dark brown) and the tunnel cross members (green) were assembled. The geo welding for this contained *16* spot welds, the first respot *10* and the second *20* welds. In the next station the other parts were added by geo and respot welding, applying another *200* spot welds.

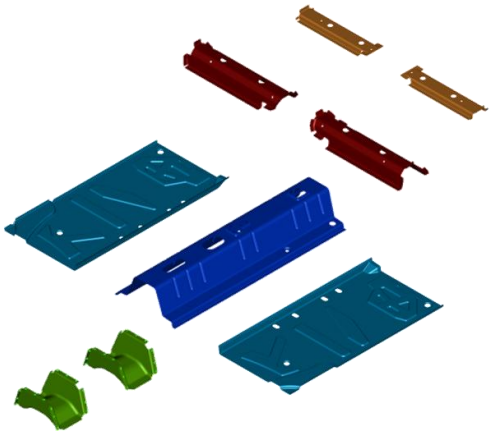

Figure 50 **Front floor subassembly of the spot welded structure**

To assemble the rear rail first the lower part of it was joined, containing the ten parts displayed in the lower end of *Figure 51*. This was the main lower rail, its extension to the rocker and the stiffening plate, and the rails suspension cradle mounts. The connection was obtained by *20* geo welds and *7* respots for each rail. The upper rail section containing the grey and the turquoise dyed parts was joined by *8* geo welds and *8* respots each, including one seat cushion support on each side.

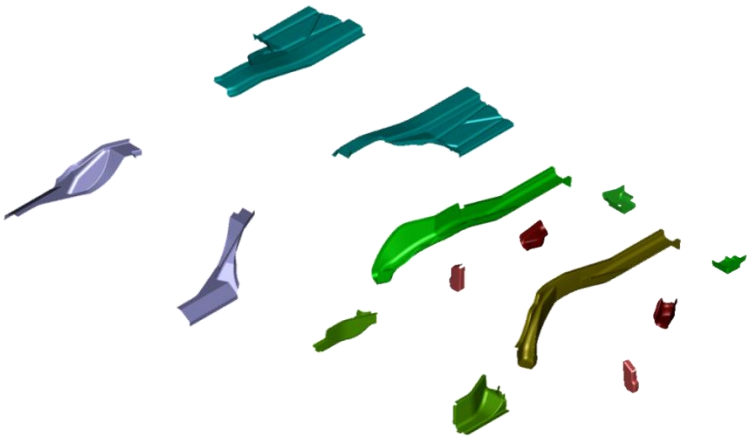

Figure 51 **Rear rail subassembly of the spot welded structure**

Coming to the floor area the rear cargo floor (bronze colored part in *Figure 52*) and the gas tank mounts (dark brown) were connected via *8* geo welds and *8* respots in total. The rear seat panel (olive) was joined with the waterfall panel (brown part to the very left) and the rear tunnel cross member (pink) with *18* geo welds and *13* respots. Before attaching those floor subassemblies to the rails both lower rails were combined by the cross member with *10* geo welds and *8* respots.

Figure 52 **Parts to be assembled to the rear floor**

Hence first the cargo floor subassembly was joined with the lower rail assembly making use of *18* geo welds and two times *11* respots in two different clamping configurations. Then the rear seat section came in, being connected by *18* geo welding spots and *10* respots. The five parts composing the inner wheel house subassembly shown in *Figure 53* were connected by *18* geo welds and *3* 2T and *3* 3T respots.

Figure 53 **Inner wheel house subassembly of the spot welded structure**

The last section belonging to the rear floor assembly was the back panel subassembly displayed in *Figure 54*. The parts are welded by *10* geo spots and three stages of respotting, with two times *20* and once *13* spot welds.

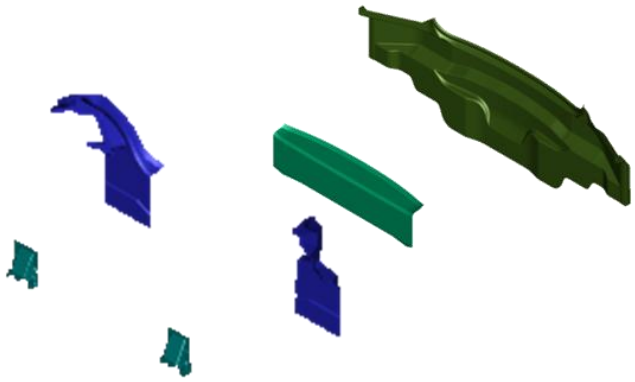

Figure 54 **Back panel subassembly of the spot welded structure**

To create the rear floor subassembly shown in *Figure 55* first the floor section was joined with the back panel, the inner wheel house and an additional cross member below the rear seat (blue). The geo welding for that operation comprehended *38* two layer and *2* three layer spot welds. Respotting was done in two steps, with *44* and *43* spot welds. Adding the upper part it was eventually possible to apply all the 3T welds coming with the rear rail. This sequence required *20* 2T and 3T spot welds each for the geo welding, *88* each for the first step of respot and *10* each for the second step of re-spot.

To complete the lower body the front structure, the front floor and the rear floor had to be assembled (see *Figure 56*). Geo welding was performed by *20* spot welds before the assembly was transferred to a buffer station. Then two respot stations followed, applying *52* and *53* spot welds. After another buffer a monitoring station checked *20* control points on the assembly before it was transferred to the next framer.

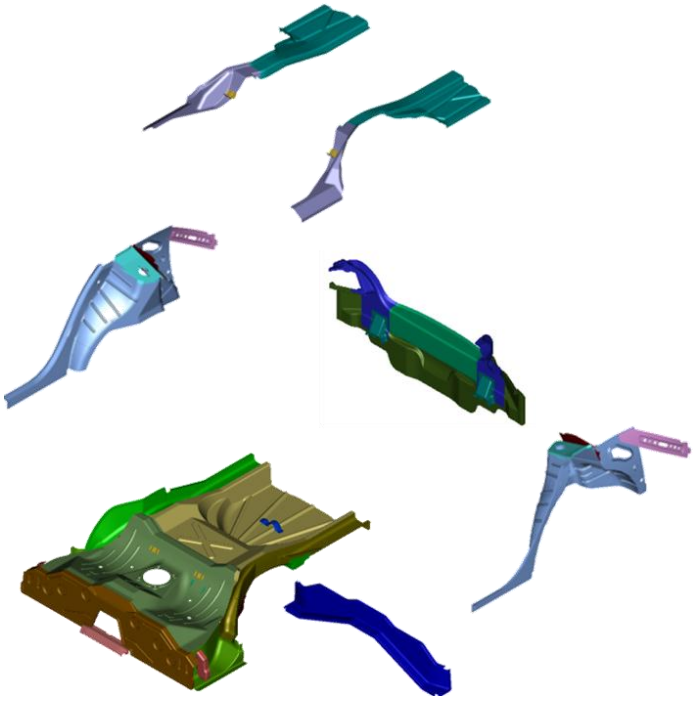

Figure 55 **Rear floor subassembly of the spot welded structure**

According to the BoM another subassembly belonged to the lower structure, thought it was not physically connected to the rest of it at that time. The package tray consists of three parts, shown in *Figure 57*. They are joined by *10* geo spot welds and three steps of respotting, containing two times *35* and one time *8* spots.

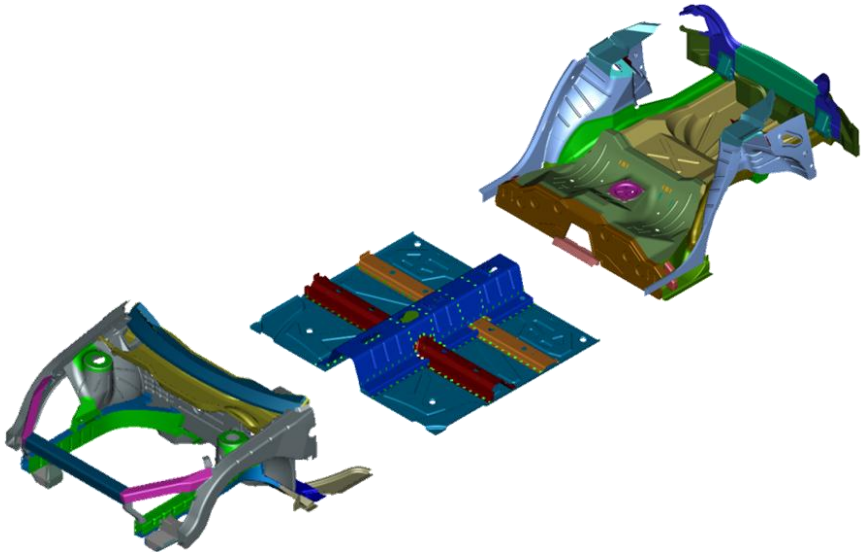

Figure 56 **Lower body assembly (framer 1) of the spot welded structure**

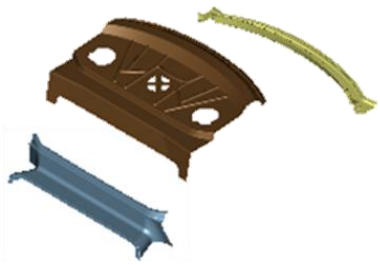

Figure 57 **Package tray subassembly of the spot welded structure**

Parallel to the lower structure the side structure was put together. The body side outer subassembly is shown in *Figure 58*, being assembled by *30* geo welds and two respot operations of *12* and *44* spot welds.

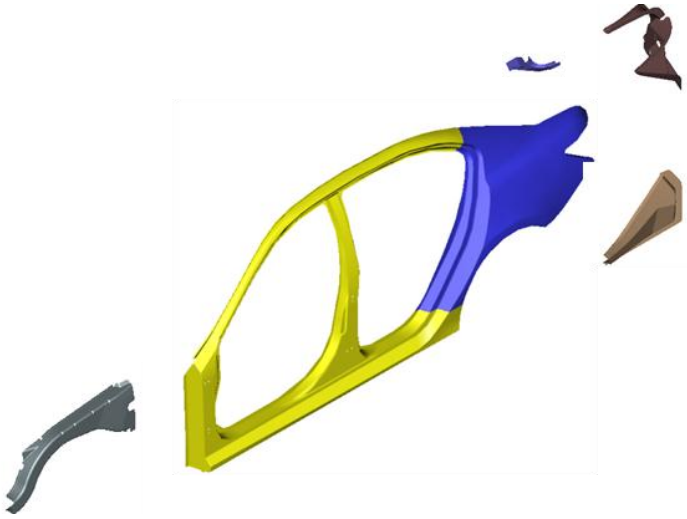

Figure 58 **Body side outer subassembly of the spot welded structure**

The other subassemblies of the side structure unfortunately were not planned in detail when this report was created. In the following there will only be an overview provided of the subassemblies. *Figure 59* shows the wheelhouse outer subassembly, which was created by *27* 2T spot welds at each side.

Figure 59 **Wheelhouse outer subassembly of the spot welded structure**

The body side reinforcement subassembly displayed in *Figure 60* was joined by *13* spot welds. *Figure 61* below shows the inner body side inner subassembly, which took *66* spot welds to be joined. Some of those welds were 3T connections, since the B-pillar inner, the front rocker cover and the inner A-pillar panel were connected to the rolled flanges of the rocker discussed above.

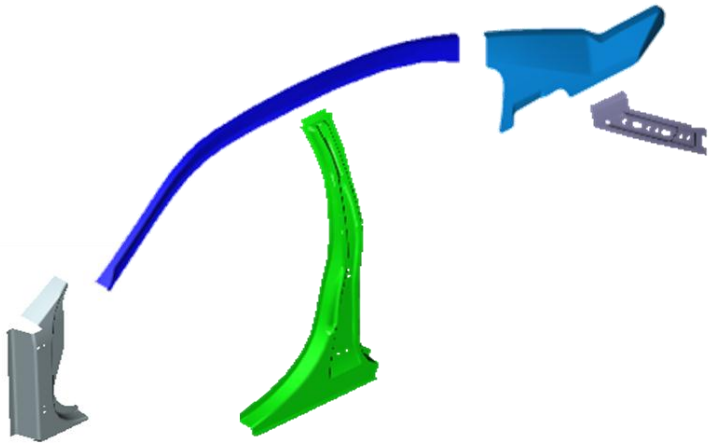

Figure 60 **Body side reinforcement subassembly of the spot welded structure**

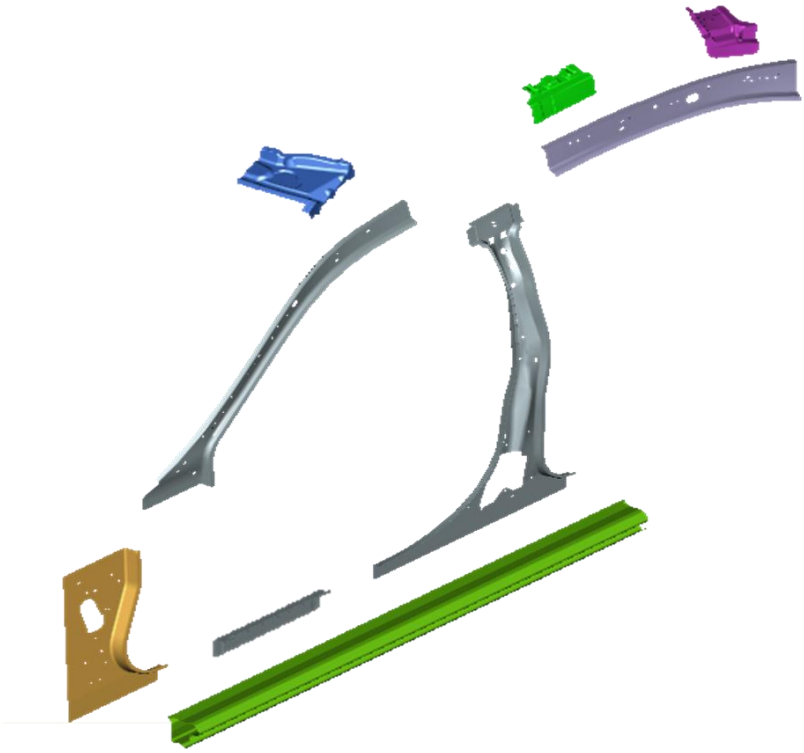

Figure 61 **Inner body side inner subassembly of the spot welded structure**

Joining the wheelhouse outer, body side reinforcement and inner body side inner subassemblies required *167* spot welds per side. Also MAG welding needed to be applied here with a length of about *715 mm*, as there was no other way to attach the reinforcements of the A- and B-pillars to the closed rocker profile. The front flange of the A-pillar actually should have solely been 3T spot welded in one of the framer stations also involving the body side outer. But due to accessibility issues the section of the flange covered by the shotgun outer in that framer was 2T spot welded already in this subassembly. Having the body side inner and outer subassemblies, which get joined to the structure at different framing stations, set up the side structure was complete.

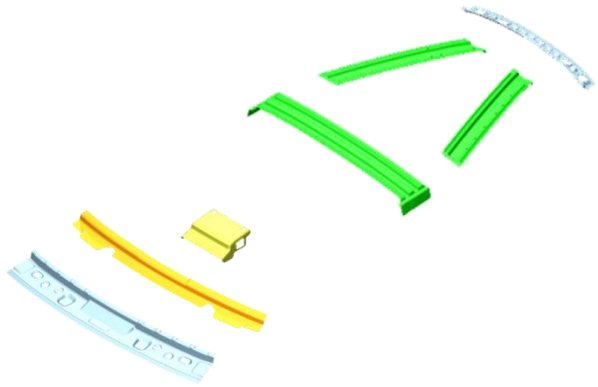

Figure 62 **The two subassemblies forming the upper structure**

Being the smallest subassembly the upper structure only comprehended two subassemblies, apart from the roof panel which was added to the structure in the last framer. The center roof assembly, displayed on the right of *Figure 62* was geo welded with *8* spots and rewelded with *2* spots. The rest of the parts, forming the front roof assembly, were joined with *14* 2T and *4* 3T geo spot welds and two times *10* respot welds.

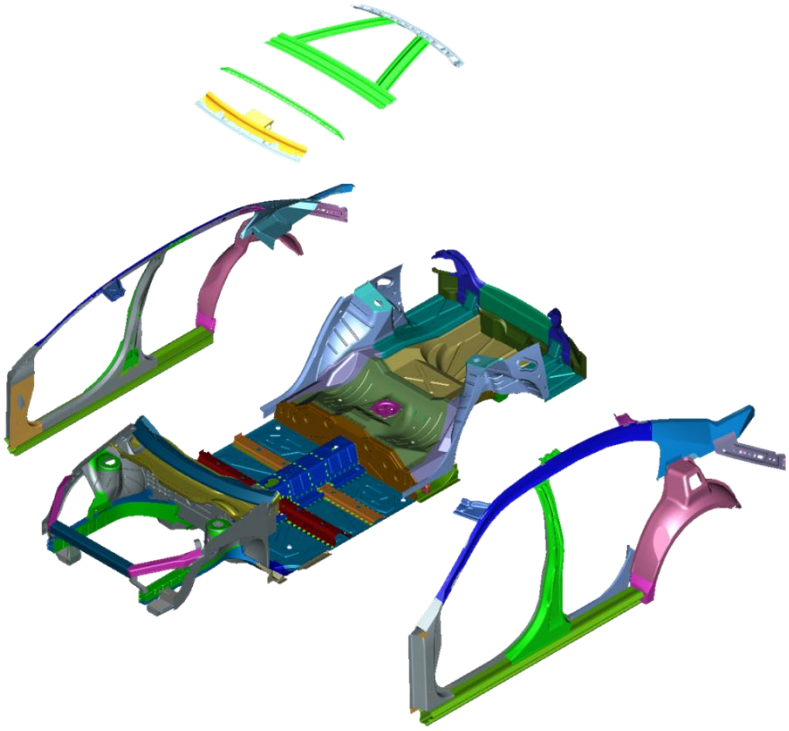

Figure 63 **Framing station two of the spot welded structure**

Having all subassemblies completed they were joined in three framing stations. Beginning with framing two – framing 1 was the last step in the assembly of the lower structure – both body sides inner and the upper structure were connected to the lower structure. Before the side subassemblies were attached to the lower structure in total *7776 mm* of adhesive were applied in the wheelhouse, rock-

er and A-pillar areas. This is common on spot welded body structures nowadays and is helping to improve the stiffness in those key areas as well as acting as a sealer. After the roof subassembly is added, inserting the parts displayed in *Figure 62* and an additional roof bow, in the next station the subassembly is connected by *48* geo welds and *84* respots. After a buffer area another three respot stations are passed through, applying two times *84* and one time *48* respots. Going through one more buffer station subsequently the subassembly is measured at 20 points for quality monitoring.

In framing station three the body side outer subassemblies and the package try was added, see *Figure 64*. About the same amount of adhesive as in framer two is applied to the rear wheel house, the rocker and a section of the A-pillar. The subassemblies were fastened by *42* geo welds. The whole framing contained *13* stations. After the unfinished structure had been lifted to the adhesive bonding station and went through the geo welding it was first buffered. Then there were two respot stations, a buffer, again three respot stations, another buffer and finally a measuring station. Those respot stations applied a total of *663* spot welds. The measuring station at the end was double checking *50* points.

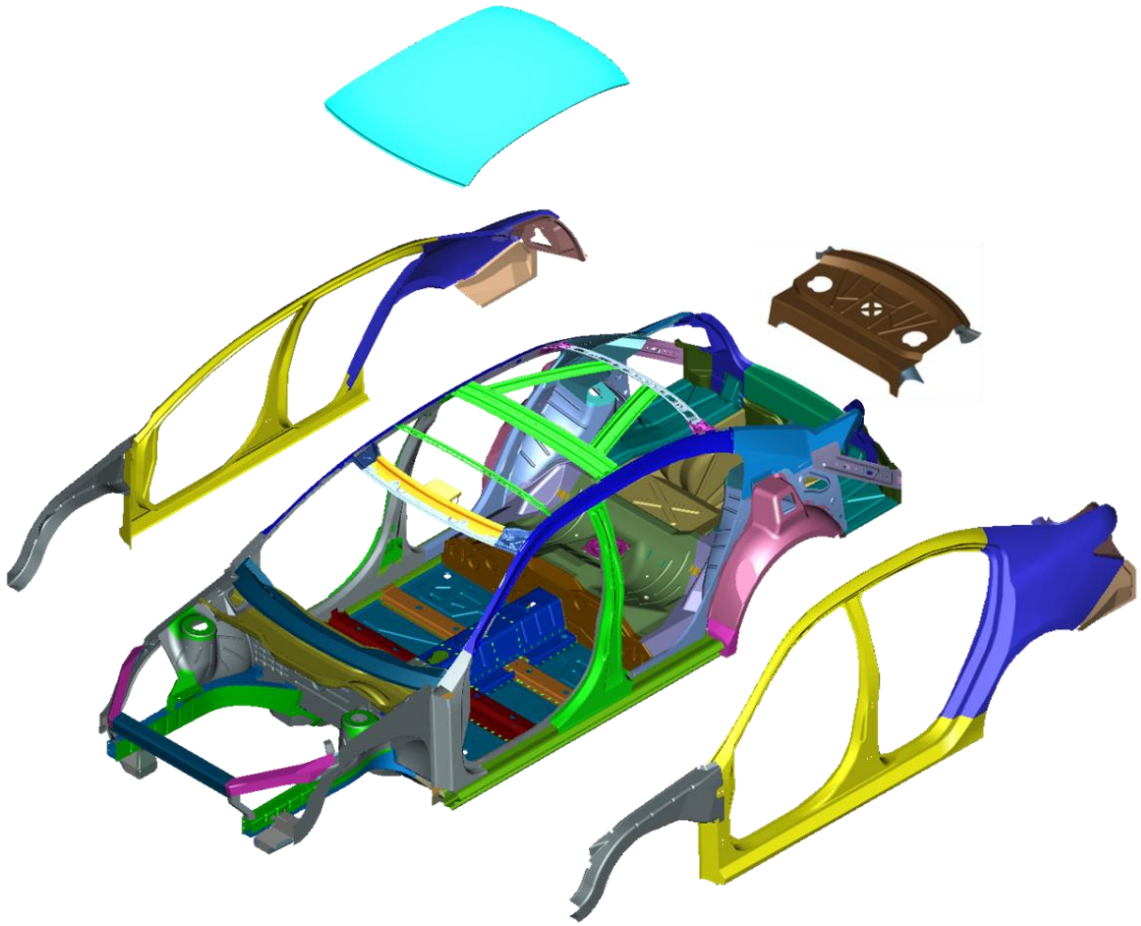

Figure 64 **Parts assembled in framing stations three and four**

Hence the framing station four finished the body in white by attaching the roof panel, which also can be seen from *Figure 64*. Again there first was adhesive applied; about *3000 mm* to the roof and *4474 mm* to the body to fit the roof panel to its support structure. After being geo welded at the

front and rear ends, the panel was laser brazed at the sides to the roof rail, creating two seams with an accumulated length of *2822 mm*. Here on the front and rear end were respotted with *46* welds and the brazed seam was brushed. After two more buffer stations spread between four quality check and finishing stations, the body structure was ready to proceed to the paint shop.

As indicated in the beginning of this chapter, the configuration of geo welding and respotting and the resulting number of stations defined the basic requirements for the assembly layout. Setting up the design of this whole manufacturing procedure gave information about how many robots, welding guns etc. were required. From that the assembly and the shop layout finally could be developed.

5.4. Costs Estimation for Resistance Spot Welding Assembly Layout

If a detailed assembly layout was provided, the costs can be calculated from that quite easily. Having the whole shop layout for the spot welded assembly planned after setting up the assembly tree, all the required machines, equipment, media etc. were known. Since the quantity as well as the kind of equipment was precisely defined, the production engineers could use their databases to find out the costs for each piece. It was essayed to include all relevant equipment in the calculations. This included for example the setup of all stations, such as fences, safety circuits and illumination; the entire power periphery required for the welding guns and the robots, for example switch boards, processing units, control units and monitoring displays; the transportation gear to move the parts and subassemblies, like robots, lifters and belt conveyors; the welding equipment itself etc.

Having cost numbers for all those components available they were added up to the total costs of the assembly layout. Depreciation was not taken into account, since it was assumed to be similar for both spot and laser welding equipment. Since the available production key figures were European based, the costs internally were calculated in Euros. After the consultation of American production engineers it was decided to just transfer the Euro-figures to US-Dollar using the current exchange rate. According to the experts the costs for equipment are globally the same due to the globally active suppliers. Manpower regarding set up of the shop layout was considered to be a bit more expensive in the USA, while the costs to operate the assembly were assumed to be lower. Those effects would cancel each other; that is why here only the exchange rate was used as well.

6. Creation and Evaluation of Solely Laser Beam Welded Structure

After the solely spot welded model was established this data set was taken to develop the solely laser welded structure for comparison. The process was similar to setting up the spot welded structure. So the annotations in the following chapter are focusing on the differences to the procedure described above.

6.1. Converting Body Structure to a Solely Laser Beam Welded Structure

The spot welded FEM model was taken as the starting point for the laser welded model to be able to use the morphing boxes created already. The same boxes used to extend the flanges which initially were too short for spot welding applications now could be used to trim the flanges as required for laser welding. Of course, many morphing boxes needed to be created additionally. This was done according to the procedures described above for all the other flanges envisaged to be trimmed. At the end *357* flanges were modified to set up the laser welded model. This was done with the help of *115* morphing parameters controlling *601* morphing boxes with *18054* control points and numerous direct morphing operations. All the morphing boxes created for the laser welded model are displayed in *Figure 65*. In the following a few examples of how certain flanges were modified are discussed.

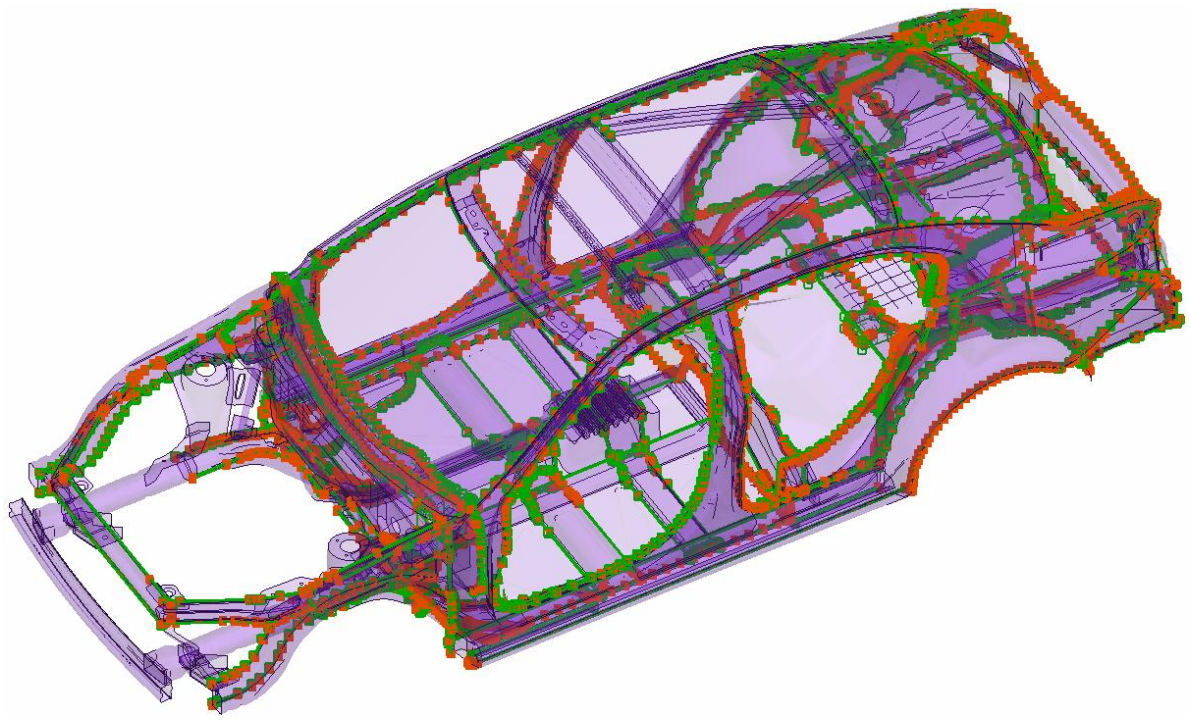

Figure 65 **Morphing boxes created to edit the laser welded model**

For the door entries mainly the morphing boxes already used in the spot welded model could be used. The shotguns on the other hand belonged to the parts whose flanges had a fitting size for spot welding, so that no changes were done while generating the spot welded model. But now to trim those flanges from *16 mm* down to *8 mm* new morphing boxes had to be created. Since all the

flanges connecting the inner to the outer shotgun (see *Figure 66*) were of the same shape all the morph boxes containing them could be gathered in one morph parameter to be morphed altogether. As the accumulated flange length for the inner and outer shotgun separately and for both sides was *12562 mm* a considerable mass saving could be achieved only for those four parts.

Figure 66 **Modified shotgun flanges (red curves) and areas not modified (arrows)**

But as mentioned in chapter 4.1 there also were flanges which were not modified at all. All areas pointed at by red arrows in *Figure 66* were not edited. For structural reasons the flanges in those areas required to be large to accommodate not just one but at least two rows of spot welds, which for example holds for the flange of the engine mount panel (grey dyed) to the shock tower (yellow). Those areas in general were not modified. Another flange like this which was not trimmed is the connection from the roof bracket bow to the roof rail, which is displayed in *Figure 67*. Since this flange plays an important role for the side impact and the roll over test it was kept at its initial size.

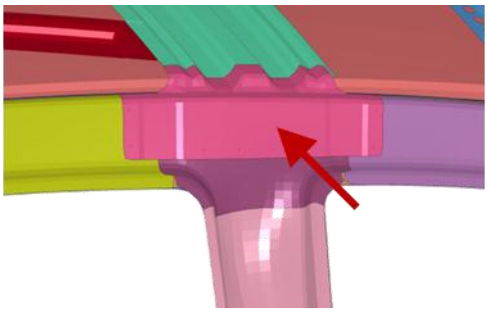

Figure 67 **The center roof bow bracket was not modified**

Another area to be mentioned for not being trimmed due to structural reasons is the region below the rear lamp can. The flange at the rear end of the rear rail was not trimmed since it creates a laminar connection to the back panel outer. Also its counterpart on the upside of the rear rail, the rear

rail inner bracket highlighted in *Figure 68*, was not trimmed. The same holds for the outer flange of the back panel inner, which also is a crucial part for the rear impact crash test.

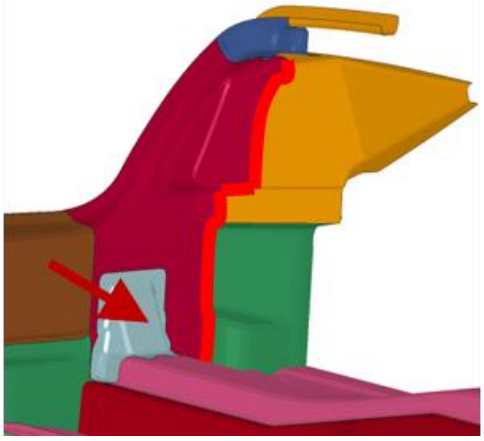

Figure 68 **Rear rail inner bracket (red arrow) and outer flange of back panel inner (red line)**

Some flanges which were very large initially but did not only gain their structural importance from their sheer size were trimmed by the delta of *8 mm* to compare spot to laser welding, no matter which original width they were. A lot of flanges like this could be found attached to the rocker, see for example the "front rail lower to rocker" flange in *Figure 69*.

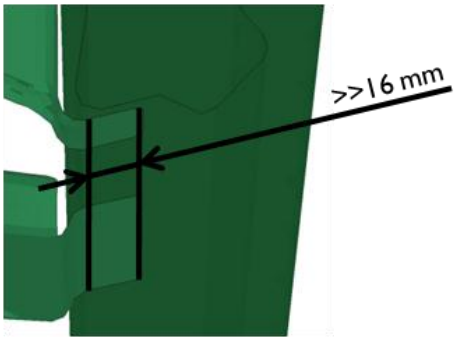

Figure 69 **Most flanges to the rocker initially were considerably wider than *16 mm***

Earlier on it was stated that to take full advantage of laser welding, a full reconstruction with respect to the much lower accessibility requirements of laser welding was required. On the other hand there were also certain areas where in a reduced scale that virtue could be beneficial for the present structure. Assuming a proper clamped support is feasible the 3T spot weld of the three cowl panels could be replaced by two double thickness laser welds, of which one is significantly translated forward avoiding the large double layer area of the green and the blue panel displayed in *Figure 70*.
One extraordinary morphing operation was performed on the rear end of the package tray towards the trunk lid frame (see *Figure 71*). Right before the package tray cross member is bent upwards to represent a part of the trunk lid frame it is bonded to the reinforcement package tray. The flange of this bonding also was subjected to trimming for the laser welded structure. Not trimming or anyhow modifying the trunk lid frame itself, it was moved forward as a whole to make the flange to the reinforcement narrower. Of course the reinforcement package tray flange was trimmed accordingly.

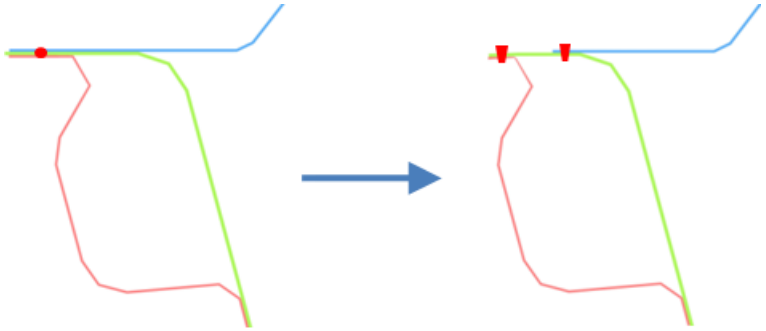

Figure 70 Y-cut through the dash panel area between wind screen instrument panel beam

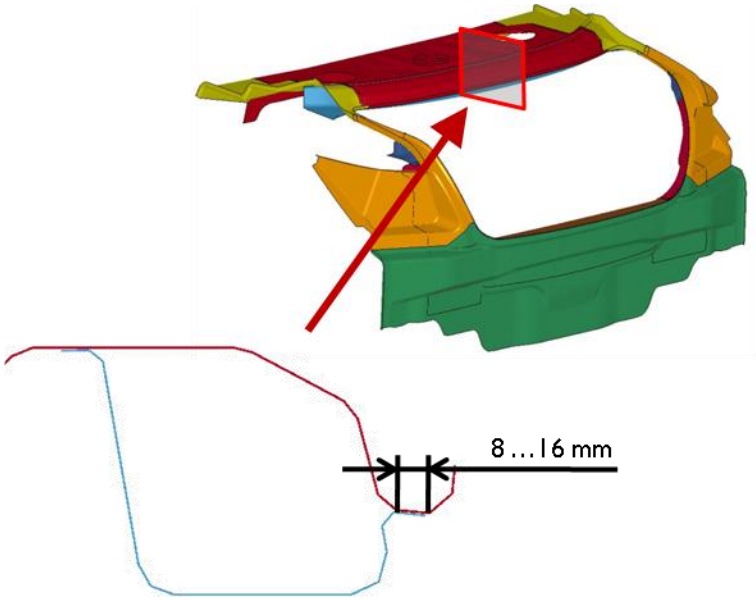

Figure 71 Package tray (red) meeting reinforcement package tray (blue) in the trunk lid frame region

As for the spot welded structure, after all these modifications the weight of the laser welded body structure could be determined very easily right from the FEM model. Also here the weight of each part of the body structure was determined separately to permit a detailed weight comparison later on.

6.2. Performance of Solely Laser Beam Welded Structure

Preparing the laser welded model for the NVH calculations was related to much more efforts than for the spot welded model. Almost the entire joining technology consisting of spot weld points was deleted and had to be redone as continuous weld lines. Those lines were created by extracting curves from the flange edges using the "feature line to curve" command as described for the creation of morphing boxes in Appendix A. The curves then were converted to adhesive lines which could be realized to create a continuous line of ACM2-connections.

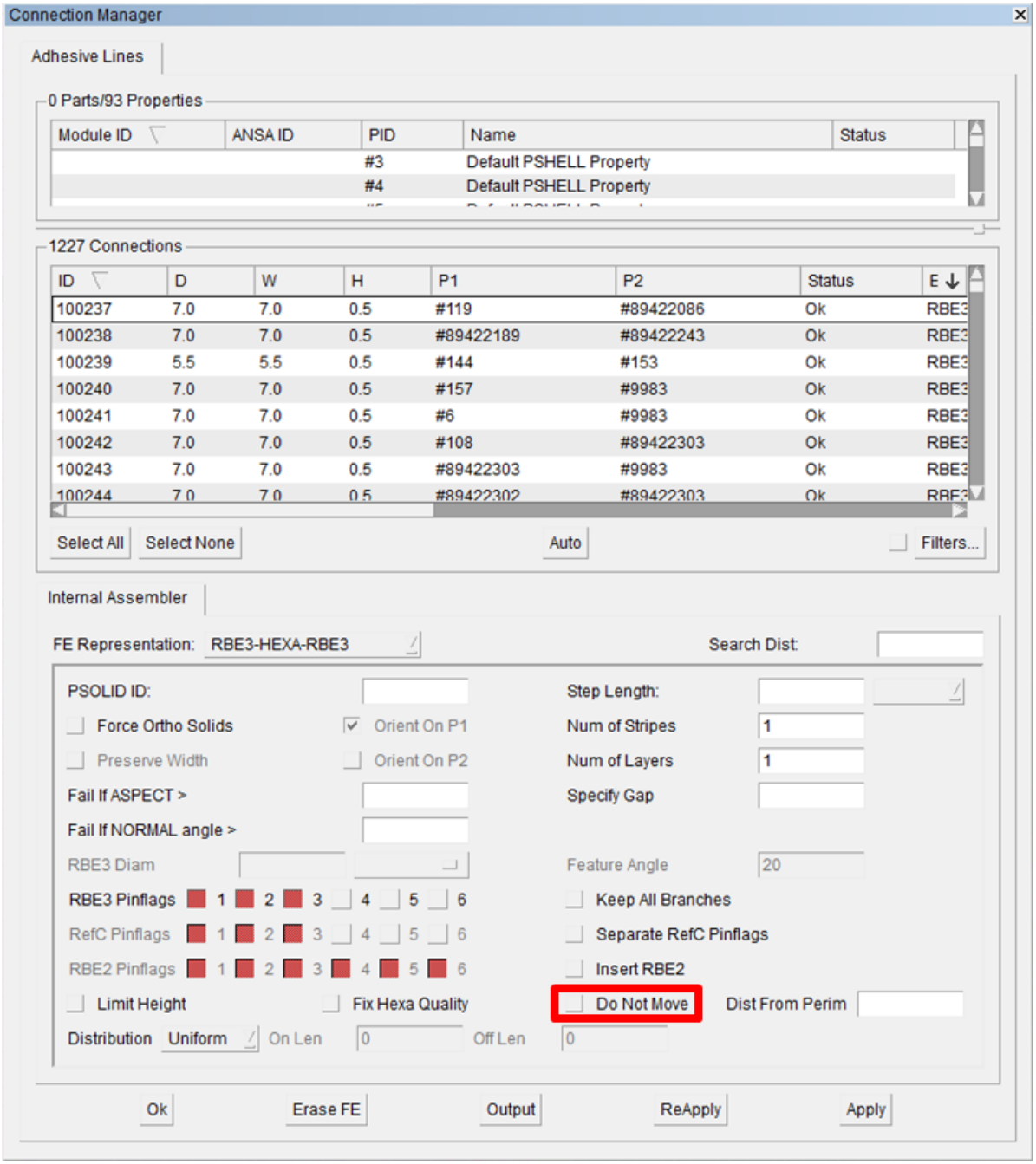

Figure 72 **Connection Manager of ANSA**

It was no problem that the weld lines were defined at the edges of the flanges and not in their middle, as explained in the following. *Figure 72* shows the connection manager of ANSA ready to edit all the adhesive lines created. Note the sub window where *1227* connections are listed. Here also the diameter *D*, width *W* and height *H* of the hexahedra representing the connection properties are chosen. The desired connections to be realized are selected within the described box and the FE representation kind is chosen, in this case RBE3-Hexa-RBE3. After further settings are made the selected connections can be realized by clicking "Apply". If the connection is allowed to move while being created, i.e. the "Do Not Move" box is unchecked (see red box in *Figure 72*), it is not hindering that

the connection line is not established in the middle of the flange. But this feature is only working with the type "adhesive line". That is why initially all continuous connections were created as this type, which is stated above. When all laser weld lines had been generated this way the properties of the hexahedrons simply were changed from adhesive connection to laser weld connection. Further changes would not be required since both connection kinds are continuous. So initially creating adhesive instead of seam weld lines was owed to the benefit of using the curves from the flange edges, which were far easier to generate.

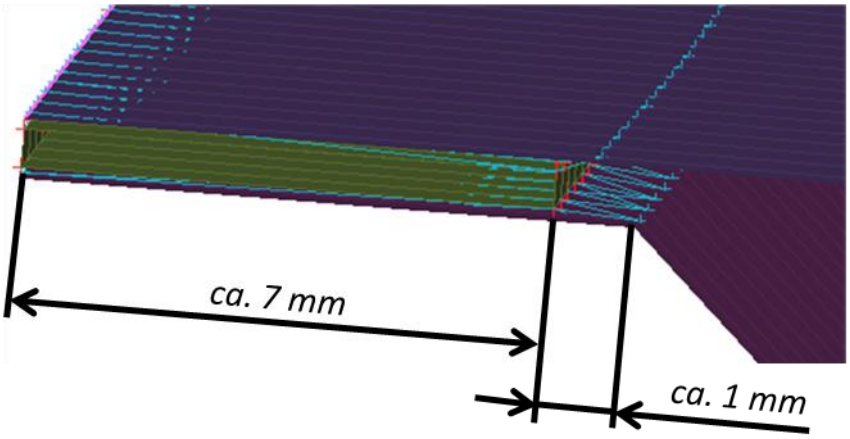

Figure 73 **Hexahedrons representing the laser weld fill almost all the flange width**

Actually the laser weld line should be positioned in the middle of the flange. If possible regarding production it should even be moved more to the root of the flange, which is beneficial for the torsion stiffness of the set up sub assembly. But the exact position of the laser weld on the flange cannot be modeled with conventional FEM methods. Though usually the maximum width of a laser seam weld does not exceed *2 mm*, a proper FEM modeling requires the representing hexahedron to fill the whole flange width (see *Figure 73*). This way it makes no difference where the laser weld actually is located on the flange. Since the flanges were modified to a width of *8 mm* the characteristic hexahedron diameter was set to *7 mm* to give only a small cushion whenever possible, as can be seen from the numbers in *Figure 72*. If the numbers in columns "*D*" were smaller, the connection was not able to be realized at a larger size.

See *Figure 74* for the illustration of a laser welding line created according to the described pattern. The pink line thereby is the foremost created adhesive line, from which the green colored hexahedrons and the turquoise colored RBE3-elements are realized.

The connections list in *Figure 72* also contains two columns *P1* and *P2*. Those are the parts to be connected. There is only room for two since both, adhesive connections and the desired laser weld connections, are only able to connect two parts at a time. Hitting the "Auto"-button the parts to be involved automatically were assigned, depending on a previously defined search distance. Nevertheless the connections where double checked to contain the right parts, especially the parts at three layer configurations had to be defined manually.

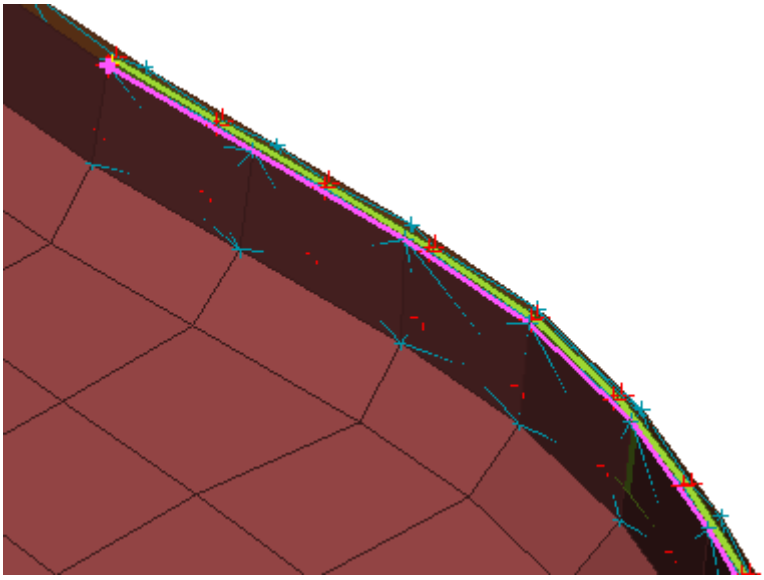

Figure 74 **Laser weld line realized with ACM2 FE connections**

To allegorize the 3T laser weld line approach described in chapter 2.2.2.3 the curve created from the flange edge was sectioned in subparts of *40 mm* length. The gap of *5 mm* or so in between two weld lines was neglected for simplification. Here on the curves were converted to adhesive lines like shown in *Figure 75*.

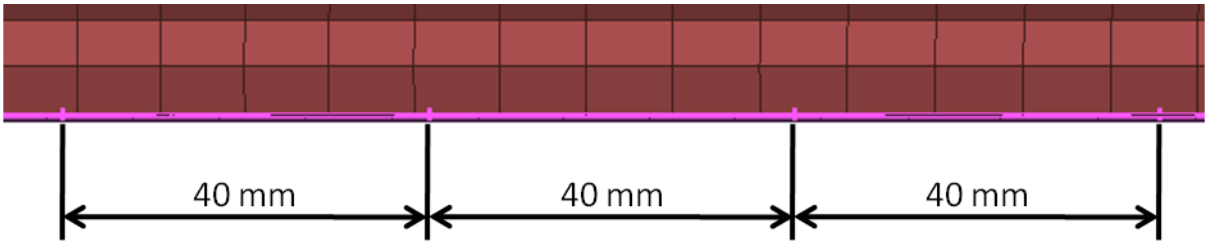

Figure 75 **Sectioned 3T laser weld line**

Then the connection manager was used to manually assign the parts to be connected to the subdivided weld lines. Every other small weld line of a flange was selected and the middle part and one outer part were assigned to them. After selecting all the other, leftover sub weld lines, again the middle part to be joined and this time the other outer part was assigned. Which outer layer was connected at the ends of the flange was decided after analyzing the structural design in the respective area. That the weld line was not located exactly at the position it was realized, i.e. that the staggered pattern was represented by a sectioned line, was no problem, since the connection automatically was realized between the assigned parts, which can be observed from *Figure 76*.

Luckily this procedure only had to be done for one side of the vehicle and all adhesive lines created could be mirrored to the other side just before they were realized. The same method was applied for the 2T weld lines. It was made possible by the fact, that mirrored parts for both sides shared the same property identification (PID), which was used for correlation to the welds. So the assignment of the parts to the welds also was mirrored with the welds. Eventually all the lines could be realized as

described above which gave the staggered pattern typical for 3T laser welds, as displayed in *Figure 76*.

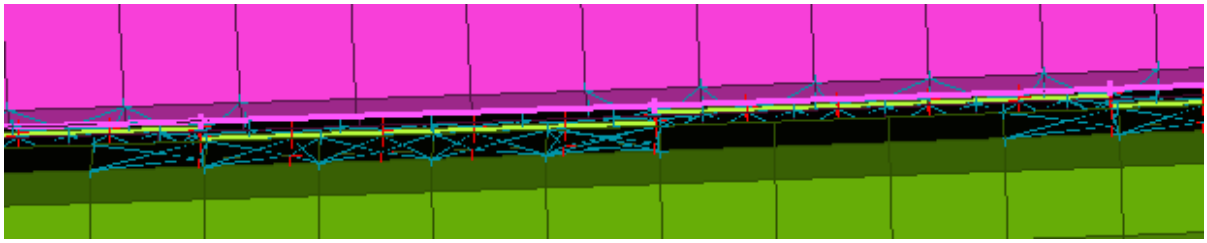

Figure 76 **Staggered pattern of laser weld connection FEM**

ANSA offers a function to automatically create spot welds along a flange with a specified distance to each other and to the flange edge. This function was used for parts which had a circumferential uninterrupted flange, since this method was less time consuming in those cases.

Actually, for FEM a truly continuous connection is not achievable. Boundary conditions can only be applied to the nodes, which always have a certain distance to each other. In between, it is not possible to establish a connection. But if every single node on a node line of a flange is connected to the same on another flange, there practically is a continuous weld created.

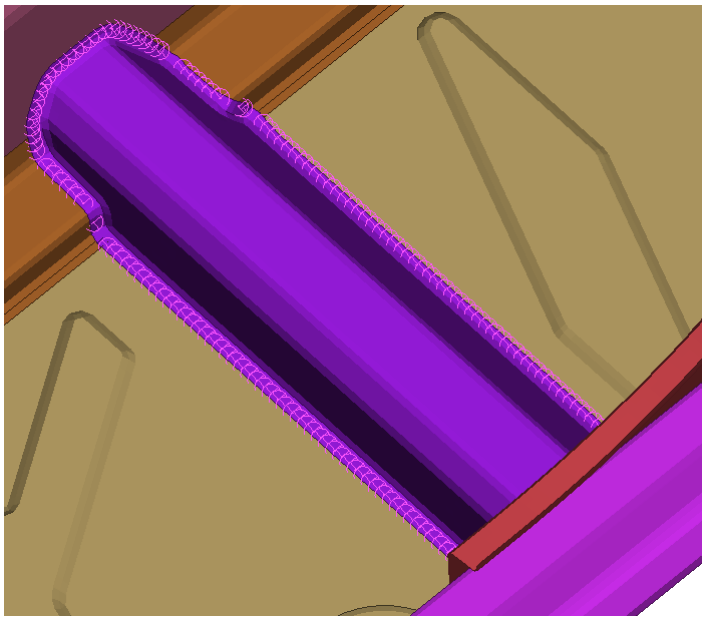

Figure 77 **Spot welds defined with very small spacing representing a continuous weld**

So this automatic spot weld tool was used to create a weld for every node by setting the spacing between the welds to *7 mm* which is below the average element length of the model of *10 mm*, creating a little safety margin. Note that in *Figure 77* the pink circles represent the spot weld connections. The spot welds which were generated at small radii of the flange geometry or at part transition zones were deleted manually. Also the parts to be connected were assigned by hand, which however did not take too long. Realizing those spot welds with the previously used ACM2-connestions actually created the same connection as an adhesive or seam line, where also just the hexahedrons are placed very close together.

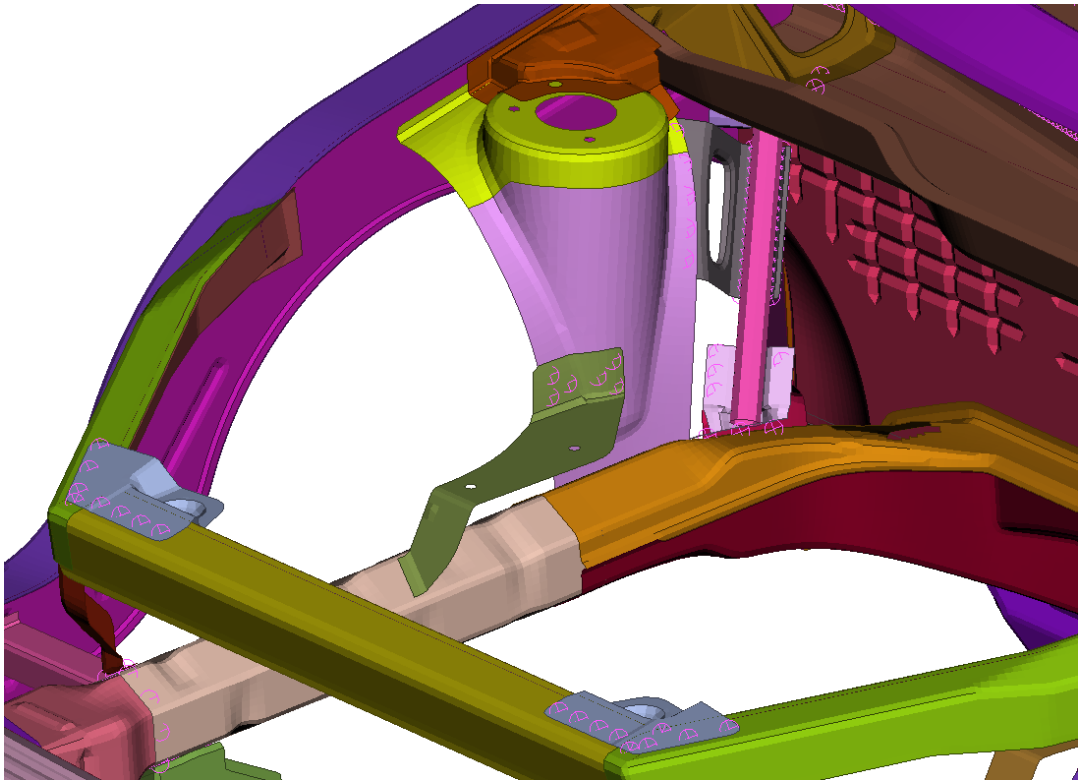

Figure 78 **Kept spot welds in the front structure**

Though the goal was to create a completely laser welded body structure, a few exceptions were made where this was not feasible or just made no sense at all, conditioning the use of a few spot weld connections. Some parts also were simply not relevant for the study, so they were kept the way they were, which was spot welded.

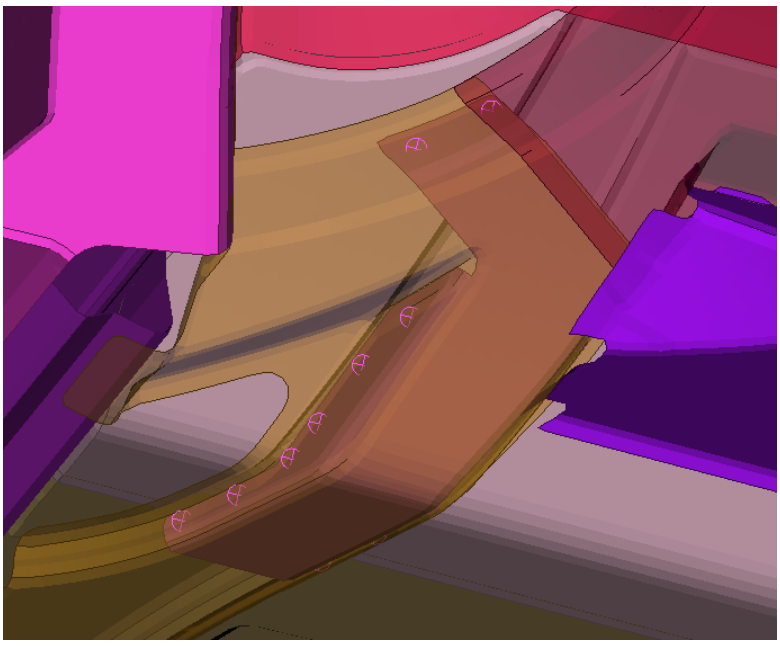

Figure 79 **Abandoned reinforcement inside lower front rail rear to rocker**

The latter applies for the radiator mounts (grey in *Figure 78*) and the previously mentioned support structure between shock tower and dash panel. The engine mount (olive) on the other hand is fixed to the shock tower with two rows of spot welds over a curvature, making it a flange requiring a large expanse. This would have been difficult to represent with a realistic laser weld.

The no relevance criterion again holds for the parts displayed in *Figure 79*, *Figure 80* and *Figure 81*. Both the reinforcement inside the connection of the front rail to the rocker and the parts in the tunnel area – the extension of the dash panel support to the rear and the structure below it – were eliminated from the NHTSA model later on, so there was no point paying further attention to those rather poorly conceived parts.

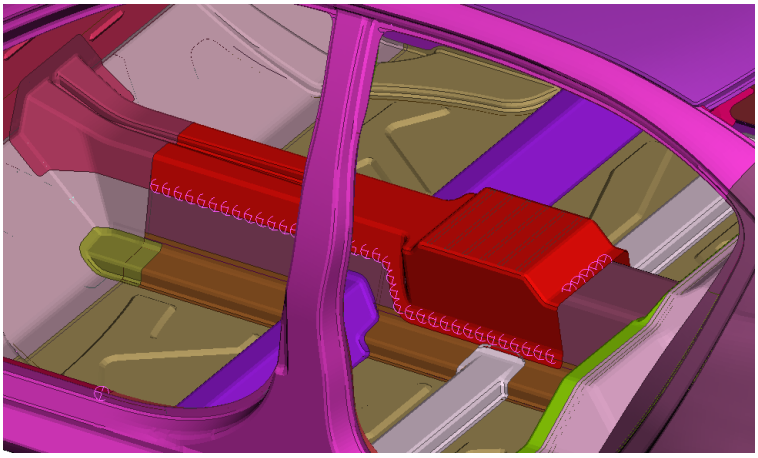

Figure 80 **Extension of dash panel reinforcement (red)**

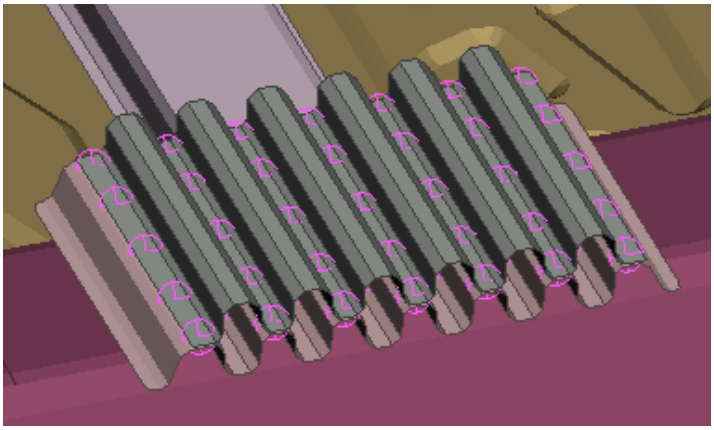

Figure 81 **Side impact support structure between front seats**

Many weld locations in the body structure offered only a very small amount of space making it impossible to introduce a reasonable long laser weld line. So either the spot welds were just kept, which regarding the production process often would require a spot weld robot just for one or two spots, or a small circular laser weld would have been created. Either way the FEM representation would be the same, obtained by a single ACM2-connection, so leaving the spot weld connection was

fine. This situation occurred quite often with the side structure in the door cutout area (see *Figure 82*) and at the trunk lid frame (see *Figure 83*), usually at corners of parts.

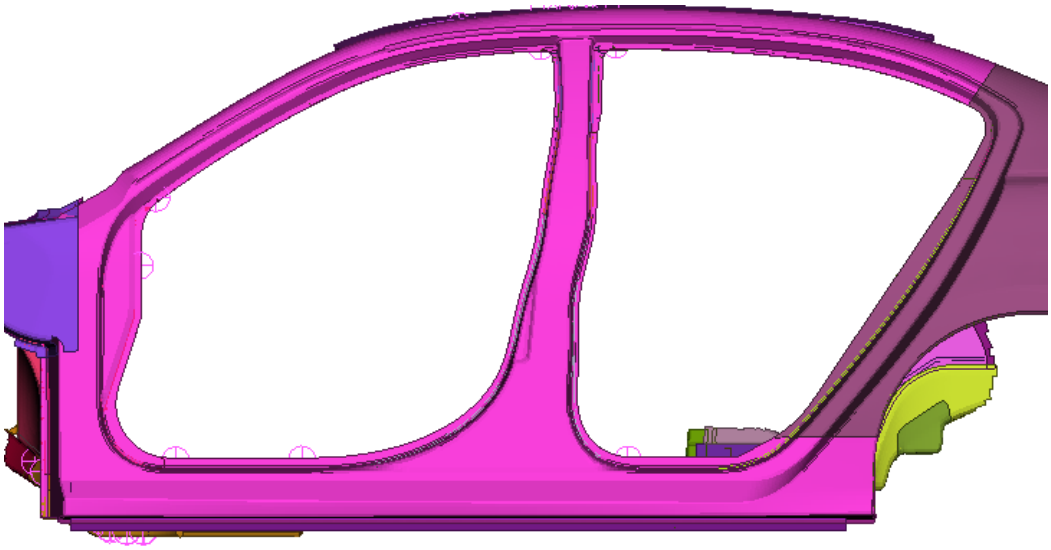

Figure 82 **Spot weld FEM representation in the body side**

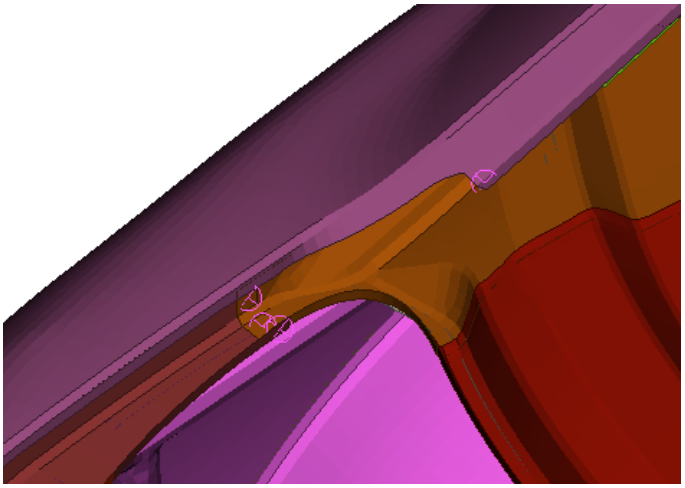

Figure 83 **FEM spot weld representations at short flanges at the trunk lid frame**

In the roof structure similar cases occurred at the diagonal supporting beams, the front roof bow, its brackets to the side structure and the connection between the main bow and its brackets, all seen by the spot weld representations in *Figure 84*. Especially at the front bow's connection to its reinforcement the punctiform contact patches designed especially for spot welding made it hard to establish laser weld lines.

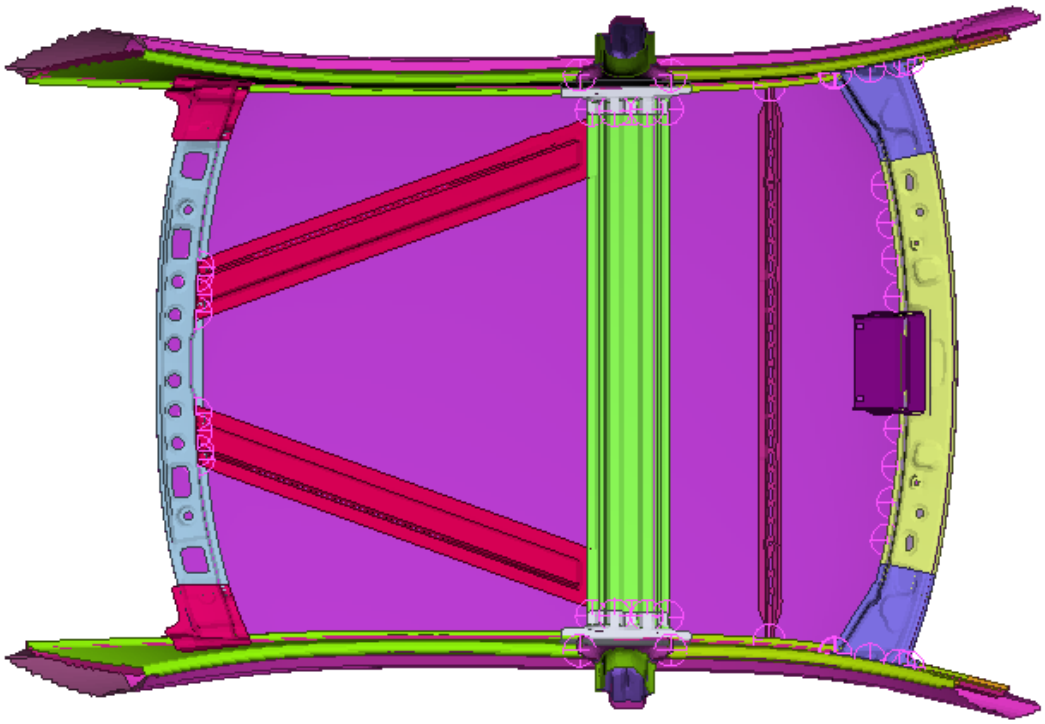

Figure 84 **Remaining spot weld representations in the roof structure**

The shape of the panel connecting the inner wheelhouse to the rear lamp can query the longevity of this kind of design. So since also this part was completely redesigned later the flange at the rear end just remained spot welded as displayed in *Figure 85*.

Figure 85 **Spot welds at rear end of panel connecting inner wheel house and lamp can**

However, self-evident most of the connections in the laser welded model where laser welds. This caused another problem; not all connections even with the right characteristic hexahedron diameter could be realized right away due to intersections. While for the spot welded model, where only one ACM2-element was created every *40 mm* along the flange or so, the number of disturbing intersections was quite low, the flange geometry for the laser welded model had to be more properly modeled. Due to the continuous connection attitude every single, slight intersection along a flange was causing problems. So fixing intersection issues for the laser welded model was in principle the same as for the spot welded model, but much more time consuming.

Before the modal and stiffness computations could be started like for the spot welded model also the same preparations were done. Exactly the same wind screens and bolted on parts were added and equally the roof panel to roof rail connections were made up for by RBE2 elements. Since there were missing connections in the added bolted on parts, which were fixed in line with the calculation preparations for the spot welded model, the updated version of those parts was taken right from the spot welded model. Eventually the same boundary conditions as described in chapter 5.2 were applied for the different load cases, providing a model to carry out the modal and the two static stiffness runs. The identified numbers then were compared to the NVH performance characteristics of the spot welded structure.

The first comparison of the two models actually indicated that the laser welded model was weaker than the spot welded one. The eigen frequencies were almost the same, but the static torsion stiffness of the laser welded model was more than *10 %* lower than for the spot welded model. Since this was contradictory to the general acceptance of stiffness increasing, continuous laser welds the laser welded model was scanned for possible errors. The spot welded model was expected to provide correct results, as only few parts of the joining technology were changed here.

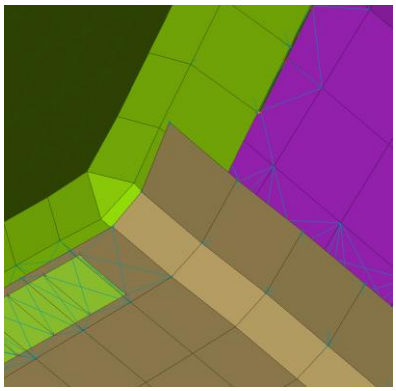

Figure 86 **Example for punctual 3T connection**

It was considered that the inability to establish true 3T welds could be regarded as the weak point of laser welding. The front end lateral mode did improve with laser welding, which would support this hypothesis, as there are no 3T joints in the front structure. The torsion stiffness on the other hand decreased dramatically, which also could be related to the weakness of 3T connections, since the side structure, containing many 3T welds, plays a decisive role here. The lack of being able to establish a 3T connection within a small, punctual flange area like the one shown in *Figure 86* was considered as another problem. If three parts meet in some corner, a single 3T spot weld easily could con-

nect them all. But for laser welding, if one sticks to the *40 mm – 40 mm* staggered pattern, it would need a flange of at least *80 mm* length plus some buffer space to establish a 3T connection. Even if the size of the single weld sections would be significantly decreased, the connection still would require much more room than a spot weld. So for configurations like those with laser beam welding only a two layer connection can be established.

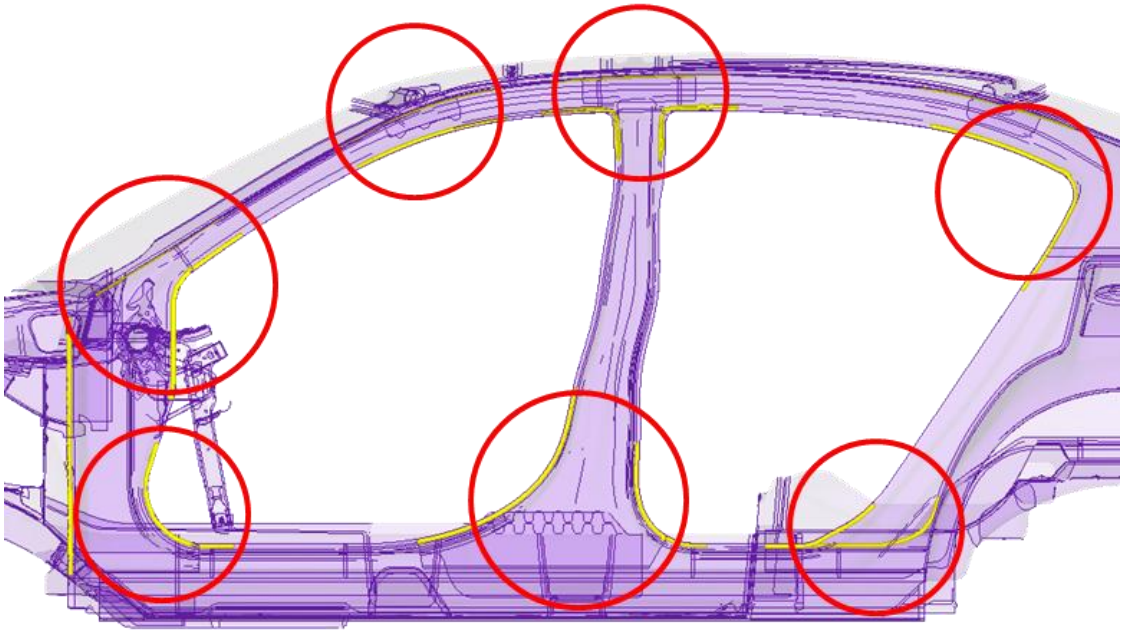

Figure 87 **Reinforcement of joints (red circles) with adhesive (yellow)**

Hence, intending to improve the assumed poor performance of the 3T welds, adhesive was added to reinforce the purely 3T welded joints in the side structure. The structural bonding was added to both gaps at the locations displayed in *Figure 87*. But this did only improve the stiffness on a negligible

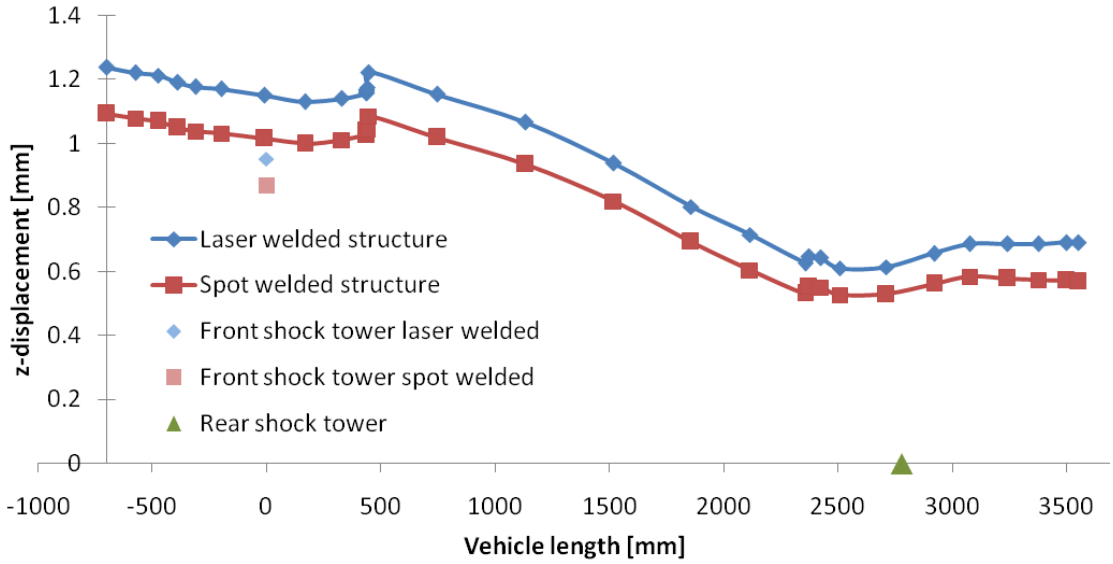

Figure 88 **Displacement of twisted trimmed body on several points of the side structure**

level, indicating that all the assumptions made in the previous paragraph did not hit the target. The next approach to find the issue was to set up a diagram to visualize the continuity of the displacement while twisting the body structure as described in chapter 5.2. The points, whose displacements are shown in *Figure 88*, are lined up on the outer shotgun, the a-pillar, as can be seen from the many nodes at the same position around *x = 500 mm*, the rocker, above the rear wheel house and along the rear quarter. The graph also includes the displacements at the more inner positioned front shock tower, whose center node also was defined as the origin of the *x*-axis, and rear shock tower, positioned ca. at *x = 2800 mm*. It would have been more accurate to relate the displacement to the *y*-value of the particular node to get the actual deformation angle at the node, which would be independent of the *y*-position. But all nodes examined except the shock towers were pretty much on the same lateral level and moreover the displacement is sufficient for a comparison study.

Looking on both graphs one notes an almost constant offset. The body is supported at the rear shock tower. In that area the displacement is at its minimum, as expected. For two body structures, which display a globally different stiffness, also the divergence should be minimal here. But instead of increasing throughout the body, reaching its maximum at the ends, a large difference is present right from the starting point at the shock tower area. Hence, there must be a local weakness between the shock tower top and the other nodes measured closest to it, which are located around the wheel arch. This crucial evidence drew the attention to the joint of the package tray and the rear wheelhouse. Compared to the spot welded structure, this connection was completed rather inadequate for the laser welded model. This being the cause for the poor performance also goes in line with the fact that the eigen frequency of the torsion mode only was slightly decreasing, while the static torsion performance decreased dramatically. The static test shows the worse results, because the force transmission is close to the bad connection. After properly reconnecting the parts in that area the stiffness performance of the laser beam welded structure considerably improved to a plausible level.

6.3. Assembly Layout for Solely Laser Beam Welded Structure

Including the same parts as the spot welded structure the assembly tree of the laser welded structure was very similar to that of the spot welded structure. Hence in this chapter the assembly tree will not be described with as many illustrations as for the spot welded structure, but the differences to the spot welded structure regarding assembly order will be elaborated.

Of course the laser weld seam specifications for the assemblies are discussed. As for spot welding there is a geo welding station which fastens the parts to each other with very small tolerances and – if applicable – one or more stations following, where more seams are established to strengthen the connection, referred to as respot laser welding in this report. Those respot operations though are applied much more seldom than for spot welding. If the 3T welding pattern is mentioned, usually this refers to only one side. Since no real 3T welding is possible, both sectioned lines are usually applied in different stations. So if *x* seams with a total length of *y* are mentioned, there are *x* separate welds between the middle and one outer part applied, while the counterpart weld to the other outer part is applied in a different station and mentioned separately.

But before the welding could be started, the parts needed to be dimpled, which still is a requirement for laser welding zinc-coated steels, as explained in chapter 2.2.2. Depending on how many clips are necessary to clamp the parts while welding, the number of dimples where defined. Usually every clip

necessitates three dimples. Since the clamping configuration is very important to laser welding, also the number of clips will be specified on the following pages. Unfortunately there were still some changes in detail made to the layout when this report was finished. Thus the information about dimpling and clamping is incomplete. This also holds for the station layout, which was not precisely defined for some subassemblies at that date.

As indicated in chapter 6.2 some small flange areas required laser welds shaped like spot welds. Those laser weld circles were just added as additional weld seams and their seam length was assumed to be *10 mm*. Also for the laser welded structure assembly the cycle time was set so *55* seconds.

For laser welding the dash panel subassembly was joined in one procedure, not having the reinforcement subassembly set up in a different step as with spot welding. *228* embossments were dimpled into the parts. There was only a single geo welding operation, creating *18* laser weld seams with a total length of *2326 mm* while the parts were fastened by *76* clips. The cowl panel subassembly required *255* dimples for *85* laser clips. *27* geo welds with a total length of *2639 mm* were created by laser. At one respot laser welding station another *10* seams with a total length of *2060 mm* were created. To join those two subassemblies *42* laser clips were required necessitating *126* dimples. The *3* geo weld seams applied accumulated to a length of *1540 mm*.

To establish the upper front rail subassembly *32* clips and *96* dimples were applied per side. The geo welding operation created *922 mm* of laser weld with *5* seams. Another *2* seams with a total length of *76 mm* were created with the 3T pattern. The lower front rail subassembly parts were dimpled *78* times which included the dimples for the next assembly step also. *26* clips fastened those two parts while they were welded to each other and to the upper front rail subassembly with *4* geo weld seams adding up to *1202 mm*, creating the outer front rail subassembly. To connect the four parts of the inner front rail subassembly to each other and to the outer front rail and thereby forming the front rail subassembly, *420* dimples for *140* clips were inserted. The connection itself was established by *9* geo laser welds with a total length of *2907 mm* on each side's subassembly.

The shot gun inner subassembly required *60* clips and *180* dimples. The four parts were joined by *662 mm* of geo laser welding distributed on *13* welds. To prepare the connection of the front rail and the shotgun inner *32* dimples were applied. Using *16* clips the assembly was created by *168 mm* of geo weld seam. Another *76 mm* were welded as the other half of the 3T pattern mentioned just above, increasing the number of seams to a total of *11*.

Creating the radiator support subassembly its ten parts were dimpled exactly *300* times. Correspondingly *100* clips were applied to geo weld *28* seams with a total length of *3534 mm*. To finalize the front structure by assembling both wheelhouse subassemblies, the radiator support and the dash subassembly, *519* dimples were introduced. The subassembly was fastened with *173* clips while *3311 mm* of geo laser welding on *34* seams was performed. Finally the structure was respot laser welded at *18* seams with a length of *2132 mm*.

Like for the spot welded assembly also the laser welded front floor was created starting off with joining the tunnel, the tunnel cross members and the seat cross members front. To prepare the connection, those parts were dimpled *138* times. The tunnel got an additional *300* dimples for subsequent joining operations. Geo welding the mentioned panels fastened by *46* clips at *22* seams established *1644 mm* of laser welds. Adding the main floor panels and the seat cross members rear necessitated another *300* dimples. Clamping the parts with *200* clips they were joined by *10* geo laser

welds with a total length of *3043 mm*. Afterwards there were two respot stations. First there were *6* seams with *2915 mm* and then *8* seams with a length of *3047 mm* created.
The assembly of the rear floor started with the connection of the two lower rails with the cross member, while the rails itself were assembled in the same way as the spot welded ones were. All this took place in one geo welding station after the parts were dimpled, creating *1808 mm* of laser welds within *30* seams. Identical so the spot welded assembly the upper rail was assembled separately first. Joining both panels and the seat cushion supports after dimpling them required *8* seams with a total length of *200 mm*. Then the lower rail set up and the gas tank mounts were connected to the rear floor cargo inside a geo welding and a respot station after passing the dimpling station, applying a total of *24* 2T and *44* 3T seam lines accumulating to a welding length of *3693 mm*. In parallel the panel rear seat subassembly was created, connecting those three dimpled parts with *13* laser welds of *1063 mm* length in one geo welding and one respot station. Joining this subassembly to the lower rear rail and cargo floor configuration required only one geo welding station, where *42* 2T seams and *8* seams with the 3T pattern were applied after the parts have been dimpled, having a total length of *2892 mm*. The back panel assembly also was created in the same order as for spot welding. All *18* seams adding up to *2886 mm* were created in one geo welding station.

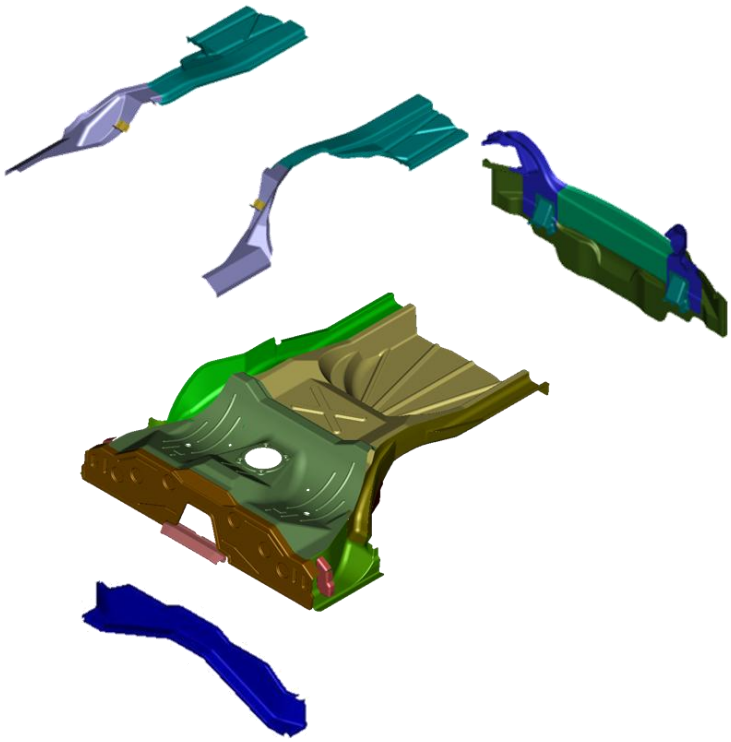

Figure 89 **Rear floor subassembly of the laser welded structure**

Hence the rear floor subassembly could be established as it was done for the spot welded structure. The difference was that the inner wheel house was not part of this subassembly, but came along with the side structure, as will be discussed later on. Connecting the three described subgroups and the cross member rear seat as displayed in *Figure 89* required of course dimpling and then *74* 2T and *64* 3T geo laser welds with a total length of *8030 mm*. The framing one operation for the laser welded structure included a loading and dimpling, a geo welding, a buffer, two respot, again a buffer, a

measuring and finally the lifter station. The front lower, the middle floor and the rear floor subassemblies were joined to the lower structure by *3000 mm* geo welding, *7000 mm* respot welding and again *3180 mm* of respot welding, creating *42* weld lines in total.
The package tray assembly was clamped by *84* clips after the parts were dimpled on *252* spots. Inside one geo welding and one respot station *4* seam lines with *3988 mm* weld were applied.

Figure 90 **Inner wheel house subassembly of the laser welded structure**

Moving on to the body side structure first the inner wheel house subassembly shall be discussed. The parts shown in *Figure 90* were first dimpled *63* times and then assembled with the help of *21* clips and of *8* 2T and *2* 3T laser seams creating a weld length of *840 mm*. The rear roof rail parts were added as shown in *Figure 91* and prepared by *51* dimples. Being fastened with *17* clips the parts were geo welded with *9* 2T and *1* 3T laser welds adding up to a length of *1295 mm*.

Figure 91 **Rear roof rail subassembly of the laser welded structure**

In the next step more parts from the body inner side were attached, see *Figure 92*. For this operation *264* dimples were required for *88* clips. *23* geo welds with a total length of *1896 mm* were applied to assemble the new parts to each other. In another geo welding station the two groups were joined by *8* weld seams of *630 mm* length. The body side reinforcement subassembly on the other hand was put together in the exact same configuration as with the spot welded structure. First ap-

plying *174* dimples for *58* clips, the parts were geo welded with *7* welds with a total length of *402 mm*.

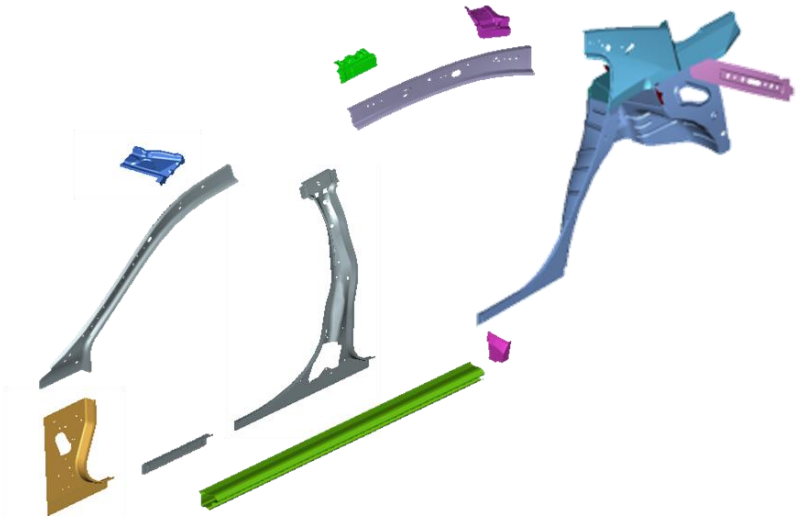

Figure 92 **Inner body side inner subassembly of the laser welded structure**

The inner wheel house panel was added to the inner body side inner subassembly by *5* geo welds having a length of *1600 mm* after the parts were dimpled (see *Figure 93*). Preparing to also add the body side reinforcement to that group the parts were dimpled *514* times. Being clamped with *128* clips welding of the parts was performed in one geo welding and one respot station. In total *17* 2T and *102* 3T weld seams were created, adding up to *7000 mm* geo and *5008 mm* respot weld length.

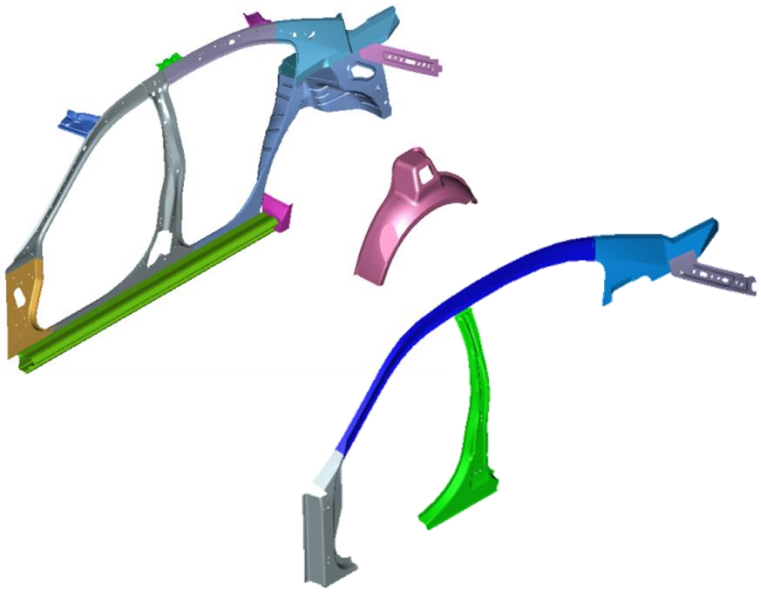

Figure 93 **Body side inner subassembly of the laser welded structure**

The body side outer subassembly again was put together like the spot welded version. Having the parts dimpled at *258* locations they were clamped together with *86* clips and geo welded with *14* seams and *1789 mm* weld length. After the dimpling operation uniting the body side inner and outer

subassemblies required *2500 mm* of geo laser welding and *6600 mm* of respot welding each in two stations, followed by another *960 mm* of respot welding. In total *13* 2T and *102* 3T laser weld seams were established.

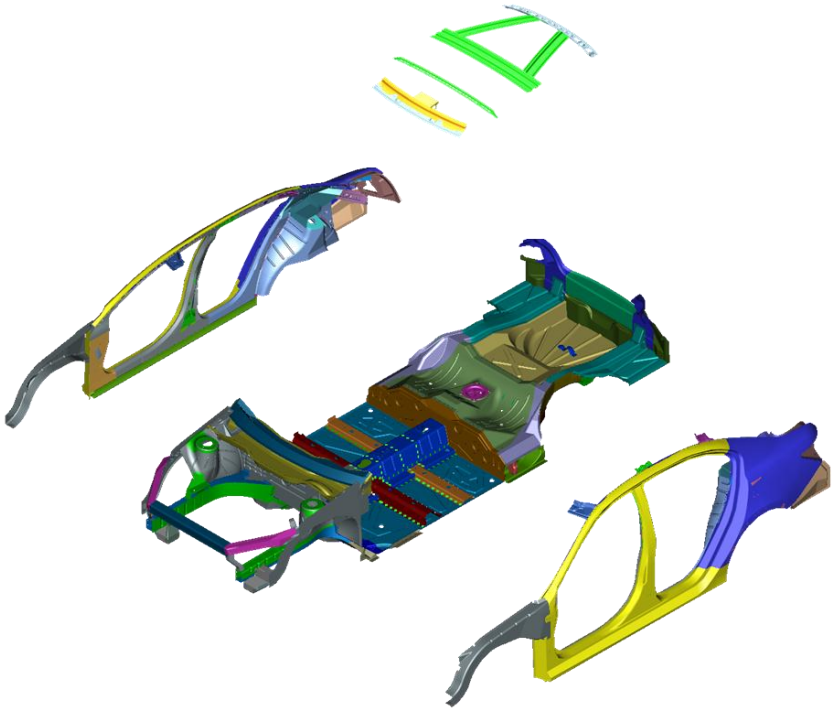

Figure 94 **Framing station two for the laser welded structure**

For the inner roof structure the assembly configuration were exactly the same as for spot welding. The rear group was joined by *6* geo laser welds after dimpling, adding up to a length of *232 mm*. The front header assembly required *10* 3T and *10* 2T geo welds to be created after the dimpling operation was performed and the parts were clamped together. This resulted in a total weld length of *435 mm*.

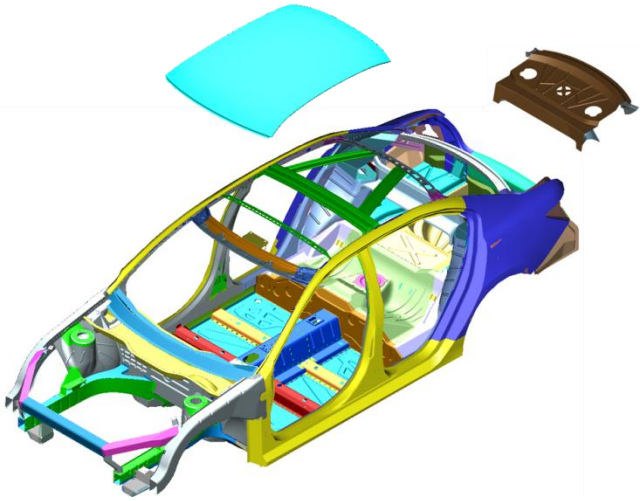

Figure 95 **Framing station three for the laser welded structure**

In the framing station two (see *Figure 94*) the side assemblies and the roof structure were attached to the lower structure. After the required dimples were introduced *7776 mm* of adhesive was applied. Then *5440 mm* of geo welds were established, followed by first *7000 mm* and then *2950 mm* of respot welding. In total *136* 2T and *6* 3T seam lines were welded. After a buffer station the assembly was measured for quality monitoring.

To complete the body structure the package tray assembly and the roof panel were added in framing station three, displayed in *Figure 95*. After dimpling *3000 mm* adhesive were applied to the roof panel and another *4474 mm* to the preassembled body. After running through a buffer station, *5170 mm* of geo laser welding is carried out on the assembly. Then *2000 mm* of respot welding is done, resulting in a total of *28* seam lines. In the next station *2822 mm* of laser brazing connects the roof panel with the roof rails. Hence a brushing station, another buffer, a seam check station, a third buffer, the measuring station, the grinding and cleaning station and a quality control station are passed.

Like for the spot welded structure the discussed assembly information was used to develop the detailed shop layout for the entire body assembly.

6.4. Costs Estimation for Laser Beam Welding Assembly Layout

In principle the cost calculation for the laser welding assembly layout was accomplished the same way it was done for spot welding. Planning regarding the actual assembly layout and cost calculation is still ongoing, while this thesis is brought to a termination. This is why this report unfortunately does not contain the complete cost information regarding laser welding. Only the cost information regarding the lower structure front and the front floor subassemblies as well as the framing station one were taken into account for the cost comparison. The other finished sections could not be considered since only for those subassemblies the spot welded and the laser welded assemblies have the same order of assembling and are thereby comparable.

7. Results and Discussion

The purpose of this study was the comparison of two body structures relying on different joining technologies. The design and process of evaluation of the structures have been described in the previous chapters in detail for each model separately. In contrast to that, for the presentation and discussion of the results those of the two body structures are analyzed in parallel to be able to better point out the differences.

7.1. Comparison Regarding Weight

As visualized in *Figure 96* the adapted spot welded structure exhibited a weight of *247.7 kg* while the laser welded body had a mass of *234.5 kg*. This resulted in a mass reduction of *12.2 kg*. Even higher than the first approximation did suggest, this is quite a considerable mass saving being equal to *4.96 %*.

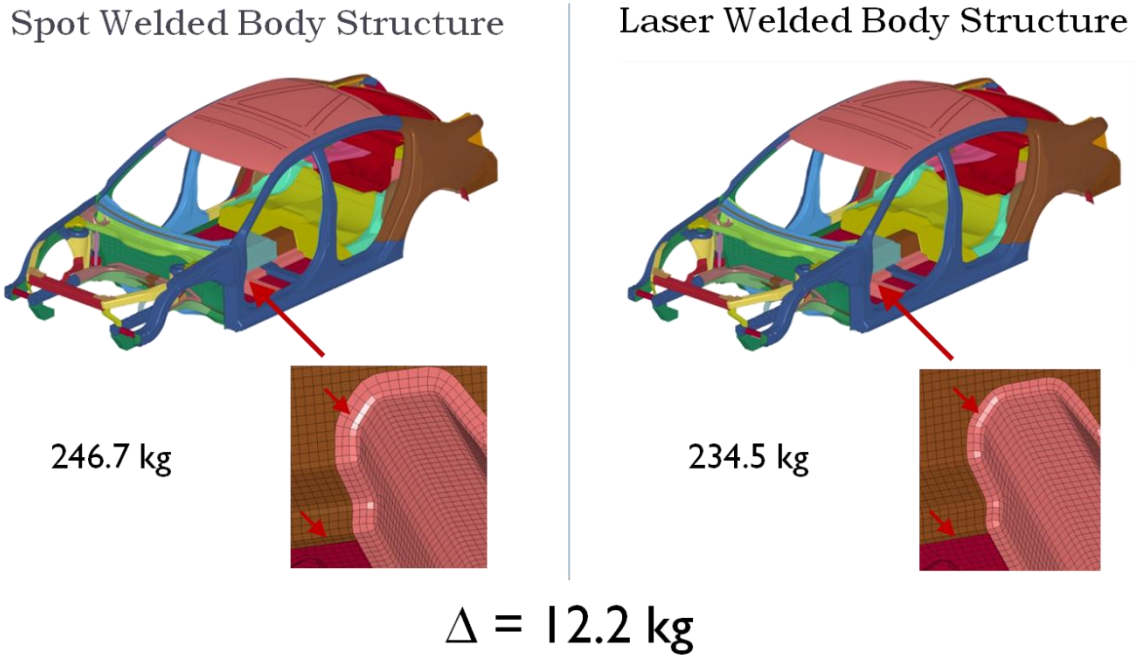

Figure 96 **Illustration of weight comparison results**

As mentioned the mass saving for every single part was determined. Information of this level of detail certainly is only of less value here, but it was used to analyze the mass savings achieved by the different sub structures of the BIW. As displayed in *Figure 97* the upper structure's contribution was quite low, also from a relative perspective. This was expected, because the massive application of adhesive bonding in that area left only few flanges to be trimmed. Considerably larger reductions could be gained from the side structure. Still the result for that region did not quite meet the expectations, since the present flanges are indeed quite elongate, but their number is small.

The by far largest share in absolute and relative terms came from the lower structure. Subdividing this part reveals that the middle also does not contribute that much; the situation is comparable to the side structure. The front end has a very large potential, which is appreciated, since this actually is

the area of the body structure where mass savings are most welcome. On passenger vehicles with nowadays standard layout of front engine and front wheel drive the center of gravity always is shifted undesirable to the front. By mass savings in this area this can be partly compensated for. The lower rear also delivers a significant share; in relative terms even the highest. However, because of the just mentioned reasons mass savings in this area are the least welcome, but still desirable.

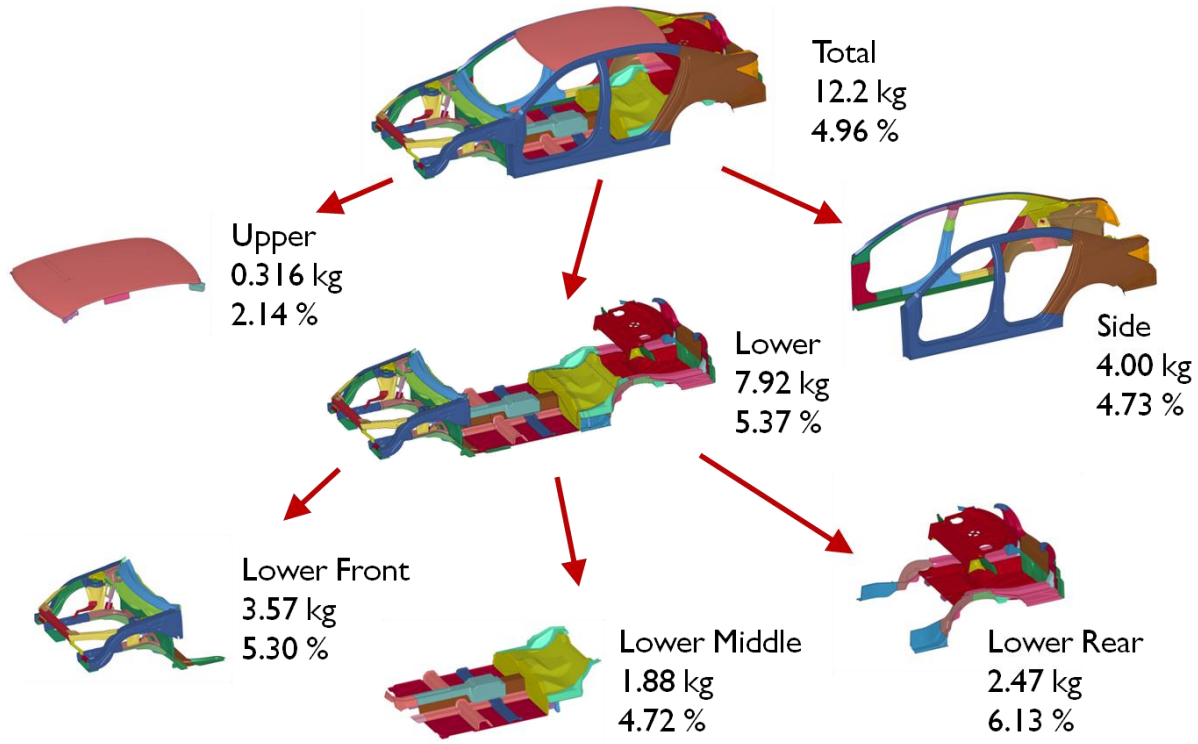

Figure 97 **Distribution of obtained mass saving**

Studying the distribution of the mass savings shows that maybe except for the roof structure every area contributes similarly. So from this point of view laser beam welding should be introduced to the entire body in white. No area shows such a low mass saving that the introduction of laser welding could be regarded as pointless there. This of course can be different looking at it from the assembly layout perspective.

7.2. Comparison Regarding Performance

After the models were improved as described in chapter 6.2 reasonable values were attained. The results are displayed in *Table 2*. The eigen frequency of the front end lateral mode did considerably increase with laser welding. This indeed could be owed to the absence of 3T laser welding in the front structure, as assumed earlier on. With only 2T welds the advantage of the continuous weld pattern with laser welding could be fully taken.

The deformation pattern of the front lateral mode is shown in *Figure 98*. All the mode shapes illustrations shown in the following are taken from the run with the laser welded structure. This shall be sufficient for demonstration, since the eigen frequencies of both models are in the same range and the patterns for the examined normal modes are very similar.

The frequency of the first bending mode did slightly decrease with the conversion to laser welding. On the other hand the static bending stiffness did increase. However, since those deviations are not only oppositional but also quite small, it could be concluded that the bending stiffness remained about the same. Though the laser welding did not improve the stiffness in that case, at least it could be assumed that the bending performance of the laser welded body structure does not degrade, since the static key figure rises more than the dynamic one goes down.
The mode shape is illustrated in *Figure 99*. Note that especially the rear bumper bended excessively, which could only be caused by an inappropriate connection to the body. Since the same bumper and connection was applied to both models, changing the connection would not have improved the relative performance of the laser welded body much.

Table 2 **Results of the performance analysis**

	Spot welded body structure	**Laser welded body structure**	**Δ**
Weight [kg]	246.7	234.5	-4.95%
Modal analysis			
Front end lateral [Hz]	34.15	35.75	+4.69%
1st order bending [Hz]	37.15	36.81	-0.92%
1st order torsion [Hz]	47.39	48.22	+1.75%
Static analysis			
Bending [N/mm]	11957	12186	+1.92%
Torsion [Nm/°]	15802	16508	+4.47%

The torsion performance of the laser welded model clearly was better than for the spot welded model. Both the static and the dynamic torsion stiffness, of which the pattern is displayed in *Figure 100*, did considerably increase. This gives room for further mass savings, as initially hoped for. A panel which mainly improves the torsion stiffness could be decreased in thickness, as for example the main dash panel, as long as the degradation of the frontal impact performance could be precluded. Further research would be required to find a proper way to use this increase in stiffness for more weight savings.

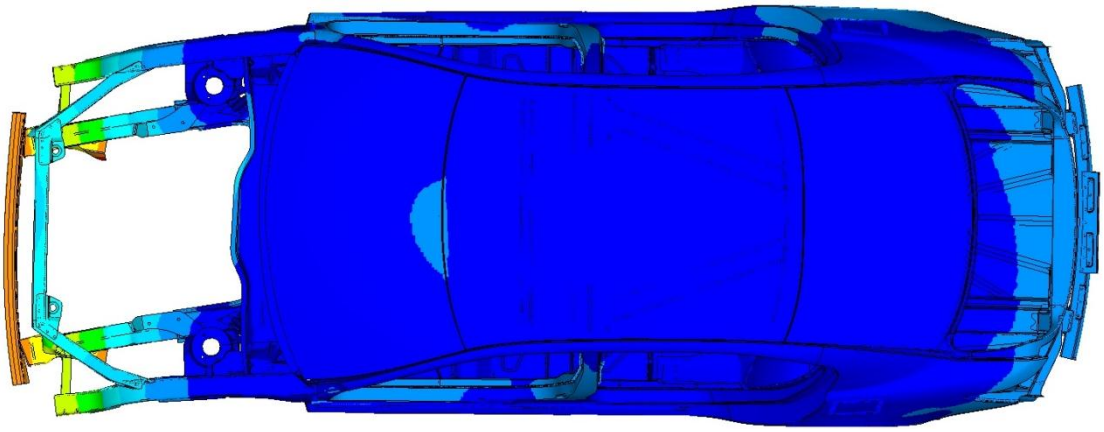

Figure 98 **Front end lateral mode of laser welded structure**

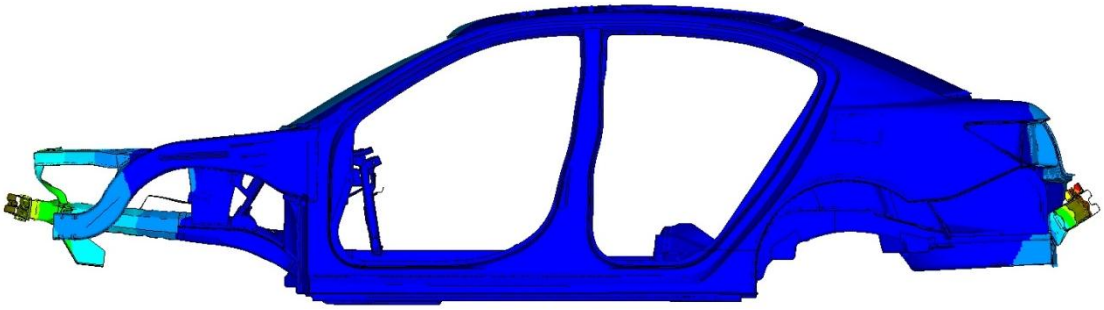

Figure 99 **First order bending mode of laser welded structure**

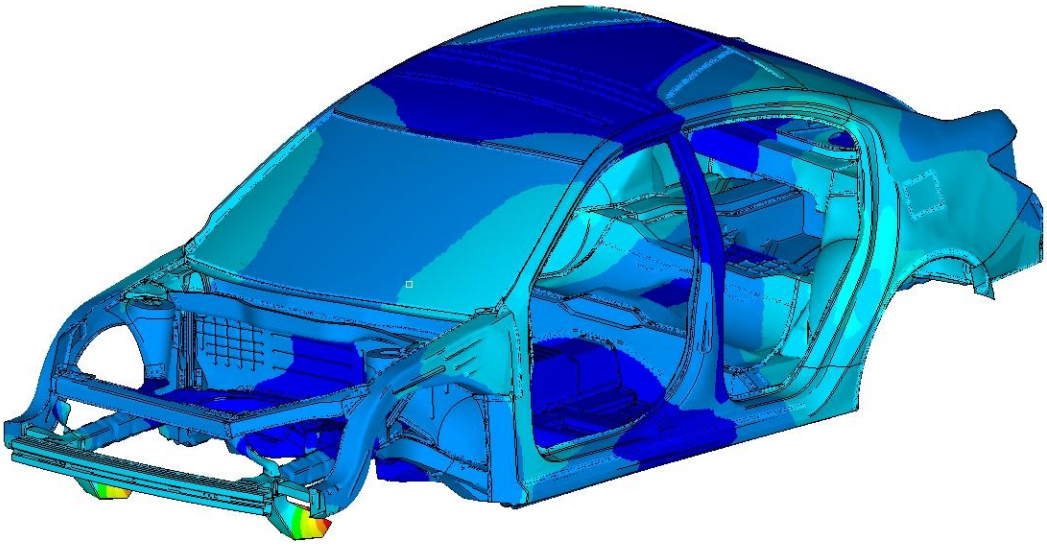

Figure 100 **First order torsion mode of laser welded structure**

7.3. Comparison Regarding Assembly Layout

The developed shop layouts for the resistance spot welded and the laser beam welded assemblies are displayed in *Figure 102* and *Figure 103*. Actually every single part entering the assembly is labeled in those drawings. But due to the size of the drawings they cannot be shown in such a level of detail here. Thus the most important assembly and framing stations are pointed out in the illustrations. As indicated the spot welding layout shown is at an almost final state, only very minor changes are expected. On the other hand the laser welding layout shown represents only a preliminary status. Thus all the results presented in this subchapter regarding the laser welding assembly are only estimates.

In both layouts an arrowed line shows the direction the unfinished body goes from framing station one to the last station, framing station three respectively four. It can be traced how the subassemblies of the lower structure – the lower structure front, the front floor and the rear floor – separately are put together, how they are joined in the framing station one and how the structure proceeds through the other framers where the side structures, the package tray and the upper structure are attached. Note that this follows the chain described in chapters 5.3 respectively 6.3. The equipment used will not be explained in detail here, since all this was set up by the production engineers. However, the most common symbols for the layout drawings are shown in *Figure 101*. Note that the robot shown on the very left can carry a weld gun but also could be just used for handling. The static welding gun also can be mounted on a slide.

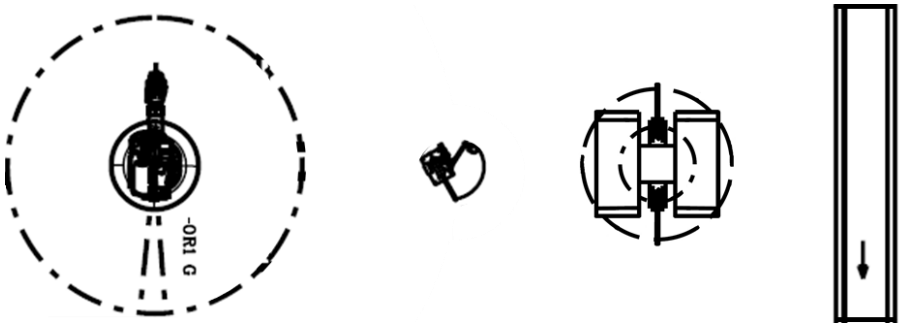

Figure 101 **Symbols for arbitrary robot, static welding gun, welding bench and conveyer belt (from left to right)**

The layout illustrations also show that the laser welding assembly needs a bit less space than the spot welding assembly does. Exemplarily comparing the number of robots required, shows that the spot welding assembly uses *416* robots of any kind, while the laser welding assembly includes only *285*. This means that the laser welding assembly needs fewer robots for the same cycle time, i.e. the same output. Beside the quicker welding speed for laser welding discussed in previous chapters another reason for this efficiency increase is the use of so called geo sets. Geo sets are special support frames for assemblies, in which the parts not only can be easily transported, but also be fastened to for welding. See *Figure 104* for an exemplary illustration of an application of a geo set conveyor system.

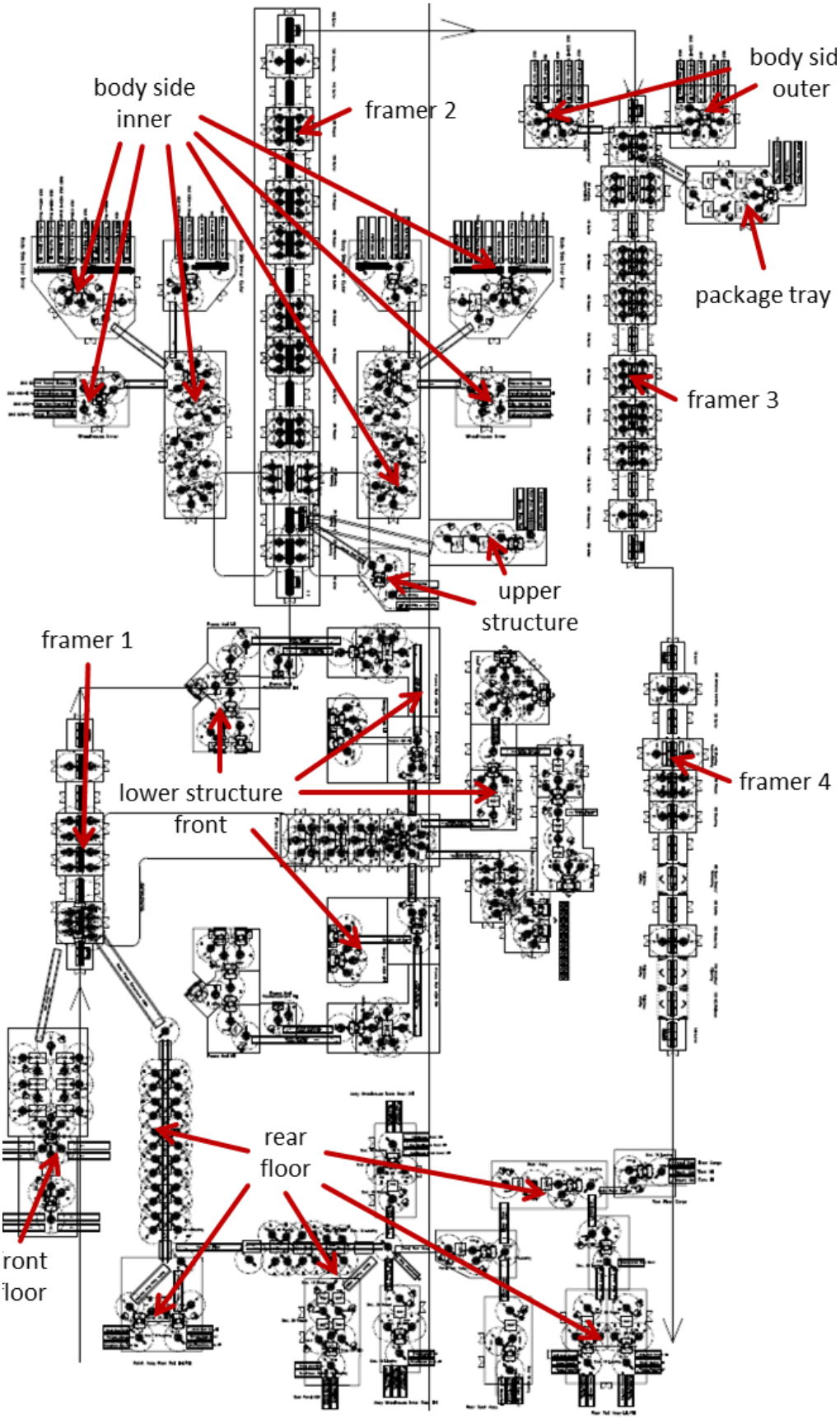

Figure 102 **Shop layout for resistance spot welded assembly**

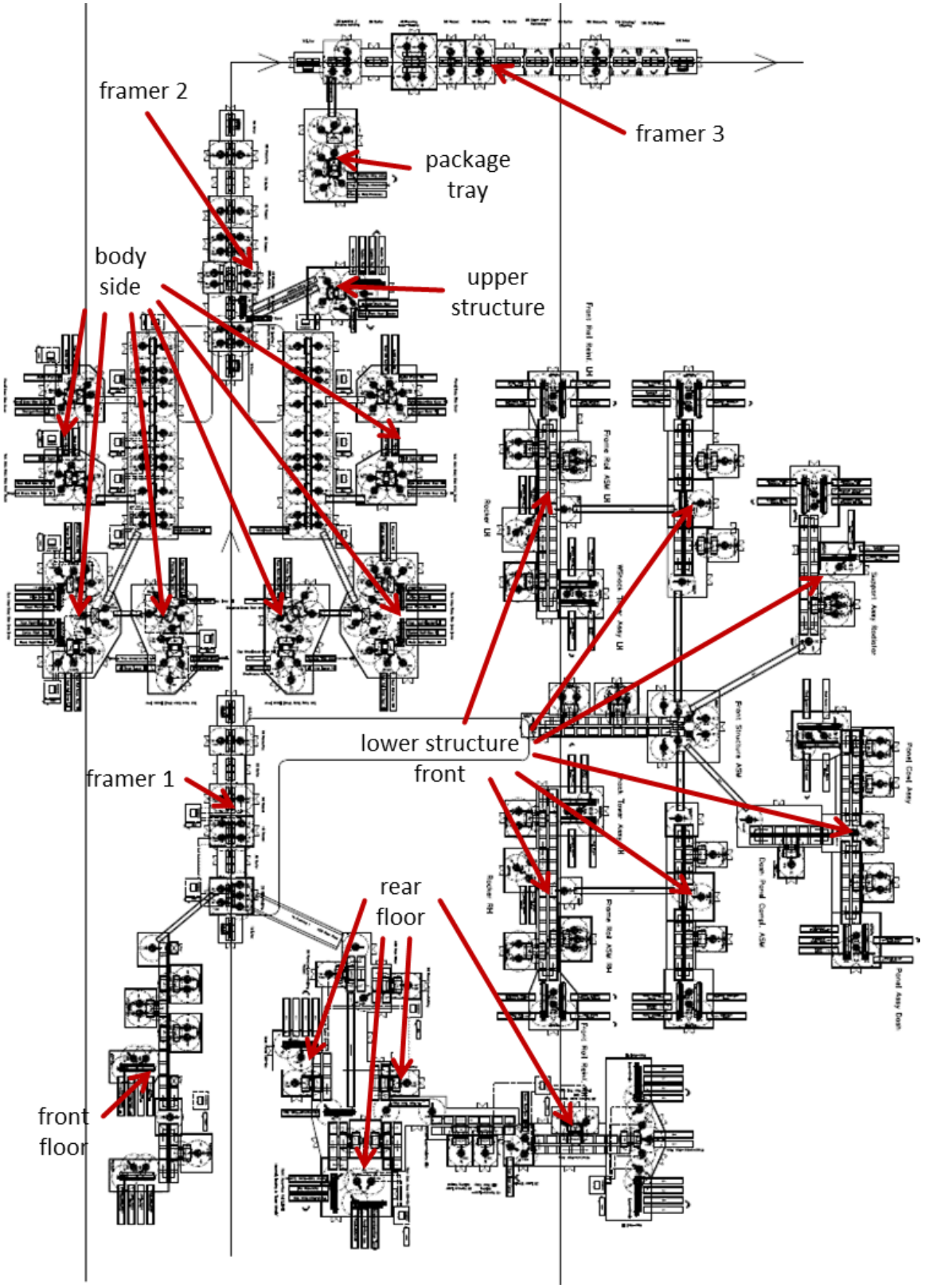

Figure 103 **Shop layout for laser beam welded assembly**

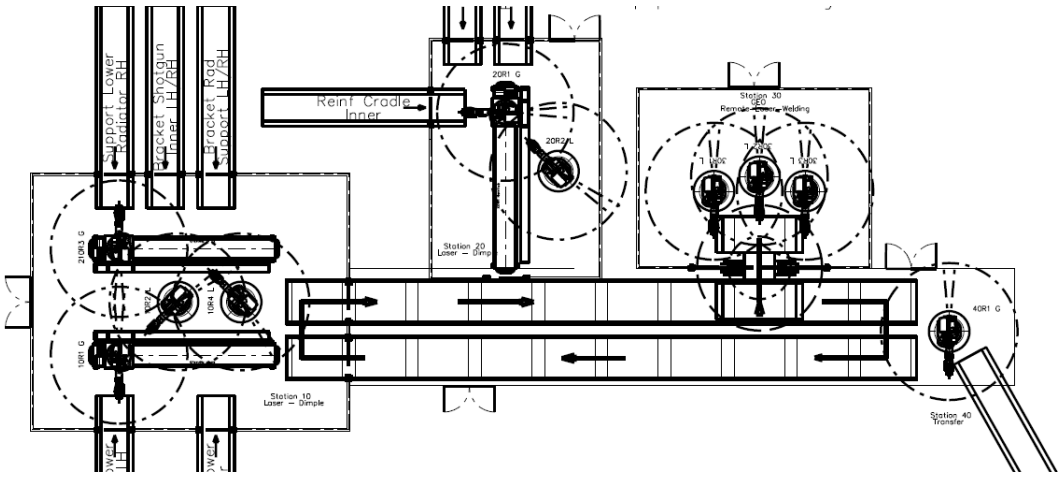

Figure 104 **Application of geo sets at the radiator support assembly**

7.4. Comparison Regarding Assembly Costs

As indicated the costs for the laser welding assembly are not completely calculated. Thus the cost comparison must be carried out inspecting only a section of the assemblies for which the costs were calculated for both versions, which is the lower structure front and the front floor. Moreover the comparison in general will be only an estimate, since there are still changes expected for the laser welded structure.

Though the number of robots significantly decreased the laser welding assembly is still much more expensive to set up than the spot welding assembly. Especially regarding transportation of parts and assemblies the laser welding system is more elaborate than the spot welding one. But also the equipment used for laser welding is, though the quantity is less, much more expensive. Only the number of robots actually was compared above, but also the count of laser welding guns is much lower than the one of spot welding guns. Additionally with modern laser welding one laser source can be used for up to four welding guns. Nevertheless the laser technology is still so expensive, that the higher number of spot welding machines ends up being more inexpensive. This might be subject to change if laser beam welding is applied on the body structure assembly on the same large scale as resistance spot welding is.

However, in the following the increase in cost is related to the weight savings achieved by laser welding regarding the lower structure front and the front floor. This includes all operations described in chapters 5.3 and 6.3 as well as illustrated in *Figure 102* and *Figure 103* up to the first framing station. Even if costing data for more subassemblies was available, it could not have been used. The lower structure front and the front floor are the only two subassemblies which contain exactly the same parts in both assembly designs, making them the only ones possible to compare if not the entire structure is analyzed. The separation between middle and rear lower structure made in chapter 7.1 though does not go in line with the separation made in the assembly tree between front floor and rear floor. But since the weight difference for every single part was determined, the weight savings to look at quickly could be adapted to the cost difference for the investigated subassemblies.

The costs were calculated from the equipment required, as indicated above. Dividing the difference in costs by the total production volume of *1 000 000* vehicles gave the value per vehicle comparable to the mass saving achieved per body structure.
A weak point of this approach are the trimmed flanges, for which no assembly operation is considered if one solely looks at the two substructures. For example the flanges of the shotgun inner connecting to the shotgun outer are trimmed and their weight saving is taken into account. But the corresponding cost increase due to the conversion to laser welding is not included. This cost difference would occur in the cost analysis of another framing operation, which of course cannot be completely included. To compensate for this the cost increase for the framing one station is included for the weight saving efficiency estimation of the two subassemblies. Regarding the connection between the lower structure front and the front floor it is correct to take this delta into account (see *Figure 56*). But since there is also the joining of the front and rear floor included, there is some extra difference in costs added which should roughly cancel the explained biased error out.

Table 3 **Results for weight saving efficiency estimation**

		Spot Welding Assembly	Laser Welding Assembly
Costs [$]	Lower Front Structure	15'992'402	34'277'369
	Front Floor	3'098'913	5'396'290
	Framing 1	2'339'221	3'545'842
	∑	21'430'536	43'219'501
	Δ	21'788'966	
	Δ per vehicle	21.79	
Mass [kg]	Δ	4.75	
Weight Saving Efficiency [$/kg]	Δ Costs per vehicle / Δ Mass	4.58	

The results from this weight saving efficiency estimate are displayed in *Table 3*. As mentioned this comparison is only taking a section of the structure into account and thereby only can be regarded as an indicator. A representative value can only be obtained when analyzing the entire body structure. This becomes evident if one examines the cost differences for the different assembly operations. While for the lower structure front the costs more than double with the conversion to laser

welding, the costs for the framing station one only increase about *50 %*. Depending on this variance throughout the body structure the value might be different for the whole body.
However, a value of *4.58 $/kg*, i.e. increasing the manufacturing costs of the vehicle about *4.58 $* to make the body structure *1 kg* lighter, is a rather disappointing result. See *Figure 105* for key figures regarding the efforts made to reduce structural mass. According to (Klein, 2011) the average accepted costs in conventional automotive engineering for lightweight design are *3 €/kg* nowadays, which converts to about *3.9 $/kg* at present. So the determined key figure for the measure of converting the body structure from spot welding to laser welding clearly lies above that value. Nevertheless it is still way below the maximum effort made, which is about *7 €/kg*.

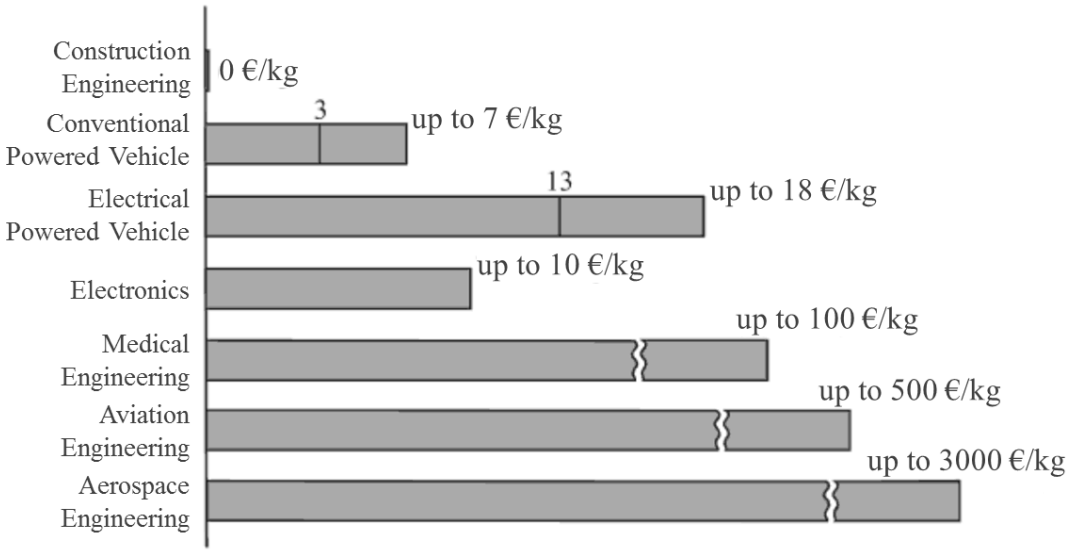

Figure 105 **Average and maximum effort taken for mass reduction (Klein, 2011, p. 9)**

As mentioned before, the determined value mainly holds for the front end structure. Due to the general vehicle dynamics, this actually is the area where the most efforts will be made to save mass. So the calculated key figure may be acceptable for this area of the body structure, though it is a rather high value concerning the entire structure. This makes it worth to give the approach of just applying laser welding in this area to consideration again, assuming that the determined figure holds for the entire structure.

8. Conclusions

In this report the analysis of the weight savings achievable by converting a resistance spot welded passenger vehicle body structure to a laser beam welded structure has been described. As well the NVH performance of both body structures was investigated and the resulting assembly costs were partly determined.

Laser beam welding thereby proved to be a joining technology approach being able to achieve considerable mass savings of *12 kg* respectively *5 %*. Overall also the structure's performance regarding stiffness did improve, which gives room for further optimization leading to the potential of more mass saving. Moreover the amount of equipment required for the body structure assembly and thereby the required shop area did decrease.

Despite all those advantages the massive increase in costs still is a major disadvantage. Though a laser weld gun is able to weld much more efficient and faster than a spot weld gun and not each laser weld gun requires its own laser light source, the equipment needed to assembly an entire body structure still is considerably cheaper for spot welding. But on the other hand there are still major improvements in the scope for laser welding while there is no great enhancement for spot welding in sight anymore, being already highly outbid. A lot of research is done at present to avoid the gap still required to laser weld zinc-coated steels. If all the dimpling operations included in the designed assembly layout could be avoided, the efficiency of laser beam welding would again increase on a large scale. Moreover there are only few applications of laser welding, especially remote laser welding, on the automotive body assembly by now. While laser technology in general already is widely spread, e.g. for laser cutting operations, laser welded tailored blanks or laser brazed roof rails, the specific application on the assembly line is not as advanced yet. Also being in use since decades already, it still is a long way off from the commonness which resistance spot welding exhibits. So there definitely is potential regarding the development of mass production capabilities for laser welding, hopefully also eventually leading to lower costs for the equipment. Examining the research in this field currently being carried out, it seems quite possible that there will be major advancements within the next decade.

However, due to the high state-of-the-art equipment costs the monetary mass saving efficiency of the measure is not very impressive. Since the determined key figure is only an estimate, the number regarding the total body structure may look a bit different. The cost numbers in *Table 3* indicate that the cost increase for simple part assemblies is larger than for framing stations, which is plausible. The advantage of the higher laser welding efficiency plays a more decisive role if a large number of connections are created within one station. For the basic joining of two parts with only a few spot welds respectively a short laser weld line, the clamping and other preparation time is dominant compared to the actual welding time. Thus the overall efficiency would be not as much improved as for a station were a lot of joining operations are carried out. This suggests that framer assemblies as well as other assemblies including a large number of joints created, such as the rear rail for example, will display a smaller cost impact with the conversion to laser welding. Completing the assembly cost analysis for the laser welded structure will allow finishing the mass saving efficiency investigation, which will show whether the explained assumption holds for the entire body assembly.

The mass saving efficiency figure could be improved by taking better advantage of the benefits of the laser beam welding technology. As mentioned several times the required smaller flanges are

only one benefit of this joining technology. Another one is the much lower demands regarding accessibility. While body structures developed for spot welding have to fulfill challenging requirements regarding two-sided accessibility, there usually are no efforts made to avoid 3T connections. As discussed three layer joints are much more complicated to realize for laser welding than for spot welding. To design a structure optimized for laser welding, one would try to reduce the amount of three layer connections. On the other hand the reduced requirements regarding accessibility would give much more latitude in design. Developing a laser welded body structure from scratch with respect to those aspects would certainly improve the performance of the carcass. Thus not just converting a spot welded body structure to laser welding, as it was done in this project, but completely redesigning it, would give a better mass saving efficiency.

But also regarding the reduction of the flange size laser beam welding has further potential. Spot welding creates a laminar connection and thereby always needs a lap joint configuration to be applied. In contrast laser welding establishes a linear connection, making it possible to create butt joints. With butt joints flanges could be made expendable. One of the parts to be joined becomes equipped with guide trenches, as displayed in *Figure 106* for the grey part. The counterpart features tongues which fit the guide trenches of the other part. This way the positioning within certain tolerance can be assured. Where the tongues are inserted into the trenches laser welds are applied, as displayed on the right in *Figure 106*.

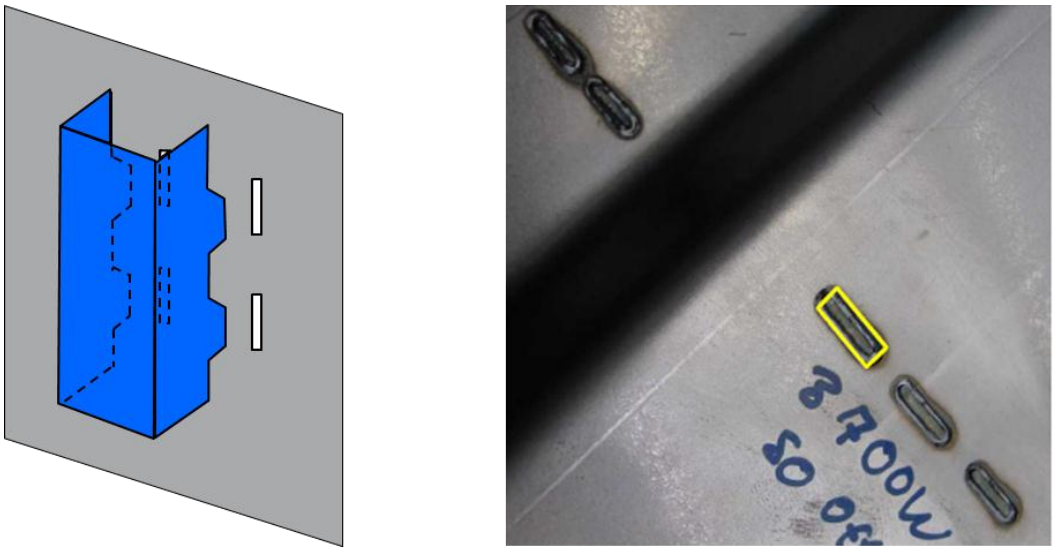

Figure 106 **Laser beam welding without flanges: schematic (left) and example of use (right) (Trumpf Inc., 2010)**

Applying this approach further weight saving could be achieved. But since this method significantly changes the design the body structure modified would have to be carefully checked regarding its crash impact and NVH performance.

9. Bibliography

autosteel.org, 2012. *autosteel.org.* [Online] Available at: http://www.autosteel.org/en/Programs/ [Accessed 16 01 2012].

cars.com, 2011. [Online] Available at: http://blogs.cars.com/.a/6a00d83451b3c669e2013484e20767970c-800wi [Accessed 21 10 2011].

Dahotre, N. B. & Harimkar, S. P., 2008. *Laser Fabrication and Machining of Materials.* New York: Springer.

Davies, G., 2003. *Materials for Automobile Bodies.* Oxford: Butterworth-Heinemann.

Dilthey, U., 2006. *Schweißtechnische Fertigungsverfahren 1.* Berlin Heidelberg: Springer.

electricore.org, 2011. [Online] Available at: http://www.electricore.org/ [Accessed 21 10 2011].

Fritz, A. H. & Schulze, G. eds., 2010. *Fertigungstechnik.* Berlin Heidelberg: Springer.

Grote, K.-H. & Antonsson, E. K. eds., 2009. *Springer Handbook of Mechanical Engineering.* Berlin, Heidelberg: Springer.

Grote, K.-H. & Feldhusen, J.-H. eds., 2011. *Dubbel.* 23 ed. Berlin Heidelberg: Springer.

Hennecke, M. & Czichos, H. eds., 2008. *Das Ingenieurwissen.* Berlin: Springer.

Klein, B., 2011. *Leichtbau-Konstruktion.* 9. ed. Wiesbaden: Vieweg+Teubner.

Klemens, U. & Hahn, O., 1994. *Nietsysteme. Verbindungen mit Zukunft.* Paderborn University: Hinrichsen.

Koether, R. & Rau, W., 2007. *Fertigungstechnik für Wirtschaftsingenieure.* München: Hanser.

Lange, K., ed., 1993. *Umformtechnik. Handbuch für Industrie und Wissenschaft. Band 4: Sonderverfahren, Prozesssimulation, Werkzeugtechnik, Produktion.* Berlin, Heidelberg: Springer.

Matthes, K.-J. & Riedel, F. eds., 2003. *Fügetechnik: Überblick, Löten, Kleben, Fügen durch Umformen.* Munich, Vienna: Carl Hanser Verlag.

Milberg, J. & Trautmann, A., 2009. *Defect-Free Joining of Zinc-Coated Steelsby Bifocal Hybrid Laser Welding,* s.l.: Springer.

Morello, L., Rossini, L. R., Pia, G. & Tonoli, A. eds., 2011. *The Automotive Body. Volume I: Components Design.* Heidelberg, London, New York: Springer.

Spur, G. & Stöferle, T., 1986. *Handbuch der Fertigungstechnik: Fügen, Handhaben und Montieren.* Munich, Vienna: Carl Hanser Verlag.

Steen, W. M. & Mazumder, J., 2010. *Laser Material Processing,* London: Springer.

Trautmann, A., 2009. *Bifocal Hybrid Laser Welding. A Technology for Welding of Aluminium and Zinc-Coated Steels.* Munich: Herbert Utz Verlag.

WorldAutoSteel, 2011. *Future Steel Vehicle. Final Engineering Report,* s.l.: s.n.

Yang, S., Carlson, B. & Kovacevic, R., 2011. Laser Welding of High-Strength Galvanized Steels in a Gap-Free Lap Joint Configuration under Different Shielding Conditions. Volume 90.

Zeissler, 2011. *http://www.uni-potsdam.de.* [Online] Available at: http://www.uni-potsdam.de/u/al/mitarbeiter/zeissler/lehre/vmh/material/schweissen.pdf [Accessed 27 07 2011].

10. Table of Figures

Appendix A: Box Morphing

Since much time during this thesis was spent on morphing operations and it was a crucial tool to create the discussed models, the method of box morphing is going to be presented in a higher level of detail in this chapter. Unlike direct morphing box morphing is a much more time consuming operation, but in return it also can handle much more complex mesh topologies. As indicated in chapter 5.1 the mesh was modified by editing the morph box which contains it. Therefore initially a morph box needed to be created which includes exactly the part of the mesh to be modified. The most often applied way was to create the boxes from curves. Those curves were derived from the outer flange edge in different ways.

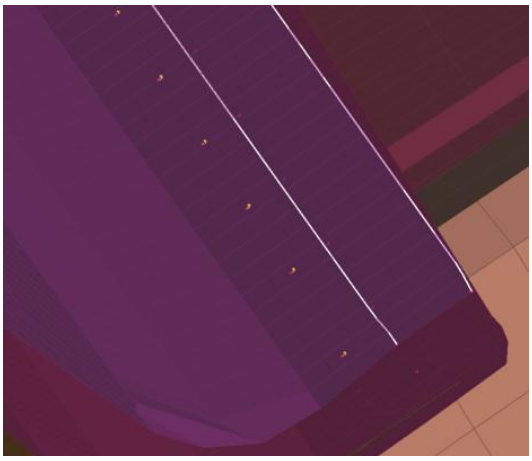

Figure 107 Extracting curves from mesh

The 'Feature Line to Curve' function of ANSA allows extracting the edge curve from the mesh, as displayed in *Figure 107*. Depending on the preset angle, the program automatically selects all the node lines which are connected to each other with an angle not larger than the one defined, starting with a line manually selected. In the example the mesh is smooth enough to also extract a second curve. Those two curves are then projected in both normal directions to the flange surface by first offsetting the start and the end point of the curves and then transferring the initial curves with respect to the new points (see *Figure 108*). From those four curves a morph box can be created which usually has a rectangular cross-section profile of about *10 mm x 10 mm* and will contain a sufficient part of the flange mesh to morph the width down to *8 mm*. Therefore the flange length which is not covered by the box, i.e. the band between the radius and the lower morph box face, must be significantly narrower than *8 mm*. If this criterion is not fulfilled, the lower face of the created morph box can be offset to enlarge its size.

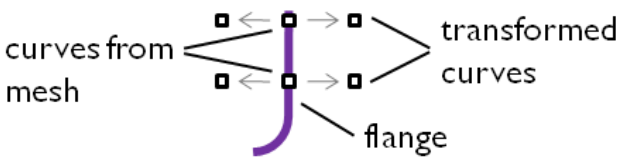

Figure 108 Two curves approach to create morph box, cross-sectional view

Eventually the flange mesh needs to be loaded into the morph box to be involved in the morph operation. If more elements than the ones inside the morph box are loaded it is implied that those elements are part of the automatic reconstruction if executed. Usually only the flange elements should be loaded, because involving the elements of the flange radius in the reconstruction operation may lead to a displacement of the node line where the curvature starts according to the mesh, which will disturb the flange width measurement.

If the ends of the edge curve are chamfered either the corner nodes are moved to create a sharp edge (see *Figure 109*) or the last node line is not included in the extracted curve. This way the curve is stretched manually to the end of the flange. Moving the corner node has no significant consequences, since the node was only moved within a extrapolation of the flange surface and the modified mesh will be, as mentioned, reconstructed any way.

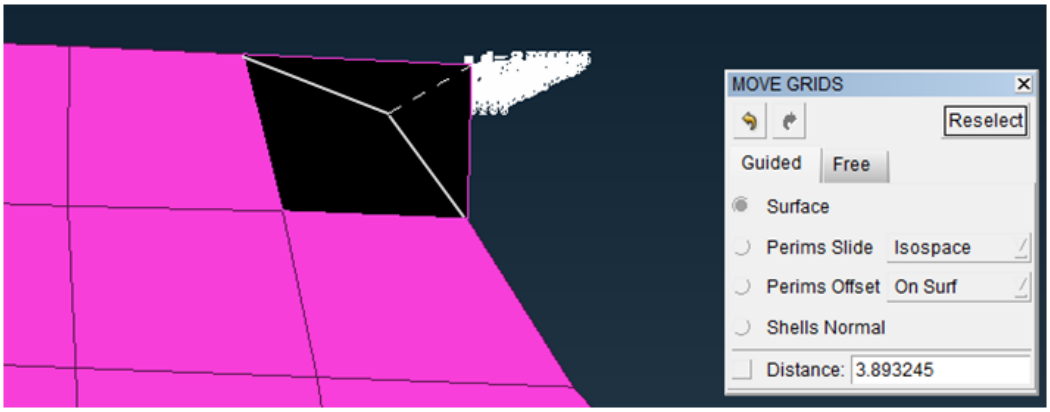

Figure 109 **Modification of flange corner**

If the mesh is not smooth enough only the edge curve is extracted. It then is sectioned to achieve a better quality of the transferred curves later on, attempting to have only one curvature per section, since the transfer function fails to follow complicated curve shapes properly. This sectioning technique can also be applied on the previously described two curves approach before the curves are transferred if the flange is overlong and includes numerous curvatures. On each section transition four points are generated creating always the same cross-section and if possible always related to the flange surface in the same way, though this is not entirely possible with an irregular flange mesh. Then the edge curves are transferred four times each with respect to the created points and the morph boxes can be generated from the new curves; see *Figure 110*. Depending on the number of

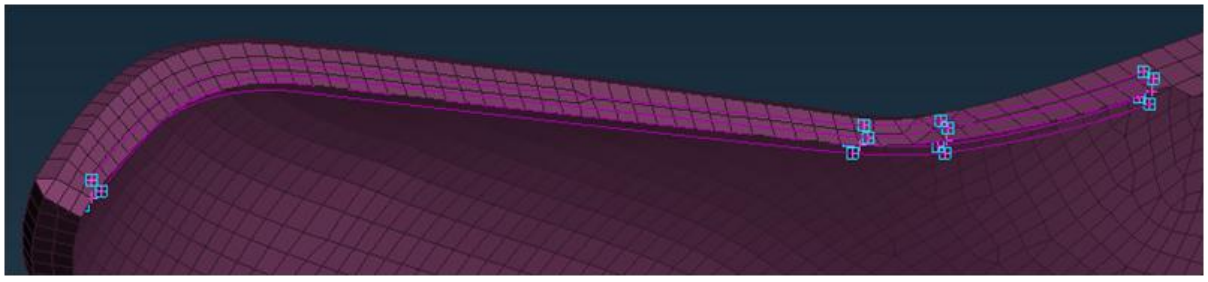

Figure 110 **Flange to be morphed sectioned into three parts**

sections a certain number of morph boxes is created. Since the morphing of all sections should happen at the same time, or if the sections have different width, at least there should be a smooth transition, the neighboring cross-sectional faces of the morph boxes are pasted together.
Two ways of extending an existing morph box are offsetting and sweeping. If a morph box just has to be linearly extended at one of its ends, e.g. because the chamfered corner is not included, the respective cross-sectional face can be offset. If the extension shall follow a guide curve, e.g. a flange edge curve, the sweep command can be applied. But again the guide curve should not include too many curvatures; otherwise the created morph box will be of poor quality.
Due to complex shaped geometries it often occurs that the morph boxes do not completely cover the flange mesh. In this case it usually is sufficient to offset the concerning face a few tenth of a millimeter. Whether there is any loaded element intersecting a morph box face can be told from the red color of the control point neighboring the face; otherwise they are represented by small green frames as shown in *Figure 111*. The control points are automatically generated when the morph box is created; their number depends on the shape of the morph box which they form. So for a pure ashlar-formed box there will only be eight points at each corner, while radii require a much higher number of control points.

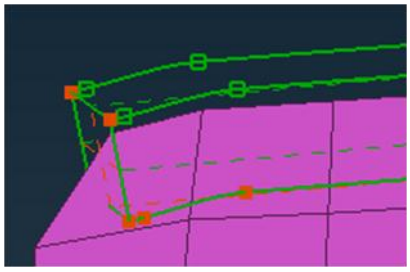

Figure 111 **Control points displayed as orange squares indicate an intersection of the embedded face**

If the described measures are not sufficient to create an appropriate morph box there are various other possibilities to further modify the box. Most of those deal with moving the control points in all kind of directions. Also the number of control points can be increased to better follow up on a complex topology shape. For the modification of the flange it is also very important that the side faces of the morph box are almost parallel to the flange surface. Otherwise the flange angle might change during morphing. So if this shape could not be fashioned when creating the box it manually needs to be remodeled by moving the control points.
Once the morph box is finalized the top face simply can be adjusted in level with the morphing flag active so that the flange reaches the desired width. But especially if several morph boxes shall be edited in the same way at a time, for example if the box is sectioned but needs to be modified at once or for a left hand and a right hand part, the creation of morphing parameters is helpful. Thereby the kind of modification is defined with the parameter; the amplitude is left as the only actuating variable.